The Development of Zinc Borate Production Process

By

H.Emre ELTEPE

A Dissertation Submitted to the

Graduate School in Partial Fulfillment of the

Requirement for the Degree of

MASTER OF SCIENCE

Department: Chemical Engineering

Major: Chemical Engineering

İzmirInstituteofTechnology

İzmir, Turkey

November, 2004

We approve the thesis of **H.Emre ELTEPE**

Date of Signature

…….. **21.12.2004**
Prof. Dr. Devrim BALKÖSE
Supervisor
Department of Chemical Engineering

…….. **21.12.2004**
Prof. Dr. Semra ÜLKÜ
Co-Supervisor
Department of Chemical Engineering

…….. **21.12.2004**
Prof.Dr. Tamerkan ÖZGEN
Department of Chemistry

…….. **21.12.2004**
Assist.Prof.Fehime ÖZKAN
Department of Chemical Engineering

…….. **21.12.2004**
Assist.Prof.Aysun SOFUOĞLU
Department of Chemical Engineering

…….. **21.12.2004**
Prof. Dr. Devrim BALKÖSE
Head of Department

ACKNOWLEDGEMENT

I would like to express my deepest gratefullness to my advisors Prof. Devrim BALKÖSE and Prof. Semra ÜLKÜ for their support, guidance and sharing their valuable experiences throughout the study and the preparation of the thesis which has been a very important experience for my future carreer.

I would like to state my special thanks to my friends Aykut ERDOĞDU, Sevdiye ATAKUL, Mehmet GÖNEN, Öniz BİRSOY and Yarkın ÖZGARİP for their help, encouragement and friendship throughout this project. I would also like to thank to Gökhan ERDOĞAN, Duygu OğuzKILIÇ, MineBAHÇECİ and Evrim YAKUT for their help for SEM, EDX and X-RAY analyses, Burcu ALP for TGA analyses and Özlem Çağlar DUVARCI and Filiz ÖZMIHÇI for FTIR analysis, Şerife Şahin ÖZALP and Belgin TUNÇEL for their help throughout the experiments.

I also present my deepest thanks to my father Kadri ELTEPE for encouriging me to be a Chemical Engineer and for teaching me the importance and vitality of science. I feel previlaged to be the son of a man who beleives in the power of production.

Finally, my thanks go to my mother and all my family members and especially to my wife for her endless support and my son for his beautifull smile giving me the inspiration to do more in life.

TABLE OF CONTENTS

ABSTRACT

The main objective of this study is the production of zinc borate which is used in large quantities as flame retardent and smoke subpressent material by making use of our country's resources which is the largest boron reserves in the world.

The development of commercially acceptable zinc borate production process was investigated from several different views and the samples obtained were characterized by using different techniques.

The physico-chemical properties of each sample were characterized by X-Ray diffraction, Fourier Transform Infrared Spectroscopy (FTIR), Scanning Electron Microscopy (SEM), Energy Dispersive X-ray (EDX) analysis, thermal gravimetric analysis (TGA).

Several forms of zinc borate with various dehydration temperatures are possible to obtain.A popular form of zinc borate which dehydrates above 290 ºC was obtained in this study.

ÖZ

Bu çalışmada alev geciktirici ve duman bastırıcı madde olarak çok miktarda tüketilen çinko boratın dünyanın en büyük bor rezervlerine sahip ülkemiz kaynaklarının kullanılarak uretimi hedeflenmiştir.

Ticari olarak kabul görebilecek çinko borat üretim işlemi araştırılmış ve değişik yönlerden değerlendirilmiş ve üretilen çinko borat numuneleri değişik teknikler kullanılarak karakterize edilmiştir.

Numunelerin fiziko-kimyasal özellikleri X-Işını Kırınımı, Fourier Dönüşümlü Kırmızı Ötesi Spektroskopi, Taramalı Elektron Mikroskobu, Enerji Dağılımlı X-Işını analizi, Termal Gravimetrik Analiz cihazlarıyla karakterize edilmiştir.

Farklı formlarda ve farklı dehidrasyon derecelerine sahip çinko borat elde etmek mümkündür.Bu çalışmada popular bir form olan 290ºC'nin üzerinde dehidrasyon derececine sahip çinko borat elde edilmiştir.

LIST OF FIGURES

LIST OF TABLES

CHAPTER 1

INTRODUCTION

Turkey has the biggest boron resources in the world 72%. Instead of processing the ore to produce high value boron compounds, Turkey is selling the material in ore form with very low values. This unfortunate situation has been the main initiative of this study. The aim of this thesis is to produce zinc borate which has a much greater commercial value than the ore. This idea has a great support by the official and commercial organizations.

Plastic materials are widely used all throughout our lives. Plastic materials release smoke and toxic gases during heating at high temperatures. Obtaining flame retardant and smoke suppressed compositions are getting more and more important day by day.

A series of different crystal structures of zinc borate (ZB) have been developed and are being used. The most widely used one is zinc borate with the formula $3ZnO{\cdot}2B_2O_3{\cdot}3.5H_2O$, but many zinc borates are used within formulations such as $4ZnO{\cdot}B_2O_3{\cdot}H_2O$, $ZnO{\cdot}B_2O_3{\cdot}1.12H_2O$, $ZnO{\cdot}B_2O_3{\cdot}2H_2O$, $6ZnO{\cdot}5B_2O_3{\cdot}3H_2O$, $2ZnO{\cdot}3B_2O_3{\cdot}7H_2O$, $2ZnO{\cdot}3B_2O_3{\cdot}3H_2O$, $3ZnO{\cdot}5B_2O_3{\cdot}14H_2O$ and $ZnO{\cdot}5B_2O_3{\cdot}4.5H_2O$. (Schubert et.al., 2003). Worldwide consumption of these zinc salts is several thousand metric tons per year.

Zinc borate, $3ZnO{\cdot}2B_2O_3$, forms a white amorphous powder or triclinic crystals depending on the method of preparation, specific gravity 3.64 (amorphous), 4.22 (crystalline); and melting point 980ºC. The amorphous form is slightly soluble in water and hydrochloric acid, the crystalline is insoluble in hydrochloric acid (Kirk-Othmer, 1970). The heat stability of hydration water of zinc borate is between 290 – 300ºC which enables the polymer processebility.

The increase in the use of synergistic mixture of zinc borate together with aluminum trihydrate has also increased the consumption of zinc borate. The reason for this usage is that the synergistic mixture of these two compounds promotes a non-halogen char formation. All around the world the consumption of halogeneous flame retardants are decreasing leading its way to compounds which are not halogeneous. Also this mixture is a smoke suppressant.

Currently, borates have a low demand in world flame retardant market. In North America, annual demand of flame retardants is 350,000 ton and the borates have a 1%

share from this market making 3,500 ton per annum. However, from 1991 onwards the share of borate compounds as flame retardants is increasing, therefore the major producer in USA, U.S.Borax has increased its capacity. The market increase of zinc borate all around the world is expected to be 12 – 15 % (Tektaş, Mergen, 2003).

In this study two main raw materials have been used for the production of ZB; zinc oxide and boric acid.

Effects of time and temperature of heating, seed crystals and refluxing on ZB product obtained were investigated.

The physico-chemical properties of each sample were characterized by X-Ray diffraction, Fourier Transform Infrared Spectroscopy (FTIR), Scanning Electron Microscopy (SEM), Energy Dispersive X-ray (EDX) analysis, thermal gravimetric analysis (TGA).

CHAPTER 2

BORON COMPOUNDS

2.1 Boron Compounds (Oxides, Acid, Borates)

A number of reviews have appeared covering the various aspects of borate glasses. The structure, physical properties, thermochemistry, reactions, phase equilibria, and electrical properties of alkali borate melts and glasses have been presented. The application of x-ray diffraction, NMR, Raman scattering, IR-spectroscopy, and ESR to structural analysis is available. Phase-equilibrium diagrams for a large number of anhydrous borate systems were included in a compilation, and thermo chemical data on the anhydrous alkali metal borates have been complied (Kirk-Othmer, 1994).

The largest single commercial use of borates is in fiber glass. There are two basic types of glass fibers: insulation (soda lime borosilicate glass) and textile (low alkali lime aluminosilicate glass) grades. Borax pentahydrate is the most common source of B_2O_3 for making insulation fiber glass. Textile or E-glass fiber requires low sodium formulations and for this reason boric acid or colemanite is commonly used. Only borates having low arsenic content are suitable for use in glass making. Smaller amounts of borates are consumed in heat-resisting (Pyrex or low thermal expansion) glass, sealing glass, glazes and enamels (frit), optical glass, nuclear waste storage glass, and in the making of vycor. The typical range of B_2O_3 content in commercial glasses is shown in Table 2.1. Borates are not generally used in container or flat glass.

Table 2.1. Borate Content in Commercial Glass (Kirk-Othmer, 1994).

Glass type	***B_2O_3, wt %***
Fiber	
Textile	6 – 13
Insulation	3 – 7
Heat resisting (pyrex)	12 – 15
Sealing glass	8 – 30
Porcelain enamel(frit)	11 – 13
Vycor	20[a]

[a] This is the percent B_2O_3 in glass prior to acid leching to form vycor.

Boron oxide B_2O_3, can be added to a glass formulation from a variety of boron-containing compounds, but because the boron is taken into vitreous solution is often

immaterial which source of boron is used. The choice of raw material is usually determined by consideration of the price per contained B_2O_3 unit uniformity of composition, purity, hydration state, and compatibility of the cation in the finished glass. In addition, boron- containing raw materials are usually the only water-containing constituents in a glass batch and because the water must be removed in the melting furnace, the dehydration characteristics important.

Boron oxide is added to borosilicate glass formulations to improve properties both in the finished glass and in the glass-making process. The benefits of B_2O_3 use in glass making are (1) creation of a low melting flux to dissolve refractory silica; (2) a lower liquids temperature and inhibition of devitrification; (3) lower melt viscosity; (4) enhanced melt rate; and (5) improved draw qualities in fiber production. The benefits of B_2O_3 in the finished glass product are (1) improved chemical durability; (2) lower thermal expansion; (3) increased mechanical strength; (4) decreased devitrification tendency; (5) improved stretching hardness; and (6) enhanced refraction, color, and brilliance.

2.2 Boron In The World

Boron was discovered by Joseph Gay-Lussac and Louis Thénard, French chemists, and independently by Sir Humphry Davy, a British chemist, in 1808 Boron is a hard, brittle semi-metallic element.

Chemical Symbol: B

Atomic number : 5

Atomic weight : 10.81

Melting Point : 2348 K

Boiling Point : 4273 K

2.2.1 Boron Minerals

Boron does not occur in nature as free element, crude borax occurs in nature as a mineral with associated clay and other impurities. There are over 200 naturally occurring boron containing minerals but the most commercially important and frequently traded minerals (salts, known as borates) are tincal, colemanite, ulexite and kernite. These ores can be refined into a pure chemical compounds. The ones that have the commercial importance are:

Boric acid H_3BO_3

Anhydrous boric acid B_2O_3

Anhydrous borax $Na_2B_4O_7$

Borax pentahydrate $Na_2B_4O_7.10H_2O$

Borax decahydrate $Na_2B_4O_7.5H_2O$

Sodium Perborate $Na_2B_4O_7.5H_2O$

Some commercially important boron minerals are;

Tincal $Na_2B_4O_7.10H_2O$

Kernite $Na_2B_4O_7.4H_2O$

Colemanite $Ca_2B_6O_{11}.5H_2O$

Ulexite $NaCaB_5O_9.8H_2O$

Datolite $Ca_2B_2O_5.Si_2O_5.H_2O$

Hydroboracite $CaMgB_6O_{11}.6H_2O$

Turkey is the largest producer of boron ore in the world. Important boron minerals of Turkey's are tincal, colemanite and ulexite. Boron minerals contain different amount of B_2O_3 in their structures. The important factor for industrial application of boron minerals are B_2O_3 content, so they can replace each other in use. This means that one boron mineral can be trade competitor to the other one.

Boron minerals can be used in some sectors in the industry as crude minerals. In general, their applications after refining and end-products are wider than crude ones. Borates find use in different sectors, however the principal markets are: Agriculture,

detergents and soaps, flame retardants, glass, glazes, frits, enamels and insulation.

2.2.2 Boron Reserves

In the world, Turkey, USA and Russia have the important boron mines. In terms of total reserve basis, Turkey has a share of 64%, the other important country USA is 9% as seen in Table 2.2.

Total world boron reserves on the basis of B_2O_3 content are 363 million tons proven, 522 million tones probable and possible, as a total of 885 million tons. With a share of 64%, Turkey has a total boron reserve of 563 million tons on the basis of B_2O_3 content.

Table 2.2 World boron reserves (Million tons)(**http://minerals.usgs.gov**, 2001)

Country	Proven Reserve	Probable Possible Reserve	Total Reserve	Percent in Total (%)	Life Span (Year)
Turkey	224.000	339.000	563.000	64	389
U.S.A.	40.000	40.000	80.000	9	55
Russia	40.000	60.000	100.000	11	69
China	27.000	9.000	36.000	4	25
Chile	8.000	33.000	41.000	5	28
Bolivia	4.000	15.000	19.000	2	13
Peru	4.000	18.000	22.000	2	15
Argentina	2.000	7.000	9.000	1	6
Kazakhstan	14.000	1.000	15.000	2	10
Total	**363.000**	**522.000**	**885.000**	**100,0**	**610**

Turkey has the highest boron reserves in the world.

2.2.3 Boric Acid

H_3BO_3 is a weak acid often used as anticeptic, insecticide, flame retardant and a component of other chemical compounds. It exists in the form of colorless crystals or a white powder and dissolves in water. It has the chemical formula H_3BO_3 and in known by the chemical name hydrogen othoborate.

The general technical specifications of boric acid used throughout the study are tabulated in Table 2.3.

Table 2.3 The general technical specifications of boric acid (Etiholding)

Chemical Properties (Typical)		
	Normal Sulphate	Low Sulphate
Purity	99.90% min	99.90% min
B_2O_3	56.25% min	56.25% min
SO_4	500 ppm max	130 ppm max
Physical Properties		
Crystalline		
Molecular Weight	61,83	61,83
Specific Gravity	1,435 gr/cm3	1,435 gr/cm3
Bulk Density	0,8 gr/cm3	0,8 gr/cm
Fractions	+1 mm 4%max	+1 mm 4%max
	-0,060 mm 4% max	-0,060 mm 5% max
Powder		
Molecular Weight	61,81	
Specific Gravity	1,435 gr/cm3	
Bulk Density	0,7 gr/cm3	
Fractions	+1 mm 0%	
	-0,060 mm 30% min	

The solubility of boric acid in water increases with respect to temperature which is shown in the solubility chart of in Figure 2.1.

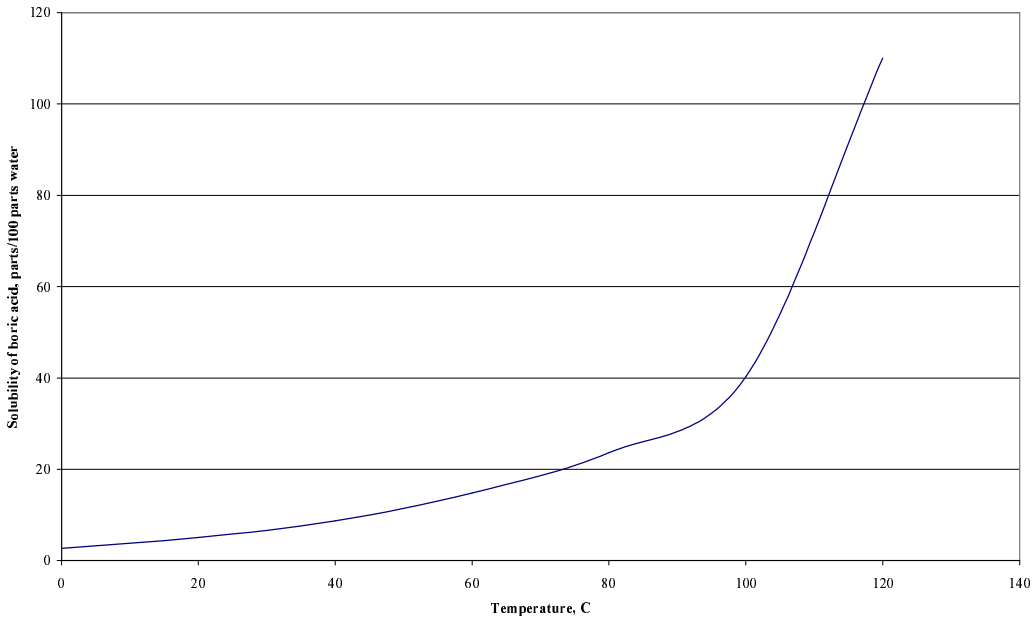

Fig.2.1 The solubility of boric acid (Kirk-Othmer, 1970).

2.3 Other Metal Borates

Borate salts or complexes of virtually every metal have been prepared. For most metals, a series of hydrated anhydrous compounds may be obtained by varying the starting materials and/or reaction conditions. Some have achieved commercial importance.

In general, hydrated borates of heavy metals are prepared by mixing aqueous solutions or suspensions of the metal oxides, sulfates, or halides and boric acid or alkali metal borates such as borax. The precipitates formed from basic solutions are often sparingly-soluble amorphous solids having variable compositions. Crystalline products are generally obtained from slightly acidic solutions.

Anhydrous metal borates may be prepared by heating the hydrated salts to 300-500 ^{o}C, or by direct fusion of the metal oxide with boric acid or B_2O_3. Many binary or tertiary anhydrous systems containing B_2O_3 form vitreous phases over certain ranges of composition (Kirk-Othmer, 1994).

2.3.1 Barium Metaborate

Three hydrates of barium metaborate, $BaOB_2O_3xH_2O$, are known. The tetrahydrate and pentahydrate both contain the $B(OH)^-_4$ anion, and are properly formulated as $Ba[B(OH)_4]_2xH_2O$ where X=0 or 1. These compounds crystallize when solutions of barium chloride and sodium metaborate are combined at room temperature. The higher hydrate is favored when excess sodium metaborate is used. Saturated aqueous solutions contain 13.5 g/L of $BaOB_2O_34H_2O$ at 25 ^oC. Both forms dehydrate at temperature above 140^oC. Barium metaborate may also be prepared from barium sulfide formed by prior reduction of barium sulfate. The presence of sulfide impurities in the product may render it unsuitable for some applications. Crystals of a hydrate, x=1.67 H_2O, form from a boiling solution having the B:Ba molar ratio <2. Dehydration of this hydrate at 300^oC gives $BaOB_2O_3$ in which boron atoms are both triangularly and tetrahedrally coordinated.

Barium metaborate is used as an additive to impart fire-retardant and mildew-resistant properties to latex paints, plastics, textiles, and paper products. Barium metaborate is marketed by Buckman Labs, Inc., Memphis, Tennessee (Kirk-Othmer, 1994).

2.3.2 Copper, Manganese, and Cobalt Borates

Borate salts of copper, manganese, and cobalt are precipitated when borax is added to aqueous solutions of the metal (II) sulfates or chlorides. However, these materials are no longer produced commercially (Kirk-Othmer, 1994).

CHAPTER 3

ZINC BORATE

3.1 General Properties of Zinc Borate

Plastic materials are widely used all throughout our lives. The importance of flame retardancy of plastics and flame retardant materials are also increasing day by day. A series of hydrated zinc borates have been developed for use as fire-retardant additives in coatings and polymers. The most widely used one is zinc borate with the formula $2ZnO{\cdot}3B_2O_3{\cdot}3.5H_2O$, but many zinc borates are used within these formulations such as $4ZnO{\cdot}B_2O_3{\cdot}H_2O$, $ZnO{\cdot}B_2O_3{\cdot}1.12H_2O$, $ZnO{\cdot}B_2O_3{\cdot}2H_2O$, $6ZnO{\cdot}5B_2O_3{\cdot}3H_2O$, $2ZnO{\cdot}3B_2O_3{\cdot}7H_2O$, $2ZnO{\cdot}3B_2O_3{\cdot}3H_2O$, $3ZnO{\cdot}5B_2O_3{\cdot}14H_2O$ and $ZnO{\cdot}5B_2O_3{\cdot}4.5H_2O$. Worldwide consumption of these zinc salts is several thousand metric tons per year. A substantial portion of this total is used in vinyl plastics where zinc borates are added (Kirk-Othmer, 1994; Tektaş, 2003).

Besides zinc borate, flame retardant materials such as aluminum trihydrate, magnesium hydroxide, antimony, phosphorus and bromine compounds are also used. Antimony trioxide and the halogenated compounds of the former have been banned because of their toxic gases during burning. The ban of halogenated compounds has increased the usage of synergistic compounds. The usage of zinc borates with aluminum trihydrate for this purpose has increased.

Zinc borate, $3ZnO{\cdot}2B_2O_3$, forms a white amorphous powder or triclinic crystals depending on the method of preparation, specific gravity 3.64 (amorphous), 4.22 (crystalline); and melting point 980ºC. The amorphous form is slightly soluble in water and hydrochloric acid, the crystalline is insoluble in hydrochloric acid (Kirk-Othmer, 1970). The heat stability of hydration water of zinc borate is between 290 – 300ºC which enables the polymer processebility. Because the refractive index of zinc borate is nearly the same to the refractive indices of many polymers, it enables the pigment load to be low. The theoretical composition and physical properties of zinc borate having 3.5 hydration water are given in Table 3.1 (Tektaş, 2003).

Table 3.1 The theoretical composition and physical properties of zinc borate(Tektaş, 2003).

B_2O_3, %	48.05
ZnO, %	37.45
Crystal water, %	14.50
Refractive index	1.58
Average particle size, μm	7 – 12
Solubility (At room temperature), %	0.28
Specific gravity, g/cc	2.77

Zinc borate $2ZnO3B_2O_3 \cdot 7H_2O$ is formed when borax is added to aqueous solutions of soluble zinc salts at temperatures below about 70°C. An x-ray structure determination has indicated that this compound is orthorhombic and has a zinc triborate monohydrate structure. $Zn[B_3O_3(OH)_5]H_2O$. Zinc borates $2ZnO3B_2O_3 \cdot 7H_2O$ and ZnO $B_2O_3 \cdot 2H_2O$ lose water of hydration when heated from 130 to 250°C (Kirk-Othmer, 1994).

3.2 Applications

Main application areas of zinc borate are listed in Table 3.2.

Table 3.2 Main application areas of zinc borate (http://www.samuelbanner.co.uk/storey/home.htm).

1. PVC	Smoke suppression,snergy,char formation
2. Halogen Free Cable Compounds	Smoke suppression,snergy,afterflame reduction,char formation.
3.Conyeyor Belting	Synergy ,after glow suppression
4.Nylon6,6	Snergy,anti-drip,electrical track property improvement
5.Glass Reinforced Polyester	Synergy,Smoke levels contained
6.Epoxy	Synergy,L.O.I. Improvements
7.Carpet Backing	Bond strength improvement,low smoke carpets e.g. Aircrafts
8.General Rubber	After glow suppression ,can be used with chlorinated paraffin to improve flame ret.
9.Cotton Fabric Treatment	Afterglow suppression , cotton polycotton latex back coating

Giudice and Benitez, [2001]; discussed the influence of ZB with molecular formulas of 3.5 H_2O and 7.5 H_2O on flame resistance of paints. Eight different paint compositions were prepared. LOI, and flame spread index (FSI) tests were carried out to test the flame retardancy. As shown in Figure 3.1, results of LOI tests indicate that the compositions having both ZB's (No.5) and having only 7.5 H_2O (No.3) with antimony trioxide have the maximum values. All sample compositions are given in Table 3.3.

Table 3.3. Composition of flame-retardant coatings, % by volume on solids[a](Guidice and Benitez, 2001).

Component	**1**	**2**	**3**	**4**	**5**	**6**	**7**	**8**
Titanium dioxide	11.5	11.5	11.5	11.5	11.5	11.5	11.5	11.5
Antimony trioxide	9.0	6.0	6.0	6.0	3.0	-	-	-
Zinc borate[b]	-	3.0	-	1.5	3.0	4.5	9.0	-
Zinc borate[c]	-	-	3.0	1.5	3.0	4.5	-	9.0
Micronized talc	22.4	22.4	22.4	22.4	22.4	22.4	22.4	22.4
Chlorinated alkyd resin	52.4	52.4	52.4	52.4	52.4	52.4	52.4	52.4
Bentone (gel)	2.8	2.8	2.8	2.8	2.8	2.8	2.8	2.8
Additives	1.9	1.9	1.9	1.9	1.9	1.9	1.9	1.9

[a] PVC (pigment volume concentration), 42.9% [b] $2ZnO{\cdot}3B_2O_3{\cdot}3.5H_2O$ [c] $2ZnO{\cdot}3B_2O_3{\cdot}7.5H_2O$ [d] 24.9% chlorine content.

Samples No.6 – 8 had the lowest LOI values with no antimony trioxide in their compositions.

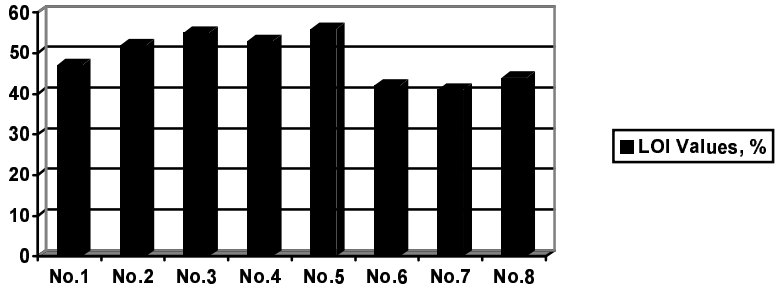

Figure 3.1 LOI Values (%) of the compositions(Guidice and Benitez, 2001).

The UL94 tests carried out also have shown that all of the compositions passed the tests in Class A.

Bourbigot et.al., [1998] have studied the recent advances in the use of zinc borate in flame retardancy of EVA. In their work, zinc borates were used as synergistic agents in EVA (Ethyl vinyl acetate)-ATH (aluminium trihydrate) and EVA-$Mg(OH)_2$ flame retardant formulations and as smoke suppressants. Moreover, the study by solid state NMR of the residues sampled at different times during cone calorimeter experiments of the formulations EVA-ATH and EVA-ATH/ZB allows proposing a mechanism of action of the flame retardant systems.

3.3 Some Manufacturers Around The World

It is marketed by the United States Borax & Chemical Corp. under the trademark FIREBRAKE ZB, BOROGARD ZB, and under AMAX, Inc. as ZB-467. This compound has the unusual property of retaining its water of hydration at temperatures up to 290^{o}C. This thermal stability makes it attractive as a fire-retardant additive for plastics and rubbers that require high processing temperatures. It is also used as an anticorrosive pigment in coatings. The 1990 selling price for FIREBRAKE ZB ranged from $ 2.40/kg to $ 2.90/kg. Zinc borates are also manufactured by Storey (UK) and Waardals (Norway). Besides these, the general producers are tabulated in Table 3.4.

Table 3.4 The general manufacturers and their capacities (Tektaş, 2003).

Country	Producer	Place	Capacity, ton/annum.
China	Hainan Zhongxin Chemical	Haiko	1.000
	Shanghai Jinghua Chemical	Wujing	-
	Wuxi Daxhong Chemical	-	-
	Zhenjiang Sulphuric Acid Plant	Zhenjiang city	1.000
India	C-Tech	Mumbai	-
Norway	Waardals	Skalevik	-
USA	Anzon	Laredo	-
	US.Borax	Wilmington	12.000

3.4 Market Share

The most consuming countries in the world are from US and West Europe. The consumptions of the flame retardant materials according to regions are given in Table 3.5.

Table 3.5 The consumption of flame retardants in 1998 (Tektaş, 2003).

Regions	Per cent consumption
North America	45 %
West Europe	32%
Japan	13%
Other Asian Countries	8%
Others	2%

The flame retardants used in US and West Europe ratios are given in Table 3.6.

Table 3.6 The ratio of other flame retardants used in US and West Europe(Tektaş, 2003).

Flame Retardants	US	West Europe
$Al(OH)_3$	39	47
Bromine based	27	13
Phosphorus based	12	23
Chlorine based	11	3
Antimony oxides	8	7
$Mg(OH)_2$	1	2
Others*	2	5

*Zinc borate and other borates are given in Others section.

85% of flame retardants produced all around the world find use mostly in plastics. For this section, $Al(OH)_3$ is the most important item and find use around 50%. The borates find a less amount in total world share of flame retardants currently. For example, of the 350.000 MT/year share of flame retardant industry in North America, borates find a market of 1%(3.500 MT/year). However, in US the share of zinc borate increased starting from 1991 and US.Borax company has also increased its capacity. The increase in world zinc borate market is expected to be between 12 and 15% per year. The price index of zinc borate is given in Table 3.7.

Table 3.7 Price index of zinc borates (Tektaş, 2003).

Year	Price, USD/MT
1980	1100
1988	1700 – 1840
1992	2420
1998	2180
2001	2340

In US, although the price of zinc borate was expected to be around 2300 USD/MT levels, there were prices between 1250 and 1470 USD/MT in world market.

3.5 Future Market of Zinc Borate

The increase in the use of synergistic mixture of zinc borate together with aluminum trihydrate has also increased the consumption of zinc borate. The reason for this usage is that the synergistic mixture of these two compounds promotes a non-halogen char formation. All around the world the consumption of halogeneous flame retardants are decreasing leading its way to compounds which are not halogeneous. Also this mixture is a smoke suppressant.

The price of zinc borate is lower than the bromine based flame retardants which will affect the consumption of zinc borate in favor of this compound.

3.6 Toxicology

Zinc borate $2ZnO3B_2O_3 \cdot 3.5H_2O$ has an acute oral toxicity in rats LD_{50} >10000 mg/kg body weight and acute dermal toxicity in rabbits LD_{50}>10000 mg/kg body weight. It is not a skin irritant and gives a negative response in the Ames mutagenicity test (Kirk-Othmer, 1994).

3.7 The Production of Zinc Borate

Zinc borate ($2ZnO \cdot 3B_2O_3 \cdot 3.5H_2O$) in general is produced with the reaction between zinc oxide and boric acid. Boric acid is solved in water between temperatures 95°C and 98°C and zinc oxide and seed crystal of $2ZnO \cdot 3B_2O_3 \cdot 3.5H_2O$ is added to this solution at a certain stoichiometric ratio. The reaction continues for a while by mixing and the zinc borate formed is filtered, dried and ground. The boric acid solution is fed to the system as reflux. The general flow sheet is given in Figure 3.2.

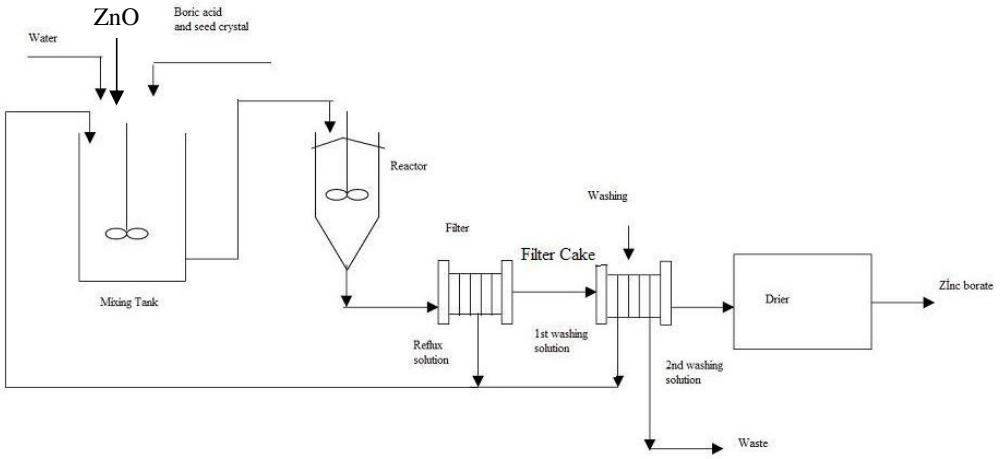

Fig.3.2. Flow sheet of a general production system of zinc borate (Tektaş, 2003).

This product has also been crystallized from solutions containing borax, zinc chloride, and sodium hydroxide (Tektaş, 2003).

3.8 Structural Characterization and Chemistry of Zinc Borate

Schubert et.al. [2003] have studied the structural characterization and chemistry of industrially important zinc borate, $Zn[B_3O_4(OH)_3]$. Several unique crystalline zinc borates are known. The structure of $Zn[B_3O_4(OH)_3]$ was determined for the first time by single – crystal X-ray diffraction, revealing it to be a complex network consisting of infinite polytirborate chains crosslinked by coordination with zinc and further integrated by hydrogen bonding.

Zinc borate is a complex inoborate (containing a borate structural unit that is an infinite chain) composed of linked triborate moieties, interconnected by coordination with pseudo-tetrahedral zinc centers and a network of H-bonds. The asymmetric unit in 1 includes one zinc atom (Figure 3.3 (a)) and one triborate moiety(Figure 3.3 (b)). There are three unique boron sites present as one trigonal BO_3 and two tetrahedral BO_4 groups. These groups share oxygen vertexes to form a B_3O_3 boroxyl ring. One BO_4 group has one attached OH group and the other has two, producing the $B_3O_4(OH)_3$ subunit (Figure 3.3 (b)). These triborate moieties link into infinite chains parallel to [101] by sharing an exocyclic oxygen (O4/O4A) between BO_3 and BO_4 polyhedra. The $BO_2(OH)_2$ group is not involved in the chain extension. Each zinc atom (Figure 3.3(a)) is pseudotetrahedrally coordinated by oxygens of three different polyborate chains. Two

zinc coordination positions are satisfied by one endocyclic boroxyl oxygen (O1) and one hydroxyl oxygen (O7) that is attached to the adjacent triborate moiety in the same chain, producing the six-membered ZnB_2O_3 rings, seen in Figure 3.4.

The boroxyl oxygen involved in zinc coordination lies between the BO_3 and BO_4 polyhedra involved in chain extension. The remaining two zinc coordination sites are occupied by hydroxyl oxygens of $BO_2(OH)_2$ groups in two separate polyborate chains. In this way, all hydroxyl groups are involved in zinc coordination.

Compound 1 exhibits a complex higher order structure. Not only does each zinc center link three separate polyborate chains, but also these chains are interconnected by H-bonds. All there OH hydrogens are involved in H-bonding with oxygen atoms of adjacent chains. Chains are connected via O5-H5…O3, O6-H6…O4, and O7-H7…O2 hydrogen bonds. Notably all three H-bonds involve B-O-B acceptor oxygen atoms and not B-O-H oxygens, which may explain the relatively high dehydration onset temperature of 1. The three hydrogens atoms in 1 are observed in the H MAS NMR spectrum. Owing to their distinct differences in H-bonding strengths, the three proton sites yield clearly resolved resonances at 4.6, 7.0, and 8.6 ppm.

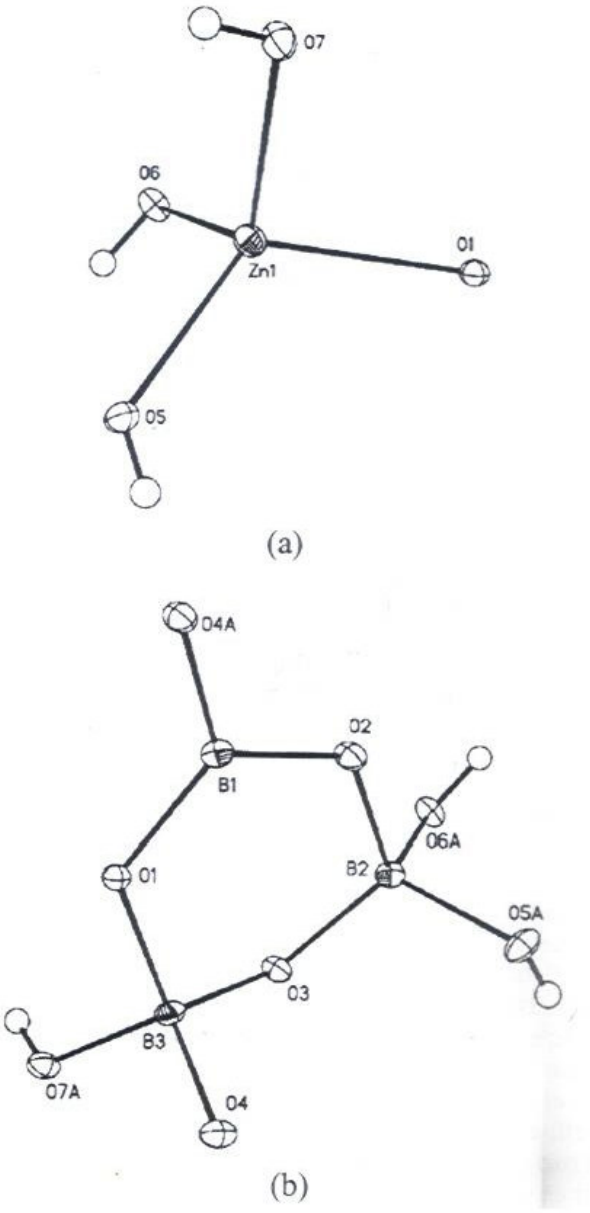

Figure 3.3 (a) Zn center and (b) B_3O_4 $(OH)_3$ units in 1. thermal ellipsoids are drawn at 30% probability level. (Schubert et.al., 2003)

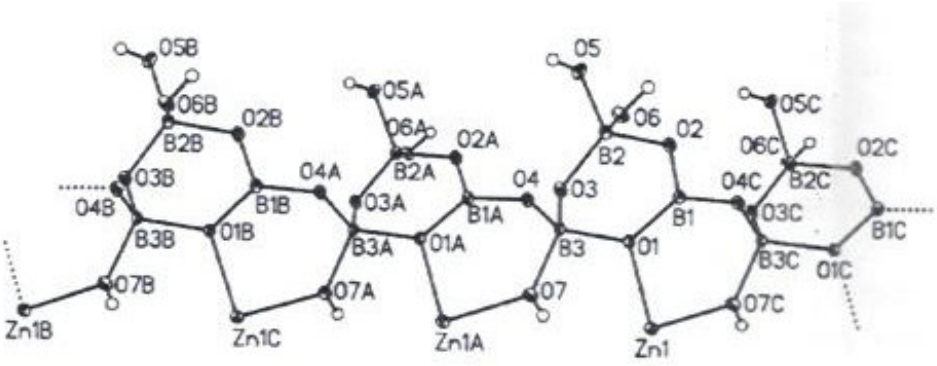

Figure 3.4. A segment of the infinite polytriborate chains in 1 showing zinc interactions. Zinc atoms are shown with only two coordination positions occupied for clarity. Thermal ellipsoids are drawn at 30% probability level. (Schubert et.al., 2003)

There are regular 4-fold centrosymmetric connections between alternating complementary pairs of triborate moieties in neighboring chains. These interactions involve two zinc centers, one in each chain, that link adjacent triborate rings via 2-fold O6-Zn-O1 coordination (corner sharing of zinc tetrahedral and borate polyhedra). The same triborate are also linked by pairs of O7-H7..O2 H -bonds. Zinc atoms lie very roughly in layers positioned between repeating pairs of polyborate chains.

Borate structures can be described in terms of compact, insular groups, referred to as fundamental building blocks (FBBs), forming the basis of classification schemes for crystalline borate compounds. These schemes define FBBs according to the number of boron atoms, the number of trigonal BO_3 and tetrahedral BO_4 groups, and the mode of polymerization between the FBBs, to give isolated, modified isolated, chain, modified chain, sheet, modified sheet, and three-dimensional network structures. Using the classification scheme devised by Christ and Clark(1977), the borate structural unit of 1 is described as ∞:3(Δ + 2T), indicating a three-boron FBB containing one trigonal and two tetrahedral boron centre. Using the more recent classification scheme proposed by Burns and Hawthorne(1995), the structural unit 1 is described as 1Δ2□:< Δ2□>, where Δ and □ refer to BO_3 and BO_4 polyhydra, respectively.

3.8.1 Comparison with mineral structures

The structure of 1 bears similarities to some borate minerals, notably the industrially important colemanite, $Ca[B_3O_4(OH)_3]•H_2O$, and the lesser known studenitsite, $Ca[B_3O_4(OH)_3]$. The industrial mineral hydroboracite, $CaMg[B_3O_4(OH)_3]_2•3H_2O$, is also related. These minerals also contain infinite polytriborate chains of the <Δ2□> type that are cross-linked by coordination with metal cations. However, significant differences exist between the structures of these minerals and 1 resulting from the different coordination demands of their metal cations.

In colemanite, calcium atoms link together by sharing oxygen to form chains running parallel to the polytriborate chains (parallel to [100]). These calcium containing chains share oxygen of the polytriborate chains and thereby interconnect them into infinite sheets. These sheets are connected by H-bonding and a relatively small number of Ca-O bonds, resulting in the perfect [101] cleavage characteristic of colemanite. In contrast, the tetrahedral zinc centres in 1 do not form chains by sharing oxygen between zinc and instead interconnect the polyborate chains into a three-dimensional network rather than sheets. Consequently, 1 is a much less friable material than colemanite.

The closest mineral analogue to 1 in composition is studenitsite, $Ca[B_3O_4(OH)_3]$. In contrast, however, this mineral contains corrugated calcium oxide sheets lying between and interconnecting parallel polytriborate chains. Some notable differences between studenitsite and colemanite are the absence of the interstitial water and a helical rather than translational extension of borate chains in the former, with $B_3O_4(OH)_3$ groups within a chain related by a 2-fold screw axis parallel to the b-axis of the crystal. Although colemanite contains one water in the coordination environment of calcium, this water uses one hydrogen to H-bond to adjacent water with the result that the total number of bonds from the interstitial complex, $Ca(H_2O)]^{+2}$, to the borate structural unit is the same as that for Ca^{+2} in the studenitsite if each metal centre is assigned the same coordination number.

Borate and polyborate structural units have associated basicities that are approximately proportional to the percentage of tetrahedral boron in their FBBs. This is also a function of the solution pH prevailing during borate crystallization since specific borate anions are stable only within a given pH range. Empirical methods based on the analysis of borate mineral structures were developed recently to estimate Lewis basicities of borate structural units. According to the *valence matching principle*, to have a stable structure, the Lewis basicity of the (anionic) borate structural unit must

match closely the Lewis acidity of the (cationic) interstitial complex. Correlations of structural features found in minerals suggest that borate structural units adjust to varying acid-base conditions, within stability ranges, by changing the average coordination number of oxygen atoms (O-CN) in the structural unit, counting hydrogen bonds and bonds to cations. Higher average O-CN values are associated with higher borate basicities. These correlations depend heavily on the assignment of coordination number to cations since this largely defines average O-CN.

Colemanite, studenitsite, and 1 have chemically equivalent borate structural units and thus have the same Lewis basicities. However, Zn^{+2} has substantially higher Lewis acidity than Ca^{+2}. The structure of colemanite was analyzed by others with the conclusion that it has an average O-CN of 3.6. Considering calcium to be 8-coordinated and examination of the studenitsite structure indicates that it also has an average O-CN of 3.6. The O-CN value of these minerals correlates well with the overall pattern for borate mineral structures. Zinc favours four-coordination and the zinc atom in 1 to be considered to be four. Each structural unit oxygen in 1 is coordinated once by either an H-bond or zinc, resulting in an O-CN of 3.0. This O-CN value is significantly below the range reported for borate minerals. Only by considering the coordination number of zinc to be higher than 4 can the O-CN be higher.

For metal coordination, some authors have included all oxygens having a metal-oxygen bond valence greater than 0.05 vu with metal-oxygen distances less than the metal-metal distance, with consideration of distance gaps. Application of the distance rules alone can over count the number of oxygens actually involved in bonding the interaction with metal. In 1, there are 24 oxygen atoms having Zn-O distances shorter than the Zn-Zn distance (4.391 A). The immediate coordination environment around zinc (Figure 1a) contains four oxygen atoms, at distances from 1.919 to 1.966 A, with geometry close to an idealized tetrahedron. Valence analysis gives a sum of bond valences for zinc of 3.8 vu, counting only these four Zn-O bonds. There is a large gap between the closest four oxygen and the next two, which have Zn-O distances of 2.707 A (O2) and 2.918 A (O7). Beyond these, the next closes oxygen lies at a distance of 3.179 A (O4).

For the borate structural unit in colemanite, studenitsite, and 1, it has been argued that the boroxyl oxygen linking the two tetrahedral boron atoms should receive two additional bonds, either from the metal or H-bonds to satisfy its valence requirements. In colemanite this oxygen receives two H-bonds and in studenitsite it is bonded to two

calcium atons. However, the corresponding oxygen in 1, O(3), receives only one H-bond and is not within the tetrahedral coordination environment of zinc. The shortest three O(3)-Zn distances are 3.282, 3.771, and 3.885 A. valence analysis, counting one H-bond and two B-O bonds gives a sum of valences for O(3) of 1.81 vu, somewhat less than the 1.90 vu calculated for colemanite. The two B-O bonds to these oxygen atoms are both slightly shorter by 0.021-0.022 A in 1 than in colemanite.

The related synthetic monomeric triborate 6, $Zn(H_2O)[B_3O_3(OH)_5]$, is an analogue of the mineral meyerhofferite, $Ca(H_2O)[B_3O_3(OH)_5]$. Here, tetra-coordination of zinc also results in a significantly lower average O-CN in the synthetic material compared to that in the mineral. Explanations offered for why synthetic borates may not match the patterns observed for borate minerals refer to the greater range of options available in nature compared with more restricted synthetic systems. Hydrolytic stability under geologic conditions may also be a factor. Clearly, geological conditions, as well as those used to crystallize most anhydrous borates, favour more thermodynamically stable products. Nevertheless, improved understanding of structure-stability relationships is important to the development of synthetic methodologies for borates having useful properties.

3.9 Zinc Borate

There are two patents regarding zinc borate production.

3.9.1 Patent by Schubert

In a US.Patent by Schubert [1995], zinc borate compositions having a $ZnO:B_2O_3$ ratio of 4:1 and anhydrous zinc borate are examined. The patent relates to improved zinc borate compositions, and more particularly, provides a new hydrated zinc borate having a high dehydration temperature which offers significant advantages for compounding with plastics and rubbers at elevated temperatures. The anhydrous form of zinc borate was also provided in this study offering advantages for compounding at even high temperatures.

Many different hydrated zinc borates are known and several find commercial application as fire retardants and smoke suppressants for various polymers. They are also used for anticorrosive pigments for coatings and have demonstrated fungistatic and bacteriostatic properties which find many applications.

In this study, a new crystalline, hydrated zinc borate having a relatively high dehydration temperature which makes it especially useful for use in polymers requiring processing at high temperatures was studied. The anhydrous form of zinc borate was also provided with this study.

The hydrated zinc borate of this study had the formula $4ZnO \cdot B_2O_3 \cdot H_2O$. It is a crystalline solid having very slight water solubility and having a dehydration temperature which begins at about 415°C with a rapid loss occurring above 425°C. Such a high dehydration temperature makes this composition especially useful as an additive for polymers requiring high processing temperatures such as polysulfones, polyamide-imides, etc.

The studied zinc borate hydrate was comprised by the reaction of zinc oxide with a near stoichiometric amount of boric acid (2:1 mole ratio) in water at an elevated temperature, according to the equation

$$4ZnO+2B(OH)_3 \rightarrow 4ZnO \cdot B_2O_3 \cdot H_2O+2H_2O.$$

The reaction takes place near the boiling point of the mixture and is promoted by the presence of previously prepared product seed. The concentration of the initial reaction mixture should be greater than about 5% by weight of starting reagents in order to provide a reasonably rapid reaction rate. Preferably, reaction mixtures in the 10 – 20% by weight range were employed, since they require only a few hours of refluxing in water to go to completion. It was also preferred that a slight molar excess (approximately 5%) of boric acid was used in order to provide complete consumption of zinc oxide in the reaction. The desired hydrated zinc borate product was readily separated from the cooled reaction solution by filtration and dried to give the desired crystalline product. It had also been found that more consistent results boiling water in at least two separate portions, thereby maintaining the pH of the reaction mixture above 5.5, and the reaction mixture was efficiently stirred or mixed during the reaction period.

Other methods of preparing the hydrated zinc borate of the patent include hydrolysis of the zinc borate $2ZnO \cdot 3B_2O_3 \cdot 3.5H_2O$ in a refluxing aqueous slurry. It has been found that the concentration of the starting material in the aqueous slurry must be less than about 5% in order to produce a complete reaction. At least five days of continuous reflux at atmospheric pressure of 5% slurry of starting material was required to give complete hydrolysis. Reflux of the reaction mixture containing free boric acid

for an excessive period of time (such as for one month) will convert the zinc borate to the compound $6ZnO \cdot 5B_2O_3 \cdot 3H_2O$ which was previously reported as a product of the hydrothermal reaction of zinc oxide and boric acid at 165°C (Lehmann, 1967).

The zinc borate of this patent may also be prepared by reacting $2ZnO \cdot 3B_2O_3 \cdot 3.5H_2O$ with a stoichiometric amount of zinc oxide in refluxing water. This reaction was also facilitated by the presence of seed crystals of previously prepared zinc borate $4ZnO \cdot B_2O_3 \cdot H_2O$. In some cases, the reaction appears to be catalyzed by the presence of zinc ion such as supplied by a small amount of zinc chloride or zinc sulphate.

A fourth method for preparing the $4ZnO \cdot B_2O_3 \cdot H_2O$ of this patent was by reaction of sodium tetraborate with a zinc salt such as zinc sulphate and zinc oxide in boiling water according to the equation.

$$Na_2B_4O_7 \cdot 5H_2O + ZnSO_4 \cdot 7H_2O + 7H_2O + 7ZnO \rightarrow$$

$$2(4ZnO \cdot B_2O_3 \cdot H_2O) + Na_2SO_4 + 10H_2O$$

The presence of about 5% seed product facilitates the reaction which goes to completion within a few hours.

The patent by Schubert [1994] written so far has given the following examples illustrating the preparation and use of the zinc borates.

Example 1

200 grams of $2ZnO \cdot 3B_2O_3 \cdot 3.5H_2O$ (0.46 mol) was added to 4.5 L of deionized water (DI) and boiled under reflux for six days. During this time the pH of the reaction solution gradually decreased from 7.8 to about 4.5. The reaction slurry was then filtered, washed with DI water and air dried to give 92.2 gr.(97% yield) of product, $4ZnO \cdot B_2O_3 \cdot H_2O$ having the analysis in Table 3.8:

Table 3.8 The analysis of $4ZnO \cdot B_2O_3 \cdot H_2O$ (Schubert, 1995)

	Calculated, %	Found, %
ZnO	78.79	78.35
B_2O_3	16.84	17.04
H_2O	4.36	4.88

Since slight variations in analyses can be expected, a typical composition of the hydrated zinc borate of this patent can be defined as 3.9-4.1(ZnO)·0.9-1.1(B_2O_3)·0.8-1.2(H_2O).

A portion of this filtrate was evaporated to dryness to give a crystalline solid which was identified as boric acid by its XRD pattern.

Example 2

A 5-L flask was charged with 100 gr. (0.23 mol) of the zinc borate $2ZnO·3B_2O_3·3.5H_2O$, 74.9 gr (0.92 mol) of ZnO, 7.2 gr.(17 mmol) of previously prepared seed product, and 2.0 L DI water. To this slurry was added 0.5 gr. Of $ZnCl_2$ (3.7 mmol). The mixture was boiled under reflux for six hours with mechanical stirring.

The reaction was then cooled, filtered, and the product air dried to give 146.4 gr.(98% yield) of $4ZnO·B_2O_3·H_2O$, identified by its XRD pattern.

Example 3

A 5-L round bottom flask was charged with 488.4 gr.of ZnO(6 mol) and 3.5 L of DI water. This slurry was brought to a boil and 28 gr.of previously prepared seed (0.07 mol) and 97.4 gr.of boric acid (1.58 mol) was added. After boiling this mixture under reflux with stirring for 2.5h, another portion of boric acid (97.4 gr., 1.58 mol) was added. After refluxing with stirring for another 2.5 h, the reaction mixture was cooled and filtered. The solid product was washed with DI water and air dried to give 629.2 gr (97% yield) of $4ZnO·B_2O_3·H_2O$.

Example 4

Sodium tetraborate pentahydrate (45.9 gr., 0.158 mol) was dissolved in 1.0 L of hot DI water in a 5-L flask. To this solution was added 43.1 gr. of $ZnSO_4·H_2O$ (0.15 mol) dissolved in 250 ml water. A white precipitate formed immediately. This mixture was brought to a boil and ZnO (85.5 gr., 1.05 mol) and 6.2 gr.of previously prepared seed (15 mmol) were added. The reaction mixture was boiled under reflux for six hours. The reaction was cooled, filtered, washed with water and air dried to give 137.2 gr. (97% yield) of $4ZnO·B_2O_3·H_2O$ containing some residual zinc oxide.

Zinc borate $4ZnO·B_2O_3$ can be prepared by the dehydration of the hydrate zinc borate $4ZnO·B_2O_3·H_2O$. The dehydration was readily accomplished by heating the

hydrated borate at a temperature above 415°C for a period of time sufficient to remove essentially all water. Generally heating at a temperature in the range of about 500°C to 550°C for about 3 to 5 hours will produce good yields of the desired $4ZnO \cdot B_2O_3$.

The zinc borate $4ZnO \cdot B_2O_3$ is non-hygroscopic and is resistant to rehydration even under high humidity conditions. This offers a significant advantage over many other anhydrous metal borate compounds which are often appreciably hygroscopic.

Example 5

A 50 gr.(0.12 mol) sample of the zinc borate hydrate of this patent was heated in a furnace at 500° - 550°C for about 4 hours. This resulted in a weight loss of 2.2 gr., corresponding to the loss of 0.12 mol of water.

To test for moisture reabsorption, a sample of the resulting anhydrous zinc borate was placed in an open container in a humidity chamber maintained at 90% relative humidity and 90°F for one month. After this time, a sample of this material was subjected to thermogravimetric analysis (TGA). Less than 0.1% weight loss was detected upon slowly heating the material over a period of about 2h from room temperature to 700°C, indicating that very little moisture was absorbed during prolonged storage under high humidity conditions. Furthermore, no significant weight loss was found when this material was heated continuously at 400°C (Schubert, 1995).

3.9.2 Patent by Igarashi

In a patent by Igarashi et.al. [2001] zinc borate having a particular crystallite size and containing very little sodium components and a method of preparing the same was studied. The zinc borate had a particular chemical composition, had a crystallite size of not smaller than 40 nm as found from diffraction peaks of indexes of planes of (020), (101), and (200) in the x-ray diffraction image (Cu-kα) and contains sodium components in amounts of not larger than 100 ppm as measured by the atomic absorptiometric method.

Example 1

An aqueous solution was prepared by dissolving 72.5 gr.of boric acid (B_2O_3 content 56%) in 1000 ml of pure water. To the aqueous solution were added 96 gr.of a zinc flower (ZnO content 99.4%) and 217.5 gr.of boric acid, and were stirred and mixed

together such that the molar ratio of B_2O_3/ZnO was 2.0. Next, the solution was stirred and reacted at 60°C for 90 minutes. The solution was further stirred and reacted at 90°C for 4 hours. The obtained product was filtered, washed with water and was then dried at 105°C to obtain a zinc borate. Table 3.10 shows the chemical composition and properties of the obtained zinc borate. Figure 3.5 shows the x-ray diffraction image of this study. Table 3.9 tabulates the x-ray diffraction of crystals that an intensity peak appears.

Table 3.9 X-ray diffraction of crystals that an intensity peak appears(Igarashi et.al., 2001).

2θ	**Spacing, A**	**Index of a plane**	**Relative Intensity,**
18.0	4.91	(020)	100
20.6	4.31	(101)	78.2
21.7	4.08	(120)	75.1
22.5	3.95	(111)	21.7
23.7	3.75	(121)	74.7
24.1	3.69	(200)	40.0
27.5	3.32	(121)	22.0
28.7	3.11	(012)	63.3

Example 2

An aqueous solution was prepared by dissolving 72.5 gr.of boric acid (B_2O_3 content 56%) in 1000 ml of pure water to which has been added 1.25 gr.of zinc borate ($2ZnO \cdot 3B_2O_3 \cdot 3.5H_2O$)as a seed in advance. To the aqueous solution were added 95.7 gr.of a zinc flower (ZnO content 99.4%) and 217.5 gr.of boric acid, and were stirred and mixed together such that the molar ratio of B_2O_3/ZnO was 2.0. Next, the solution was stirred and reacted at 60°C for 90 minutes. The solution was further stirred and reacted at 90°C for 4 hours. The obtained product was filtered, washed with water and was then dried at 105°C to obtain a zinc borate. Table 3.10 shows the chemical composition and properties of the obtained zinc borate. Figure 3.6 shows the x-ray diffraction image of this study.

Example 3

An aqueous solution was prepared by dissolving 72.5 gr.of boric acid (B_2O_3 content 56%) in 1000 ml of pure water. To the aqueous solution were added 95.7 gr.of a zinc flower (ZnO content 99.4%) and 217.5 gr.of boric acid, and were stirred and mixed together such that the molar ratio of B_2O_3/ZnO was 2.0. Next, the solution was stirred and reacted at 45°C for 120 minutes. The solution was further stirred and reacted at 90°C for 4 hours. The obtained product was filtered, washed with water and was then dried at 105°C to obtain a zinc borate. Table 3.10 shows the chemical composition and properties of the obtained zinc borate. Figure 3.7 shows the x-ray diffraction image of this study.

Example 4

An aqueous solution was prepared by dissolving 72.5 gr.of boric acid (B_2O_3 content 56%) in 1000 ml of pure water. To the aqueous solution were added 95.7 gr.of a zinc flower (ZnO content 99.4%) and 217.5 gr.of boric acid, and were stirred and mixed together such that the molar ratio of B_2O_3/ZnO was 2.0. Next, the solution was stirred and reacted at 60°C for 120 minutes. The solution was further stirred and reacted at 80°C for 8 hours. The obtained product was filtered, washed with water and was then dried at 105°C to obtain a zinc borate. Table 3.10 shows the chemical composition and properties of the obtained zinc borate. Figure 3.8 shows the x-ray diffraction image of this study.

Example 5

An aqueous solution was prepared by dissolving 72.5 gr.of boric acid (B_2O_3 content 56%) in 1000 ml of pure water. To the aqueous solution were added 95.7 gr.of a zinc flower (ZnO content 99.4%) and 217.5 gr.of boric acid, and were stirred and mixed together such that the molar ratio of B_2O_3/ZnO was 2.0. Next, the solution was stirred and reacted at 60°C for 120 minutes. The solution was further stirred and reacted at 85°C for 6 hours. The obtained product was filtered, washed with water and was then dried at 105°C to obtain a zinc borate. Table 3.10 shows the chemical composition and properties of the obtained zinc borate. Figure 3.9 shows the x-ray diffraction image of this study.

Example 6

An aqueous solution was prepared by dissolving 72.5 gr.of boric acid (B_2O_3 content 56%) in 1000 ml of pure water to which has been added 1.25 gr.of zinc borate ($2ZnO \cdot 3B_2O_3 \cdot 3.5H_2O$). To the aqueous solution were added 95.7 gr.of a zinc flower (ZnO content 99.4%) and 217.5 gr.of boric acid, and were stirred and mixed together such that the molar ratio of B_2O_3/ZnO was 2.0. Next, the solution was stirred and reacted at 65°C for 80 minutes. The solution was further stirred and reacted at 90°C for 4 hours. The obtained product was filtered, washed with water and was then dried at 105°C to obtain a zinc borate. Table 3.10 shows the chemical composition and properties of the obtained zinc borate. Figure 3.10 shows the x-ray diffraction image of this study.

Example 7

An aqueous solution was prepared by dissolving 72.5 gr.of boric acid (B_2O_3 content 56%) in 1000 ml of pure water. To the aqueous solution were added 95.7 gr.of a zinc flower (ZnO content 99.4%) and 217.5 gr.of boric acid, and were stirred and mixed together such that the molar ratio of B_2O_3/ZnO was 2.0. Next, the solution was stirred and reacted at 55°C for 120 minutes. The solution was further stirred and reacted at 75°C for 7 hours. The obtained product was filtered, washed with water and was then dried at 105°C to obtain a zinc borate. Table 3.10 shows the chemical composition and properties of the obtained zinc borate. Figure 3.11 shows the x-ray diffraction image of this study.

Example 8

An aqueous solution was prepared by dissolving 72.5 gr.of boric acid (B_2O_3 content 56%) in 1000 ml of pure water. To the aqueous solution were added 95.7 gr.of a zinc flower (ZnO content 99.4%) and 217.5 gr.of boric acid, and were stirred and mixed together such that the molar ratio of B_2O_3/ZnO was 2.0. Next, the solution was stirred and reacted at 60°C for 90 minutes. The solution was further stirred and reacted at 110°C for 4 hours. The obtained product was filtered, washed with water and was then dried at 105°C to obtain a zinc borate. Table 3.10 shows the chemical composition and properties of the obtained zinc borate. Figure 3.12 shows the x-ray diffraction image of this study.

Table 3.10 The chemical composition and properties of obtained zinc borate samples (Igarashi et.al., 2001).

	Ex.1	Ex.2	Ex.3	Ex.4	Ex.5	Ex.6	Ex.7	Ex.8
Seed	No	Yes	No	No	No	No	Yes	No
Synthesizing Temperature, °C(1^{st} step)	60	60	45	60	60	65	55	60
Synthesizing Temperature, °C(2^{nd} step)	90	90	90	80	85	90	75	110
Crystallite size (020), nm	67.6	90.0	78.9	89.2	92.6	73.5	63.3	82
Crystallite size (101), nm	64.1	59.1	60.0	42.0	71.0	40.3	46.1	56.3
Crystallite size (200), nm	64.5	73.5	70.7	78.3	82.2	86.1	88.0	76.1
Median diameter, μm	2.8	2.7	2.9	3.4	3.2	3.9	2.5	3.1
Na, ppm	15	20	18	16	16	15	19	16
Mole ratio (B_2O_3/ZnO)	1.49	1.50	1.47	1.49	1.48	1.49	1.46	1.51
Mole ratio (H_2O/ZnO)	1.60	1.61	1.63	1.62	1.63	1.61	1.65	1.61

Table 3.10 shows that for the heating temperature at 45 – 60ºC for the first and 75 – 110ºC for the second step the same product was obtained whether there is seed crystal or not. The product has nearly the same B_2O_3/ZnO ratio 1.47 – 1.51 and same water content H_2O/ZnO 1.60 – 1.65. The median diameter of the particles were in the range of 2.7 – 3.8 μm. Same X-ray powder diffractor diagram was obtained for all products obtained. The synthesis solution had B_2O_3/ZnO ratio of 2.0 and the product had B_2O_3/ZnO ratio of 1.47 – 1.51. Thus the mother liquor of the filtered zinc borate crystals showed unreacted boric acid and should have an acidic pH value.

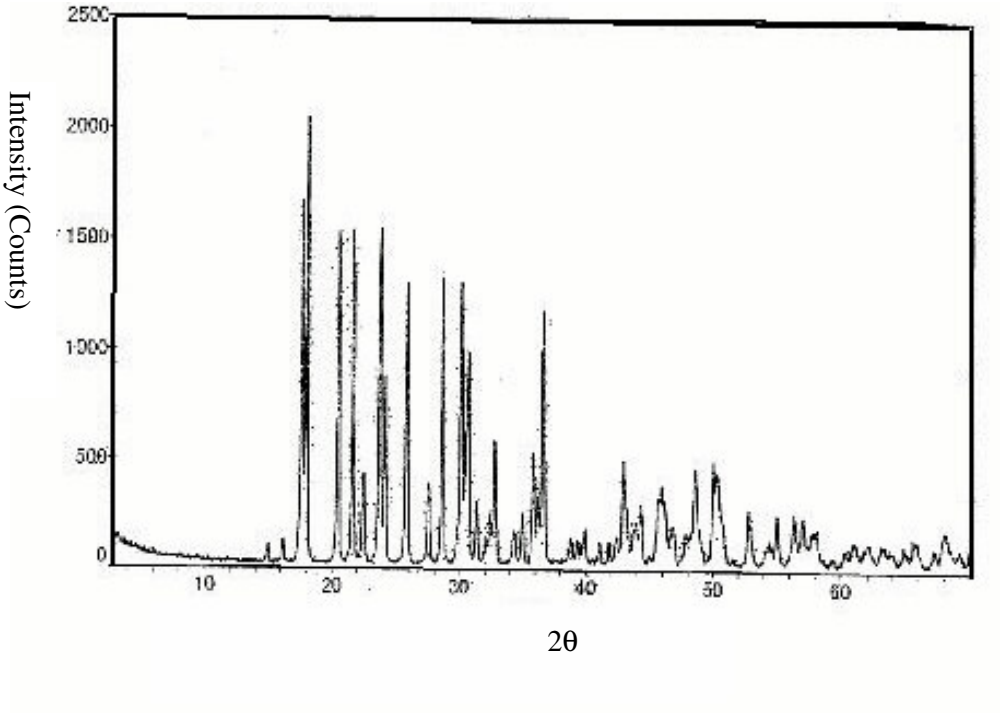

Figure 3.5 X-ray diffraction image of example 1(Igarashi et.al., 2001).

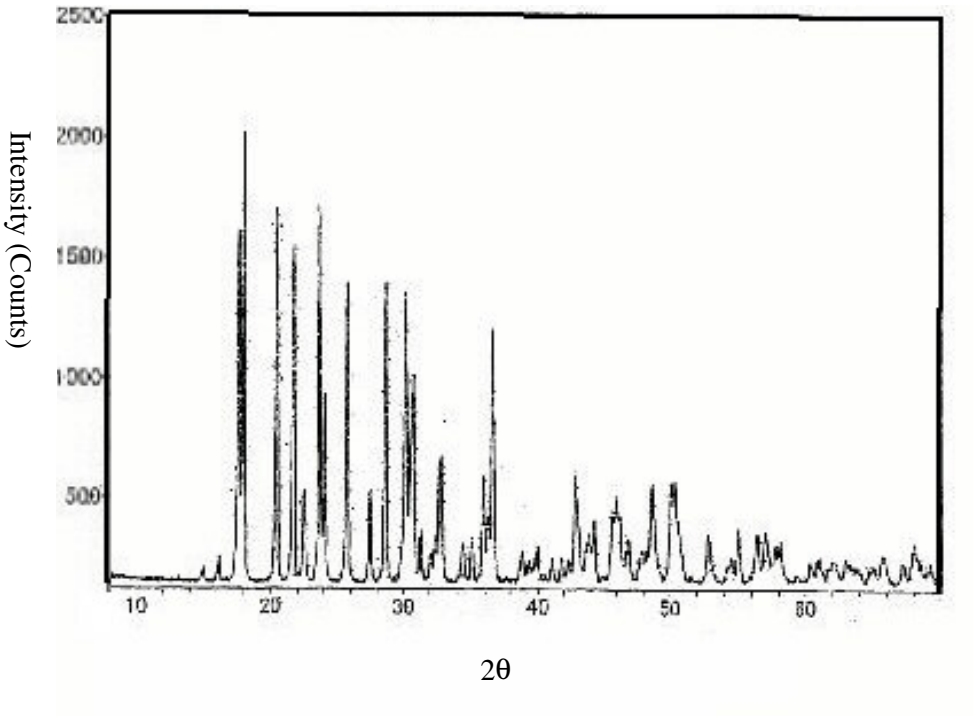

Figure 3.6 X-ray diffraction image of example 2(Igarashi et.al., 2001).

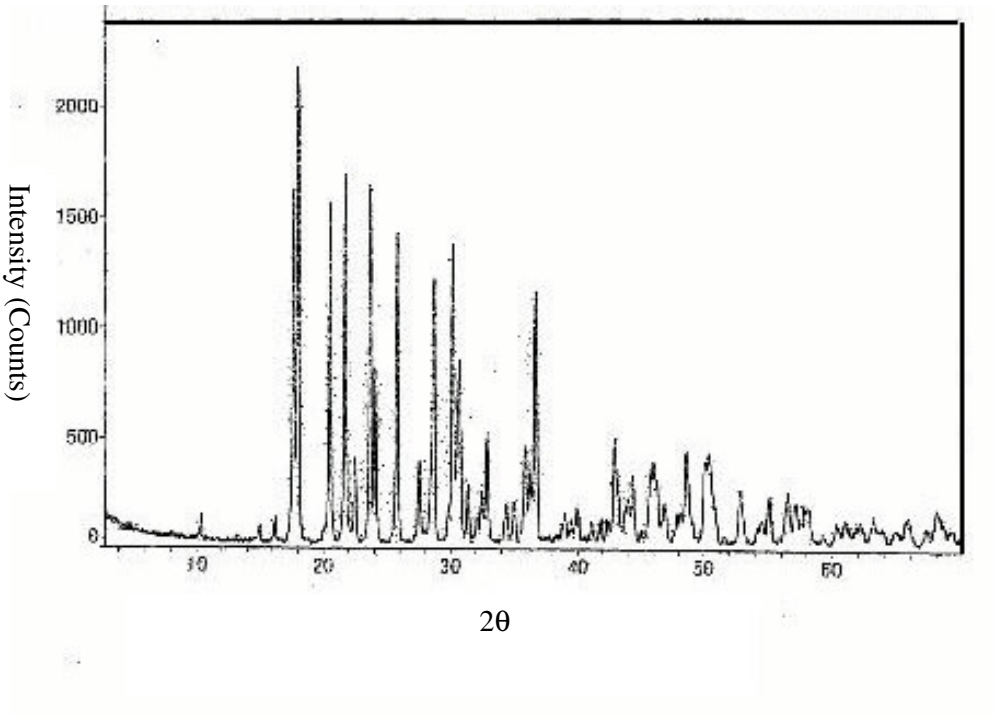

Figure 3.7 X-ray diffraction image of example 3(Igarashi et.al., 2001).

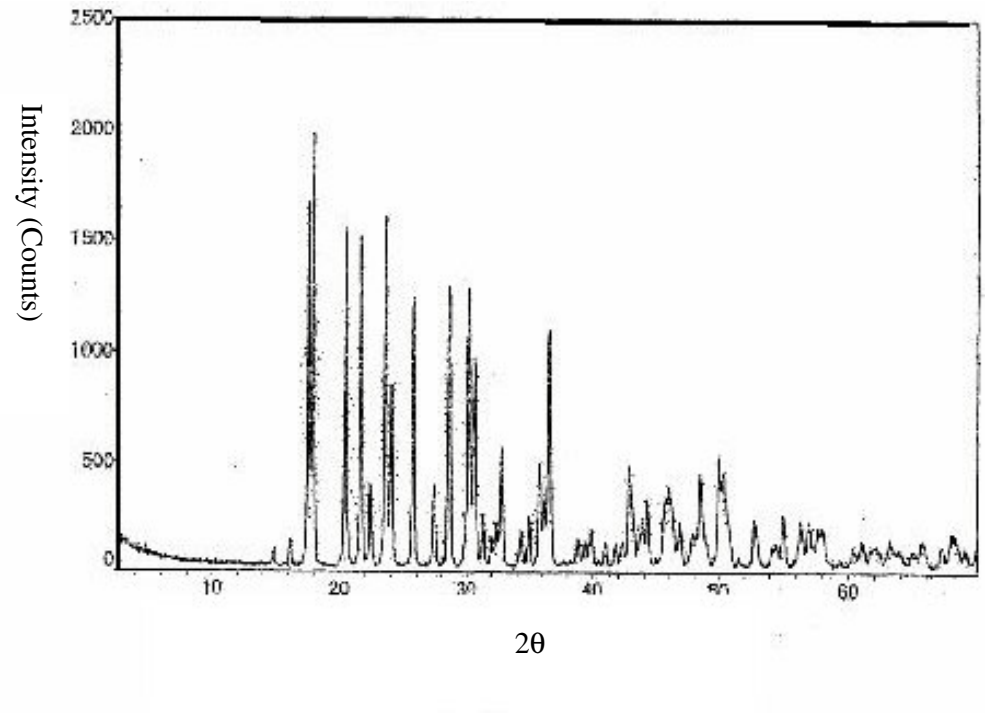

Figure 3.8 X-ray diffraction image of example 4(Igarashi et.al., 2001).

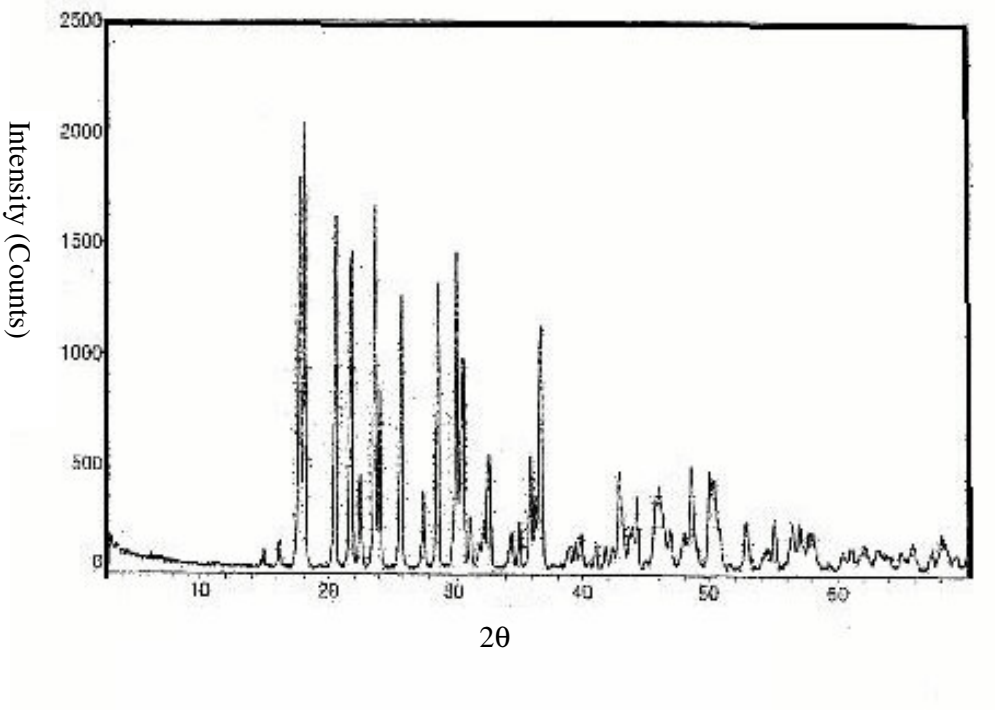

Figure 3.9 X-ray diffraction image of example 5(Igarashi et.al., 2001).

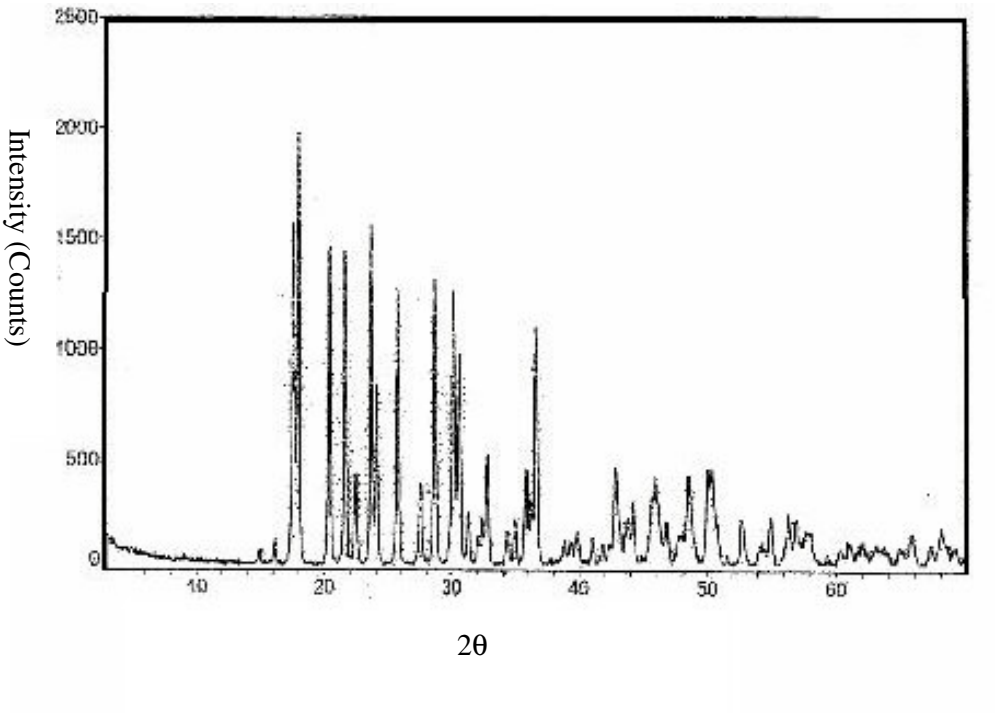

Figure 3.10 X-ray diffraction image of example 6(Igarashi et.al., 2001).

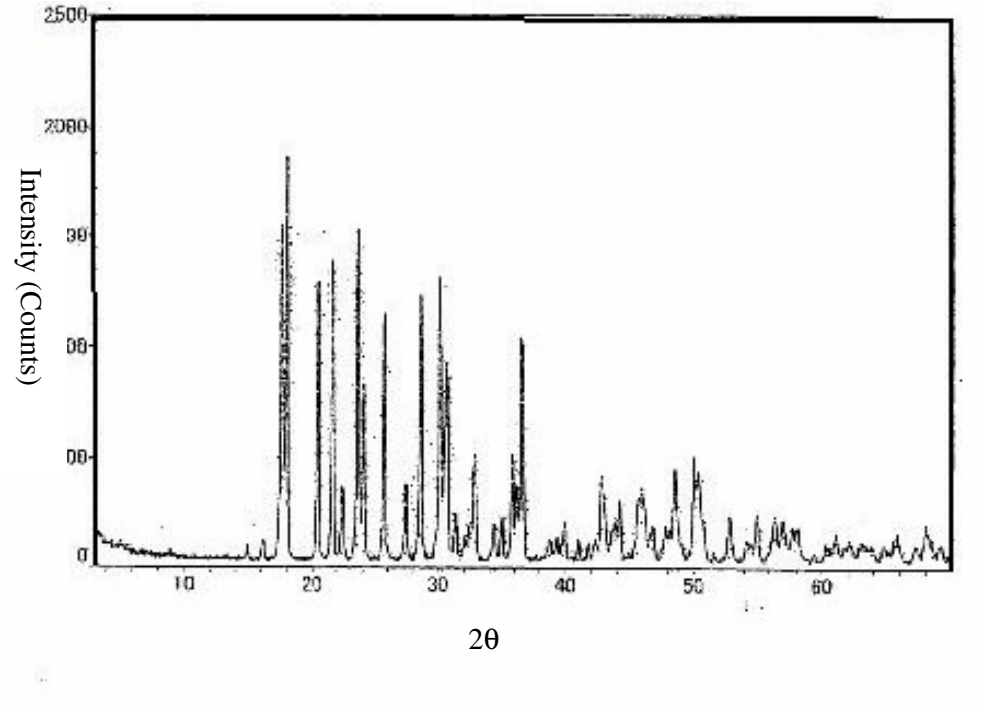

Figure 3.11 X-ray diffraction image of example 7(Igarashi et.al., 2001).

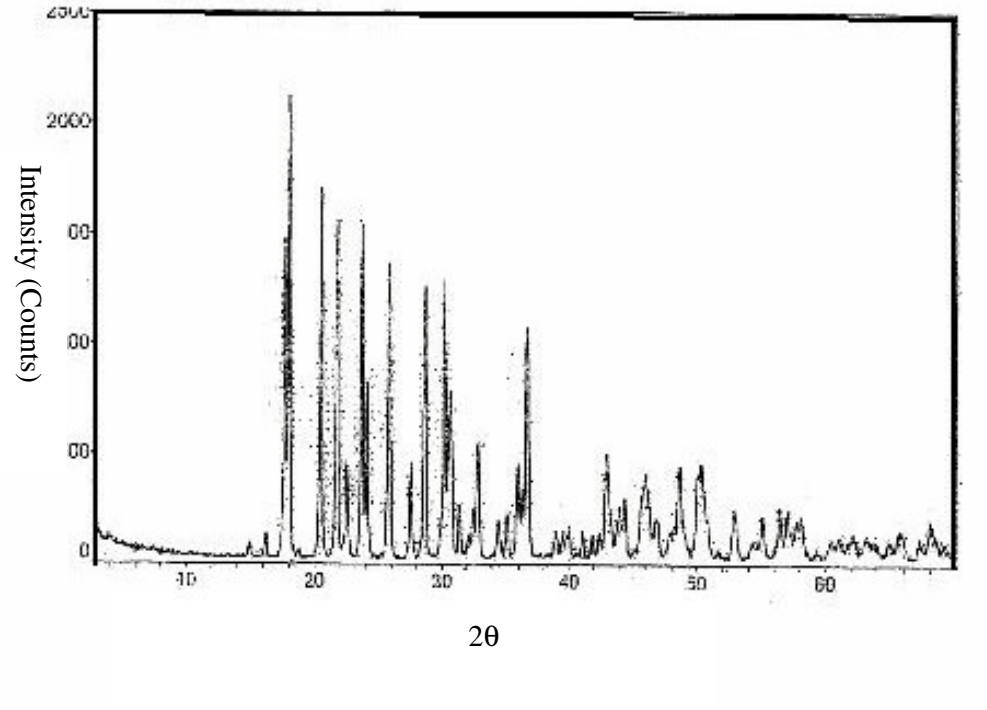

Figure 3.12 X-ray diffraction image of example 8(Igarashi et.al., 2001).

3.10 IR Studies

3.10.1 Infrared Spectra of Copolymer Having Zinc Borate

Xie et.al., [2001], have studied the dynamic thermo-oxidative degradation (TOD) of expandable graphite (EG)-based intumescent halogen-free flame retardant (HFFR) LLDPE blends in the condensed phase at 300 or 400°C by real time Fourier transform infrared spectroscopy. They were examined extensively for several LLDPE/EG blends with different additives such as the phosphorus-nitrogen compound, ammonium polyphosphate, red phosphorus and zinc borate.

Figure 3.13 (a) and Fig.3.13 (b) show the dynamic FTIR spectra from the thermo-oxidative degradation of LLDPE/EG/ZB blends at 300 and 400°C, respectively. The small peak at 3227 cm^{-1} and several peaks between 900 and 1300 cm^{-1} are characteristics of ZB additive. It can be seen that the intensities of several peaks between 900 – 1300 cm^{-1} decrease slowly with increasing TOD times which is due to the dehydration or breakdown of ZB on heating in temperature range of 300 – 400°C and the formation of boric acid to promote the formation of surface-expanded carbonaceous char structures between flame and polyolefins in the condition of a fire.

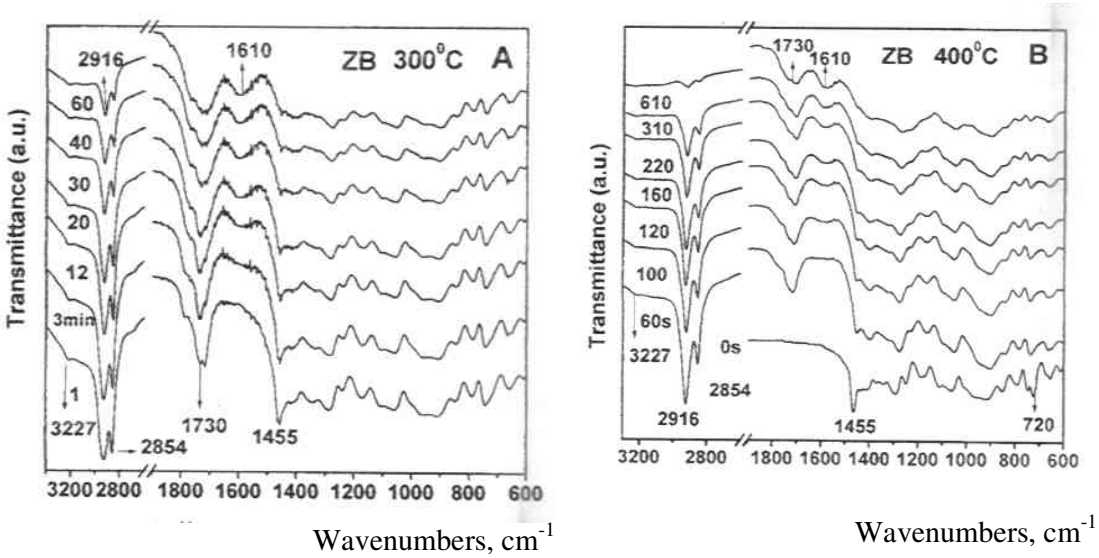

Fig.3.13 Changes of dynamic FTIR spectra obtained from the thermo-oxidative degradation of LLDPE/10% EG/20% ZB blends in the condensed phase with different pyrolysis times. (a): 300°C, (b) : 400°C(Xie et.al., 2001).

3.10.2 IR Spectra of Borate Anions

Yongzhong et.al.[1999] investigated the FTIR spectroscopy of supersaturated aqueous solutions of magnesium borate. Its acidized solutions with azeotropic hydrochoric acid and its diluted solutions with water have been recorded. The FTIR spectra of borate in solution are obtained by difference, subtracting the FTIR spectrum of water from that of magnesium borate supersaturated aqueous solution. All of the results showed that various polyborate anions in the supersaturated aqueous solutions exist. The bands of symmetric pulse vibration of the corresponding polyborate anions were indicated in this study. The observed frequencies of FTIR spectra of solid $MgB_6O_{10}\cdot 7H_2O$ are given in Table 3.11.

Table 3.11 The observed frequencies of FTIR and Raman spectra of $MgB_6O_{10}\cdot 7H_2O$ and its supersaturated aqueous solution (Yongzhong et.al., 1999)

FTIR	Assignment
1662 m	δ (H-O-H)
1423 w	ν_{as} ($B_{(3)}$-O)
1351 w	
1240 m	δ (B-O-H)
1098 w	ν_{as} ($B_{(4)}$-O)
1026 m	
957 s	ν_s ($B_{(3)}$-O)
898 m	
863 s	ν_s ($B_{(4)}$-O)
812 vs	
676 m	γ ($B_{(3)}$-O)
641 m	$\nu_p[B_6O_7(OH)_6]^{-2}$/ $\nu_p[B_3O_3(OH)_4]^-$
581 w	$\delta(B_{(3)}\text{-O})/\delta(B_{(4)}\text{-O})$
529 vw	$\delta(B_{(3)}\text{-O})/\delta(B_{(4)}\text{-O})$
436 w	$\delta(B_{(4)}\text{-O})$

m: middle, s: strong, v: very, w: weak. $B_{(3)}$-O means three coordinate boron, $B_{(4)}$-O means four coordinate boron.

3.11 Kinetics of zinc borate formation by the reaction of boric acid and zinc oxide

Shete et.al.[2003] have studied the kinetics of fluid – solid reaction of zinc borate by the reaction between zinc oxide and boric acid. Mixing parameters influencing the final particle size and conversion of zinc oxide were studied for the formation of zinc borate. The formation of zinc borate is via a fluid – solid reaction. The process was kinetically controlled above the minimum speed for particle suspension. The reaction kinetics was developed and the rate constant was estimated in this study.

Most precipitation reactions are homogeneous but for the particular reaction which was studied in this work, one of the reactants, boric acid, was in solution while the other reactant, zinc oxide, was in solid form. Therefore the reaction is homogeneous. Some assumptions were made, namely;

1. both zinc oxide particles and zinc borate particles were assumed to be spherical.
2. zinc oxide particles were assumed to be insoluble in water.
3. boric acid ions in boric acid solution react with zinc oxide particles on the surface of the latter.

The reaction studied in this work was a fluid – particle forming an insoluble reaction product. It has been suggested that an unreacted-core model applies in such circumstances. The successive steps visualized during the reaction have been described by Levenspiel, 1995.

Step 1: Diffusion of borate ions from the bulk phase of the boric acid solution to the surface of zinc oxide particles (physical).

Step 2: Penetration and diffusion of borate ions through the blanket of ash layer covering the unreacted core to the surface of the unreacted core of zinc oxide (physical).

Step 3: Reaction of borate ions with zinc oxide particles at reaction surface (chemical).

Step 4: Formation of zinc borate and diffusion of co-product water molecule through the ash layer covering the unreacted core back to the bulk phase (physical).

Step 5 (possibility): Peeling of zinc borate layer due to shear/collissions, etc.

The fluid – solid nature of the reaction makes it necessary to study the effect of mixing conditions on conversion of the zinc oxide along with the mean particle size of zinc borate.

To determine the effects of mixing, the following parameters were studied:

1. Speed of agitation.
2. Impeller type.
3. Mean particle size of zinc oxides.
4. Temperature.
5. Initial concentration of boric acid.

3.11.1 Effect of impeller type

Six – bladed pitched blade turbine down flow (PTD), impeller – disc turbine (DT) and three – bladed hydrofoil impellers (HF3) having a diameter 0.05m equal to one third of the vessel's diameter (0.15m) were used in this study. These were located 0.05m from the vessel bottom. The minimum suspension speed is an important parameter in fluid – solid reactions since only when all the particles are suspended will the entire particle surface be available for the reaction. Each impeller has a minimum suspension speed, N_s. For the conditions employed, the N_s values were 4.92 rev s^{-1} and 5.8 rev s^{-1} for PTD and DT, respectively. The minimum suspension speed was 10 rev s^{-1} for the HF3 which was measured experimentally by suspending particles in a non-reacting medium having the same physical properties.

Conversion of zinc oxide was higher for the DT impeller and lower for each of the PTD and HF3 impellers as shown in Fig.3.14(a). The effect of impeller type on mean particle sizes of zinc borate is shown in Fig.3.14(b). Mean particle sizes shown in the graphs are the values obtained at Ns. As seen from Fig.3.14(b), the HF3 impeller gave the lowest particle size.

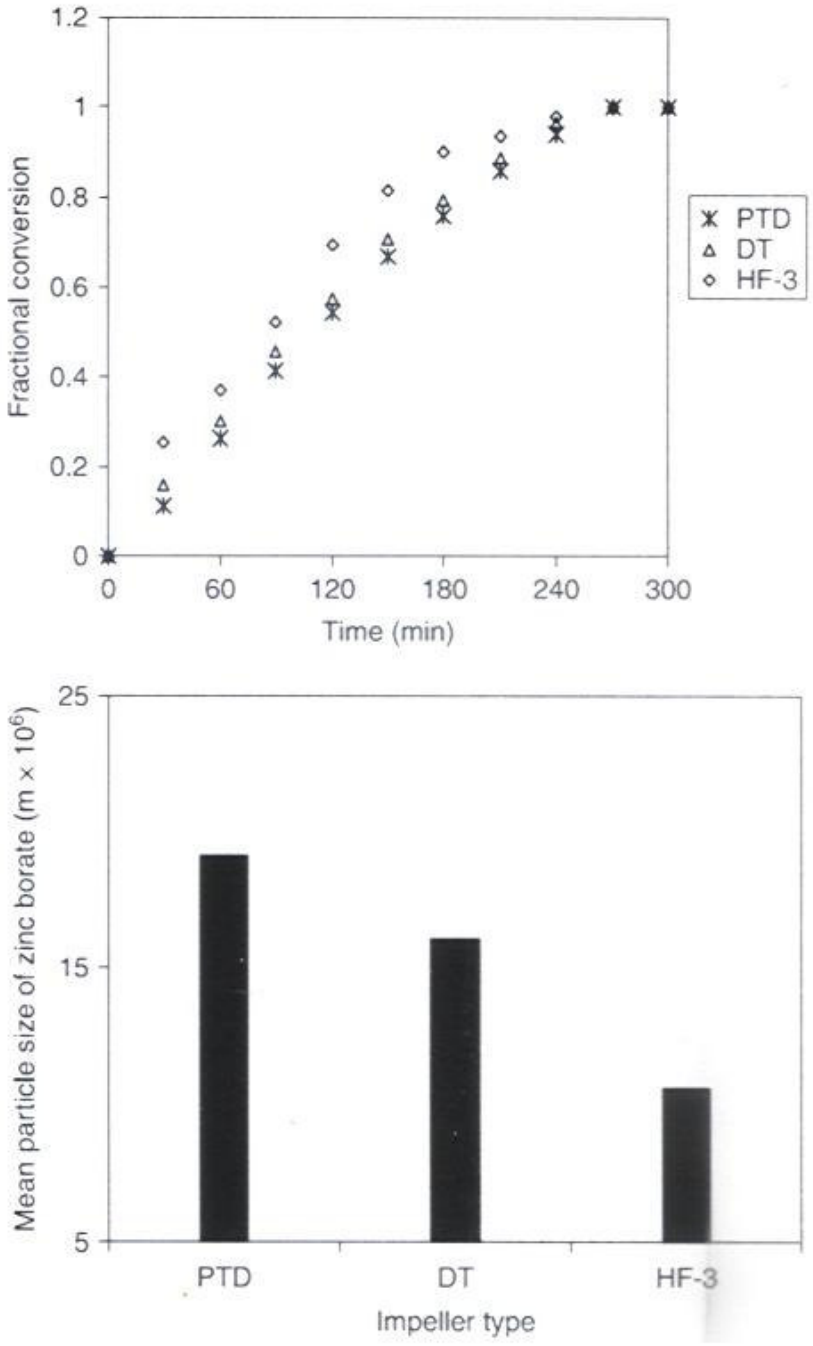

Figure 3.14. (a) Effect of impeller type on conversion of zinc oxide. Impeller DT, PTD and HF3. temperature of reaction 90C. concentration of boric acid – 3:1 mole ratio. Initial particle size of zinc oxide particles – 20.3µm. (b) Effect of impeller type on mean particle size of zinc borate. Impeller –DT, PTD, HF3. Temperature of reaction – 90C. Concentration of boric acid – 3:1 mole ratio. Initial particle size of zinc oxide particles – 20.3µm. (Shete et.al.,2003)

This was probably due to the higher absolute value of speed of agitation for the HF3 which caused significant secondary nucleation. Figure 3.15 shows a plot of the mean particle size against power input per unit mass, P/m, for the three different impellers used. Apparently there is no direct correlation between mean particle size and P/m. However, the HF3 impeller gave the lowest mean diameter when compared at the same P/m. A marginally higher speed than the minimum suspension speed gave 20% lower particle size and better conversion than that achieved at minimum suspension speed, while the particle size was higher and conversion was lower for speeds slightly lower than minimum suspension speed. Aeration effects were observed for some initial experiments carried out at very high speeds greater than the minimum suspension. The ratio of actual speed of rotation N to N_s is a significant operating parameter which defines the degree of suspension of the particles at the actual impeller speed with respect to the just-suspension condition at impeller speed N_s. the fraction of unsuspended solids was correlated uniquely with the ratio N/N_s. For $N/N_s < 1$, some particles were settled, while at $N/N_s > 1$ all particles were suspended. Therefore a value of $N/N_s \approx 1.2$ proved to be the desired condition of operation.

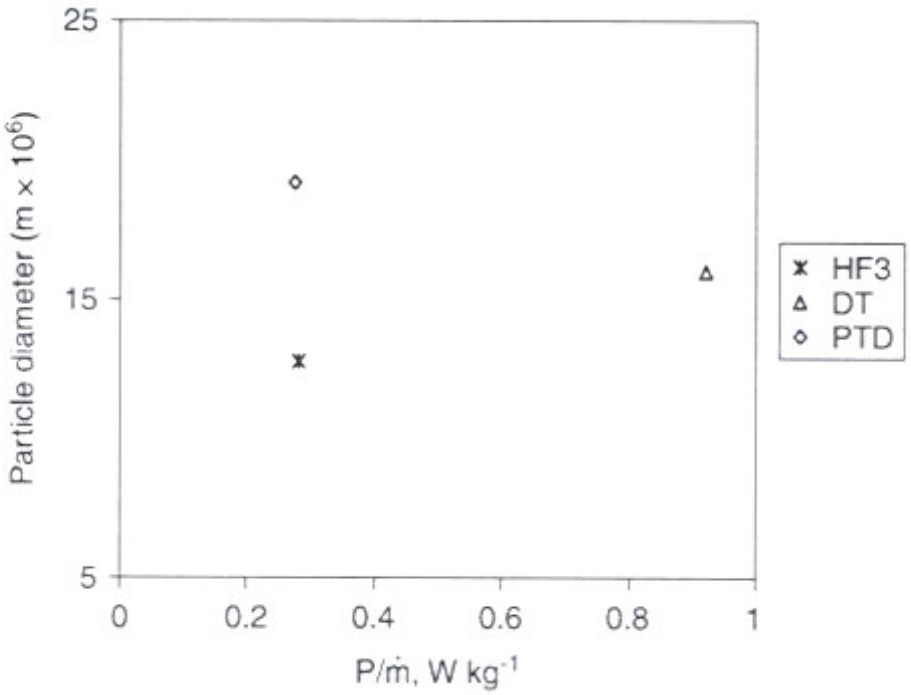

Figure 3.15. Plot of the mean particle size against P/m at $N/N_s = 1$ for three different impellers used. (Shete et.al.2003)

3.11.2 Effect of speed of agitation

To study the effect of speed of agitation on conversion of zinc oxide and mean particle size of zinc borate, the speed of agitation was varied for $0.83 < N/N_s > 1.2$. Typical results are shown in Fig.3.16(a). As the speed was increased conversion also increased. With increasing speed of agitation, the mass transfer of borate ions in solution to zinc oxide particles increased. Thus higher conversion was achieved with the increase in speed of agitation in a shorter time. It is evident that initially the conversion increased with speed of agitation ($N/N_s < 1$). However at higher speed ($N/N_s \geq$) the speed of agitation has no effect on conversion, indicating that the diffusional resistance is eliminated (Step 2).

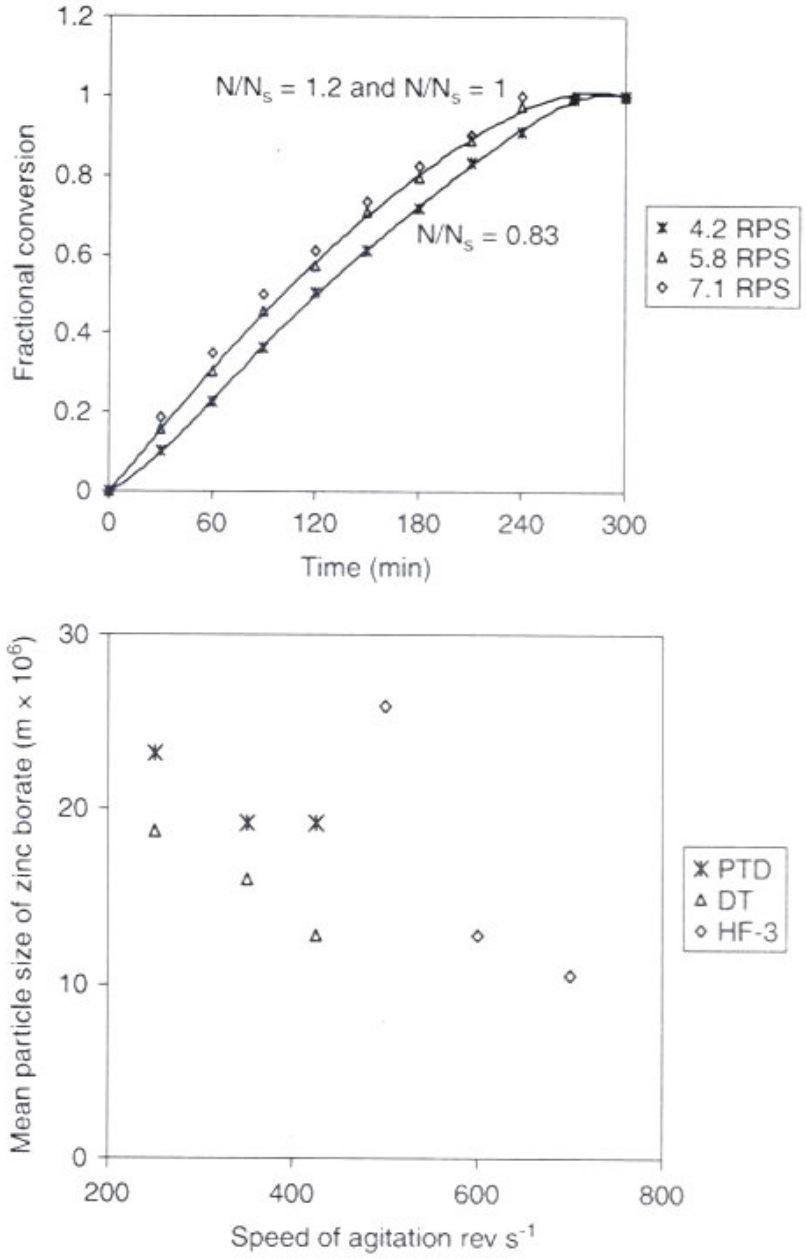

Figure 3.16. (a) Effect of impeller speed on conversion of zinc oxide. Impeller – HF3. Temperature of reaction 90ºC. Concentration of boric acid, 3:1 mole ratio. Initial particle size of zinc oxide particles, 20.3µm. (b) Effect of impeller speed on mean particle size of zinc borate for different impellers. Impeller, DT, PTD, HF3. Temperature of reaction, 90ºC. Concentration of boric acid, 3:1 mole ratio. Initial particle size of zinc oxide particles, 20.3 µm(Shete et.al.,2003).

Figure 3.14(b) shows the effect of speed of agitation on mean particle size of zinc borate. Mean particle size decreased with increase in speed as expected since the higher speed of agitation caused greater secondary nucleation due to higher strength and frequency of collisions.

3.11.3 Effect of mean initial particle size of zinc oxide

To study this effect, three different mean particle sizes of zinc oxide were used. These are 20.30 (50-100 μm), 26.29 (100-150 μm) and 26.98 (150-180 μm). The impeller used was the DT at N/N_s = 1. Figure 3.17(a) shows that the mean initial particle size affected the conversion of zinc oxide. The time needed for conversion of zinc oxide was longer with increase in mean particle size of zinc oxide. This is indication that the process is surface reaction controlled. The mean particle size of zinc borate was higher for higher mean initial particle size of zinc oxide, as shown in Fig.3.17 (b).

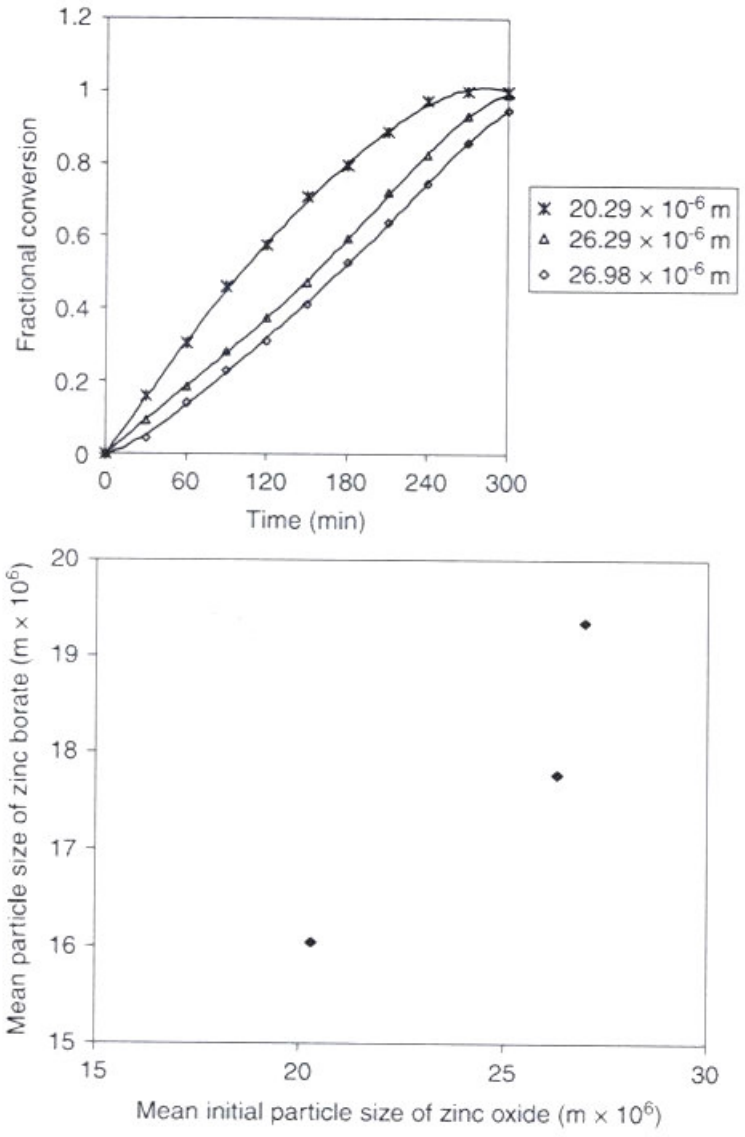

Figure 3.17. (a) Effect of mean initial particle size on conversion of zinc oxide. Impeller, DT. Temperature of reaction, 90ºC. Impeller speed, 5.8 rev s^{-1}. Concentration of boric acid, 3:1 mole ratio. (b) Effect of mean initial particle size of zinc oxide on particle size of zinc borate. Impeller, DT. Impeller speed, 5.8 rev s^{-1}. Temperature of reaction, 90ºC. Concentration of boric acid, 3:1 mole ratio(Shete et.al.,2003).

3.11.4 Effect of temperature of reaction

The temperature range selected was 90 to 110°C. The impeller used was the DT at $N/N_s = 1$. From Fig.3.18 (a), it is clear that with rise in temperature, the rate of reaction increased sharply. Complete conversion was achieved after 3.5 h at 110°C while the time needed for complete conversion at 90°C was 4.5 h. Figure 3.18(b) shows the effect of temperature on the mean particle size of zinc borate. There was an approximately linear decrease in particle size with increase in temperature.

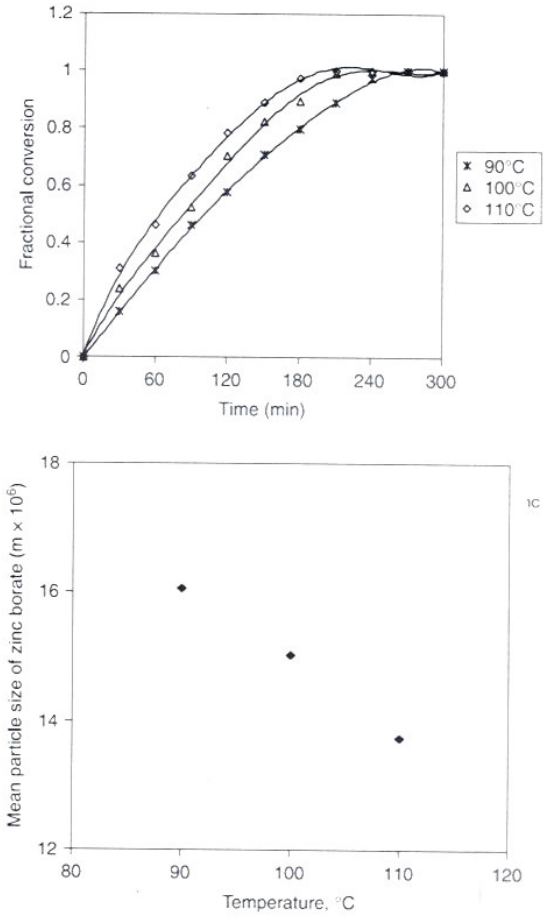

Figure 3.18. (a) Effect of temperature of reaction on conversion of zinc oxide. Impeller, DT. Impeller speed, 5.8 rev s^{-1}. Concentration of boric acid, 3:1 mole ratio. Initial particle size of zinc oxide particles, 20.3 μm. (b) Effect of temperature of reaction on mean particle size of zinc borate. Impeller, DT. Impeller speed, 5.8 rev s^{-1}. Concentration of boric acid, 3:1 mole ratio. Initial particle size of zinc oxide particles, 20.3 μm(Shete et.al.,2003).

3.11.5 Effect of concentration of boric acid

Three different boric acid to zinc oxide mole ratios were used, viz 3:1, 4:1, and 5:1. The impeller used was the DT at $N/N_s = 1$.

Figure 3.19(a) shows the variation of conversion with increase in concentration. When boric acid was added in an amount in excess of the stoichiometric quantity, there were more borate ions available to react with zinc oxide particles. Therefore, conversion of zinc oxide increased with increase in concentration of boric acid. Also, complete conversion was achieved in a shorter time.

Figure 3.19(b) gives a plot of the mean particle size of zinc borate against the concentration of boric acid. In this case, the reverse effect was observed for mean particle size. The size of zinc borate particles increased with increase in quantity of boric acid. This was because an additional quantity of boric acid forms a layer around the zinc borate particles.

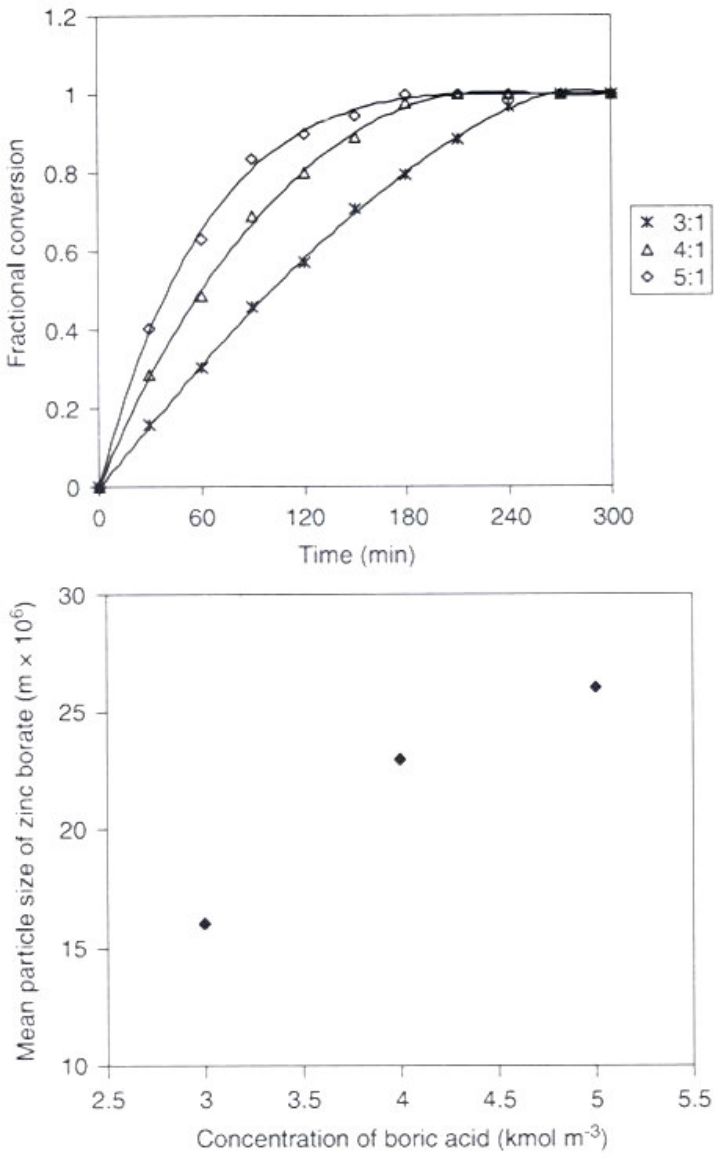

Figure 3.19 (a) Effect of concentration of boric acid on conversion of zinc oxide. Impeller, DT. Impeller speed, 5.8 rev s^{-1}. Temperature of reaction, 90ºC. Initial particle size of zinc oxide particles, 20.3 μm. (b) Effect of concentration of boric acid on men particle size of zinc borate. Impeller, DT. Impeller speed, 5.8 rev s^{-1}. Temperature of reaction, 90ºC. Initial particle size of zinc oxide particles, 20.3 μm(Shete et.al.,2003).

3.11.6 Reaction kinetics

For the particular reaction of formation of zinc borate, the majority of the experiments were conducted at the speeds having ratios of N/N_s greater than 1. Pangarkar et.al. have presented an exhaustive discussion on the particle – liquid mass transfer coefficient, k_{SL}, in two/three-phase stirred tank reactors. They concluded that for $N/N_s > 1$, k_{SL} is practically constant. Thus the effect of mass transfer rate of this particular reaction is negligible at $N/N_s > 1$.

The various kinetic expressions considered for fitting the experiments were:

1. Reaction between dissolved zinc oxide and boric acid. However, this possibility is very remote due to the very low solubility of zinc oxide in water.

2. First/second order surface reaction between boric acid and zinc oxide. However, the data showed a very poor fit for the second order surface reaction. The first order reaction kinetics on the other hand gave an excellent fit of the data, indicating that this represents the intrinsic kinetics of the surface reaction.

From Fig.3.20, it is seen that ln (rate of consumption of boric acid), ln r, is a linear function of 1/T. the slope of this line yields an activation energy value of 6.1×10^4 J mol^{-1} and is sufficiently high to ensure that the process is kinetically controlled. Thus, the controlling regime is likely to be the reaction between boric acid and zinc oxide on the surface of zinc oxide particles.

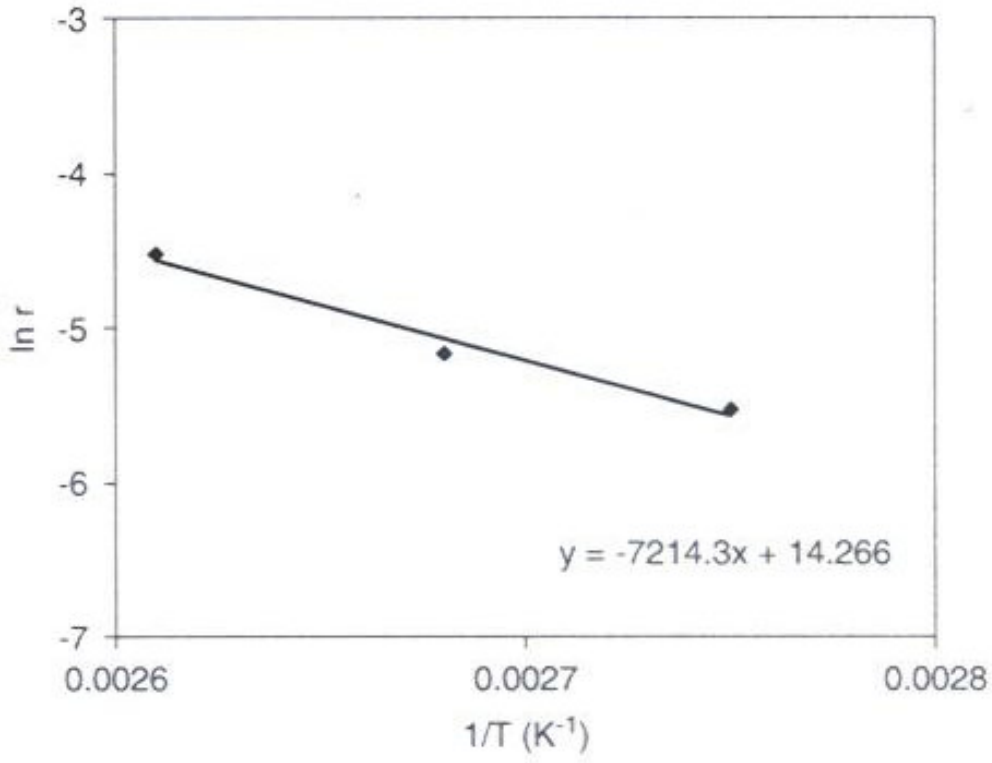

Figure 3.20. Plot of ln r vs 1/T for calculation of activation energy(Shete et.al.,2003).

3.11.7 Estimation of rate constant

The general rate expression for a first order surface reaction is:

$$\frac{dC_{Bt}}{dt} = k_r a_p c_{Bt} \qquad (3.1)$$

$$a_p = 6/d_{pt} \qquad (3.2)$$

where d_{pt} is diameter of zinc oxide particle at time t (which is an unknown quantity). This can be eliminated with the help of weight of zinc oxide and fractional conversion of zinc oxide.

The weight of zinc oxide is given by:

$$w = \frac{\pi}{6} d_{pt}^3 \rho N \qquad (3.3)$$

while the fractional conversion of zinc oxide in terms of weight of zinc oxide is:

$$x = \frac{weight\ of\ zinc\ oxide\ reacted}{initial\ weight} \tag{3.4}$$

$$x = \frac{\left(w_{in} - w_t\right)}{w_{in}} \tag{3.5}$$

This can be written in terms of the diameter of the particle of zinc oxide:

$$x = \frac{\left(d_{pin}^3 - d_{pt}^3\right)}{d_{pt}^3} \tag{3.6}$$

From eqn.4.6 the diameter of the particle of zinc oxide at time t is:

$$d_{pt} = d_{in}\left(1 - x\right)^3 \tag{3.7}$$

Substituting this value of d_{pt}, eqn.4.1 becomes:

$$\frac{dc_{Btc}}{dt} = k_r \frac{6}{d_{pt}\left(1 - x\right)^{1/3}} c_{Bt} \tag{3.8}$$

C_{Bt}, the concentration of boric acid at time t, can be written as:

$$c_{Bt} = c_{B0} - \frac{3\left(w_{in} - w_t\right)}{mv} \tag{3.9}$$

where m and v are molar mass and volume of the solution respectively. Also w_t, the remaining weight of zinc oxide at time t is:

$$w_t = w_{in}\left(1 - x\right) \tag{3.10}$$

Substituting w_t in eqn.3.9 gives:

$$c_{Bt} = c_{B0} - \frac{3\left(w_{in} - \left(1 - x\right)w_{in}\right)}{mv} \tag{3.11}$$

Therefore,

$$c_{Bt} = c_{B0} - \frac{3w_{in}x}{mv} \tag{3.12}$$

Substituting the value of c_{bt} in eqn 3.7:

$$\frac{dc_{Bt}}{dt} = k_r \frac{6}{d_{pt}} (1-x)^{-1/3} \left(c_{B0} - \frac{3w_{in}x}{mv} \right) \tag{3.13}$$

The above equation can be rearranged as:

$$\frac{dc_{Bt}}{dt} = k_p^{'} f(x) \tag{3.14}$$

where

$$k_r^{'} = k_r \frac{6}{dpt} \tag{3.15}$$

$$f(x) = (1-x)^{-1/3} \left(c_{B0} - \frac{3w_{in}x}{mv} \right) \tag{3.16}$$

In Eqn.3.14, the values of dc_{Bt}/dt and f(x) can be obtained from experimental data. Therefore, dc_{Bt}/dt was plotted against f(x). The straight line plot obtained further supported the assumption that the reaction is first order with respect to boric acid. The slope of this line gives the value of $k_r^{'}$. As the initial particle size of zinc oxide was a measure quantity, it was substituted in Eqn.3.15 and k_r was calculated. According to the first order surface reaction kinetic expression given by Eqn.3.1, the dimension of k_r are LT^{-1}. The value of rate constant for the experiments using DT is 3.83 x 10^{-5} cm s^{-1}.

The corresponding values of k_r for the PTD and HF3 are 2.7 x 10^{-5} cm s^{-1} and 1.61 x 10^{-5} cm s^{-1} respectively. The difference in the values is most likely due to variation in d_{pin}, dp_t and the the shape factor which vary with the type of the impeller. However, the differences are less than an order of magnitude and are explainable on the basis of different d_{pin}, dp_t and shape factors given above.

The effect of hydrodynamic and operating conditions was studied for the formation of zinc borate in a batch stirred reactor. From the results, it was observed that mixing parameters show an influence on the particle size of zinc borate. It was also observed that the rate controlling step is a surface reaction between dissolved boric acid and zinc oxide. To achieve rapid conversion and lower crystal size of the zinc borate, a speed marginally higher than the minimum suspension speed of the impeller should be

used. Also, higher temperatures and low mean initial particle size of zinc oxide beneficial in obtaining a lower final product size.

CHAPTER 4

EXPERIMENTAL

4.1 Materials Used

The boric acid used was supplied from ETİBANK with a molecular weight 61.83 and a molecular formula of B_2O_3. The general technical specifications are given in Table 4.1.

Table 4.1 The general technical specifications of boric acid.

Purity, % min.	99.9
B_2O_3, % min.	56.25
SO_4, ppm.max	130
Molecular weight	61.83
Specific gravity, g/cm³	1.435
Bulk density, g/cm³	0.8

The zinc oxide used throughout the experiments was supplied from Ege Kimya. Its general technical specifications are given in Table 4.2.

Table 4.2 The general technical specifications of zinc oxide.

Appearance	White, powder
Zinc oxide % min.	99
Loss on ignition at 105°C % max	0.1
Loss on calcination, % max.	0.2
Sieve residue on 325 mesh, % max.	0.05
Insoluble matter in acetic acid, % max.	0.05
Water soluble salts, % max.	0.05
Density, g/cm³ ± 0,1	5.56
Appearent density, g/lt	500 – 600

Commercial zinc borates called ZB-2335 and Chinese zinc borate were used in the experiments.

The general technical specifications of the commercial two zinc borates are tabulated in Tables 4.3 and 4.4.

Table 4.3 Commercial zinc borate ZB-2335.

Appearance	White amorphous powder
Volatile loss at 1h, 105°C, % max.	1.5
Bulk density, g/cm³	0.3 - 0.5
pH	7.0 –8.0
Sieve residue on 200 mesh, % max.	0.2
Ignition loss at 950°C, % max.	15.5
ZnO content, % min.	37
B_2O_3 content, % min.	47
Water of crystallization, % max.	16

Table 4.4 Commercial Chinese zinc borate.

Appearance	White powder
ZnO content, % min	37.5
B_2O_3 content, % min.	48
Ignition loss at 450°C, % max.	14.5
Free water at 105°C, % max.	1.0
Sieve residue on 325 mesh, % max.	1.0

4.2 Methods

4.2.1. Production of ZB

The synthesis of $2ZnO{\cdot}3B_2O_3{\cdot}3.5H_2O$ by following the US Patent by Igarashi (2001) was done. The amounts of the raw materials used in the experiments and their reaction conditions are reported in Table 4.5. Experiment No.1 and No.2 were carried in glass beaker seen Figure 4.1(a) and a glass flask under reflux was used for experiment 3. These experiments were carried out at Pigment Sanayi A.Ş. laboratories. Temperature control was done manually. In open beaker long heating times at 90ºC caused evaporation of water, thus a reflux condenser is attached to a glass flask for the third experiment.

For good temperature and agitation control thermostated shaking bath at Izmir Institute of Technology laboratories was used. An Erlenmeyer flask was used as the reactor. Experiment 4 and 5 were done in this system. Samples were taken at the end of 90 minute heating at 60ºC for experiment 4 and 5. They are called as experiment 4a and 5b.

The experiments were carried out by first dissolving the required amount of boric acid in a separate beaker in pure water. Since the solubility of boric acid at room temperature (20°C) is 5.04%, the solubility was achieved by heating the mixture to 60°C. After boric acid was completely dissolved in water, part of the solution was fed to the reactor.

Then zinc oxide and remaining portion of boric acid was added so that the molar ratio of B_2O_3 to ZnO is 2. This mixture was stirred for 90 minutes at this temperature. The same solution was further stirred and reacted at 90°C for 4 hours.

The upper limit for reaction temperature is boiling point of water (100°C) under atmospheric pressure. In the first three experiments, the agitation was achieved by using a magnetic lab stirrer (Velp Scientifica) having a speed around 200 to 250 rpm whereas in experiments 4 and 5 the mixing was achieved by shaking the flasks in a water bath at a rate of 170 rpm. Temperature control was monitored by water bath which is shown in Figure 4.2.

In experiment 3 different than experiments 1 and 2, seed crystals and reflux has been used as seen in Figure 4.2(a) and the experimental setup for the first two experiments is shown in Figure 4.2(b).

(a)

(b)

Figure 4.1 (a) The experimental setup for the first two experiments, (b) The experimental setup for the third experiment.

(a)

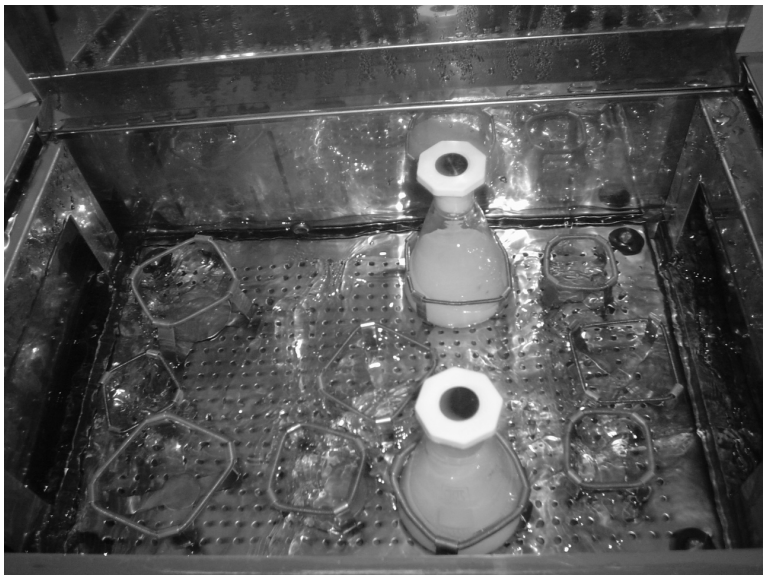

(b)

Fig.4.2 The water bath system (a) Exterior view, (b) Interior view.

In experiments 4 and 5, the flasks were sealed to achieve reflux effect. The only difference between two experiments is that experiment 4 has seed crystal where experiment 5 does not. The seed crystal was used to be able to observe its effect on the ZB yield.

The obtained product was filtered, washed with water and was then dried at 105°C in an oven to obtain zinc borate.

Two of the experiments contained seed crystals. The amounts of seed crystals, boric acid and zinc oxide are summarized in Table 4.5 for each experiment.

Minimum suspension speed depends on type of impeller. It was 4.92, 5.8 and 10 rev s^{-1} for six bladed, impeller – disc testing and three bladed impellers (Shete et.al., 2003). The rpm used in this thesis is 350 and 170 rpm corresponding to 5.8 rev/min and 2.8 rev/min close to minimum suspension speed of different types of impellers. While a magnetic stirrer was used at 350 rpm, an orbital shaking movement was done at 170 rpm.

The experimental conditions are given in Table 4.5.

Table 4.5 Conditions of experimental runs.

	Time, min	**T, ºC**	**H_2O, g**	**H_3BO_3,g 56% B2O3**	**ZnO,g**	**ZB seed crystal, g**	**Reflux**	**Reactor type**	**Reactor rpm**
Experiment No.1	90 240	60 90	1000	290	96	_	_	1	350
Experiment No.2	90 240	60 90	1000	144,7	48	_	_	1	350
Experiment No.3	90 240	60 90	500	145	47.85	0.625	+	1	350
Experiment No.4-a	90	60	100	29	9.6	0.125	+	2	170
Experiment No.4-b	90 240	60 90	100	29	9.6	0.125	+	2	170
Experiment No.5-a	90	60	100	29	9.6	_	+	2	170
Experiment No.5-b	90 240	60 90	100	29	9.6	_	+	2	170
Experiment No.6	90	60	500	21	6.97	-	-	1	630

4.3 Characterization

The physico-chemical properties of each sample were characterized by X-Ray diffraction, Fourier Transform Infrared Spectroscopy (FTIR), Scanning Electron Microscopy (SEM), Energy Dispersive X-ray (EDX) analysis and thermal gravimetric analysis (TGA).

X-Ray Diffraction: All of the samples were characterized by X-Ray diffractometer (Philips Xpert-Pro) to analyse the crystal structures of the ZB with CuKα radiation at 45 kV and 40 mA. The registrations were performed in the 5-60° 2θ range. FTIR Spectroscopy: To determine which functional groups are present in the samples, FT – IR instrument (the FT-IR 8601 by Shimadzou) was used. In the preparation of $ZnSt_2$ samples KBr disc method wad used. 4.0 mg of ZB weighed and 196 mg of KBr was added to it and mixed together. A pellet was obtained by pressing the powder under 8 tons of pressure. Scanning Electron Microscopy: Microstructural characterization of the samples was done by X-Ray energy spectrometer (the XL-305 FEG SEM instrument by Philips) for identification of particle size and product purity. Energy Dispersive X-ray (EDX): The samples were characterized by an Energy Dispersive X-ray (EDX) instrument (the XL-305 FEG SEM instrument by Philips) to investigate the elemental analyses of the samples. Thermal Gravimetric Analyses (TGA): Thermogravimetric analyses TGA utilized (Schimadzu TGA-51), ZB samples (10-15 mg) were loaded into an aluminum pan and heated from 30°C to 600°C at 10°C min^{-1} under N_2 flow (40 $ml.min^{-1}$). pH Measurement: pH of the experiments were measured by Methrohm pH-meter at different time periods at 25°C.

CHAPTER 5

RESULTS AND DISCUSSION

5.1 Characterization of Commercial Zinc Borate and Raw Materials

The Fourier Transform Infrared spectra of commercial ZB and raw materials are given between Figures 5.1 and 5.4.

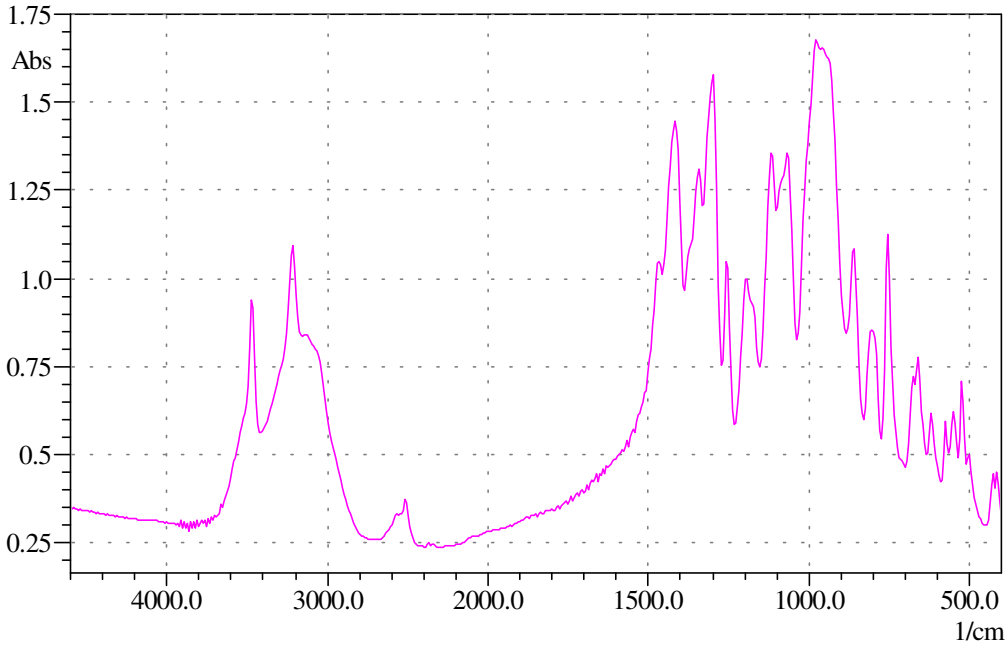

Fig.5.1 FTIR spectrum of ZB-2335.

The main characteristic peak of $ZnO{\cdot}B_2O_3$ at 3227 cm^{-1} is clearly seen in Figures 5.1 and 5.2. Both ZB samples had the same IR spectrum. Their peak values are tabulated in Table 5.1.

Table 5.1 The observed peaks of commercial ZB samples.

ZB 2335		Chinese ZB	
Wavenumber	Absorbance	Wavenumber	Absorbance
3460	0.94	3460	0.7
3210	1.1	3217	0.75
2510	0.37	2510	0.425
1415	1.45	1420	1.04
1300	1.58	1340	1.0
1255	1.05	1290	1.05
1195	1.0	1195	0.85
1120	1.35	1120	1.05
1070	1.35	1065	1.04
975	1.68	927	1.18
860	1.1	860	1.0
800	0.85	800	0.88
750	1.12	750	1.0
575	0.6	575	0.69
550	0.62	550	0.72
525	0.7	525	0.77

ZnO had a characteristic peak between 400 and 500 cm^{-1} as clearly observed in Fig.5.3.

In IR spectrum of boric acid which is seen in Fig.5.4. The following bands were observed at 3400, 1400, 1200 and 590 cm^{-1}.

TGA curve of ZB samples indicated they start to dehydrate at 350ºC. They lost 8 and 6% of their mass at 600ºC for ZB 2335 and Chinese ZB, respectively.

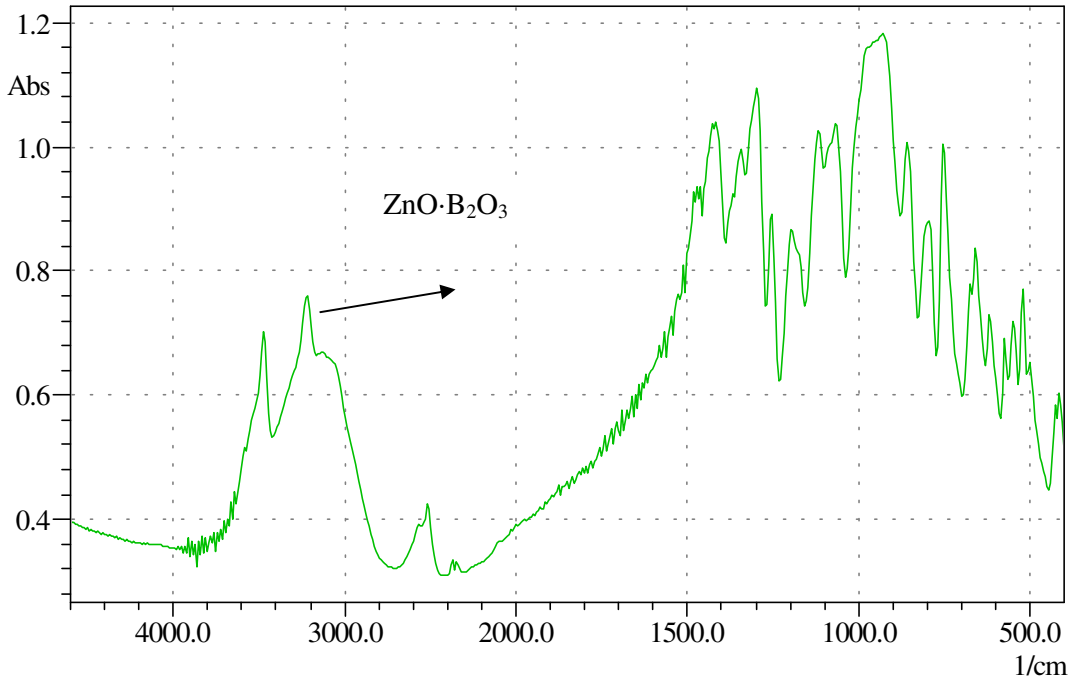

Fig.5.2 FTIR spectrum of Chinese ZB.

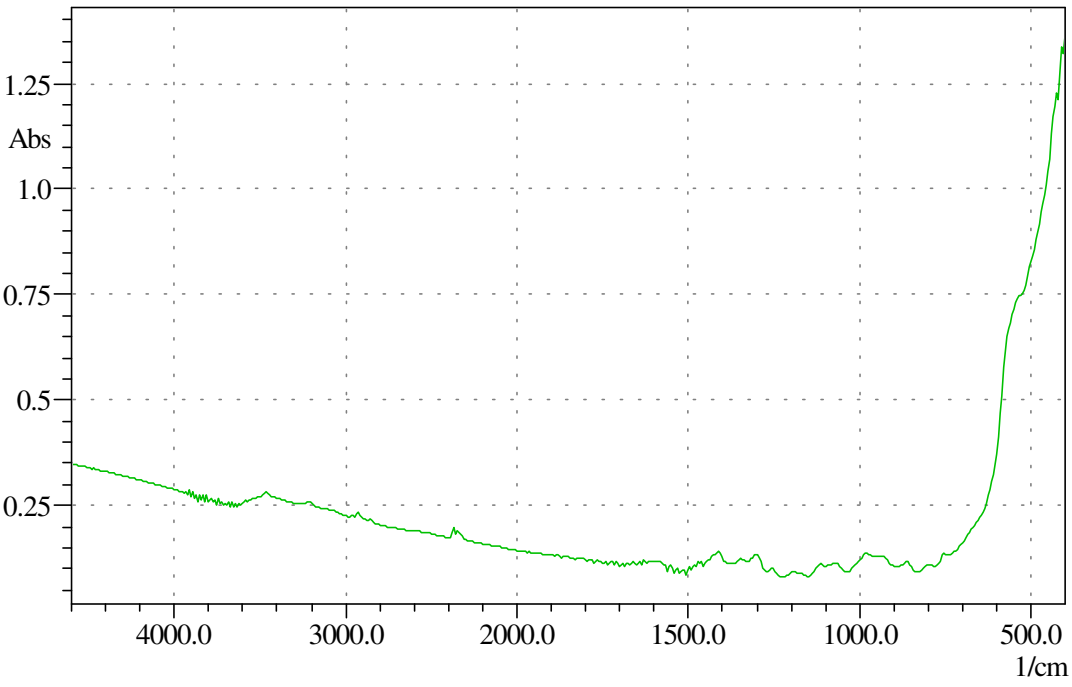

Fig.5.3 FTIR spectrum of Zinc oxide

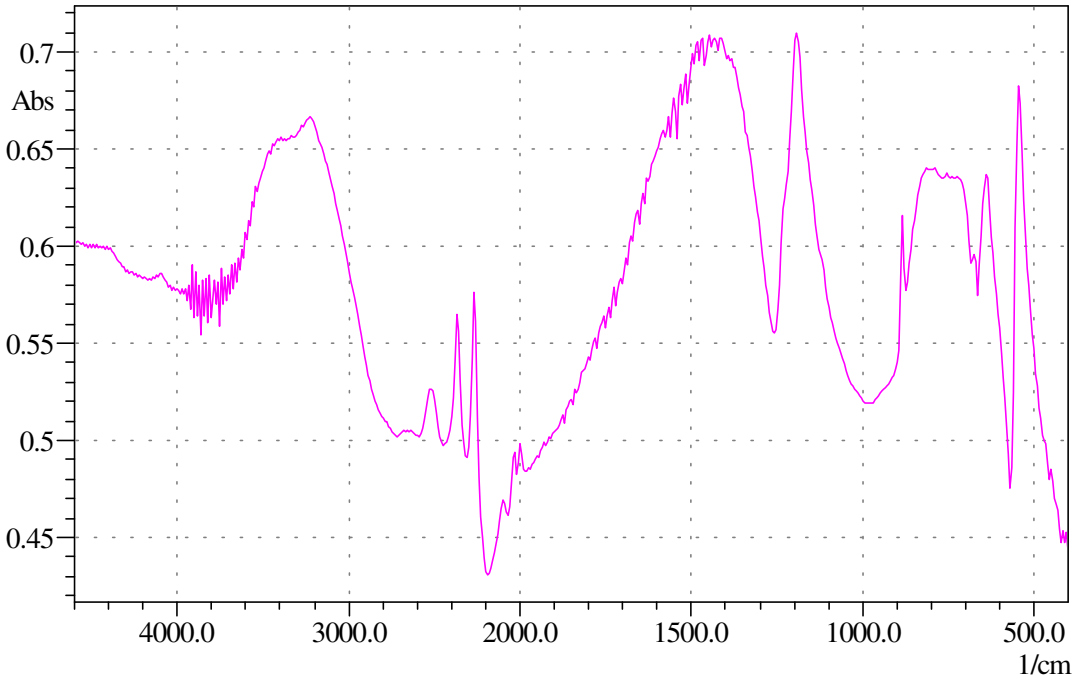

Fig.5.4 FTIR spectrum of boric acid

The thermogravimetrical analyses of the commercial ZB are also given in figure in Fig.5.5.

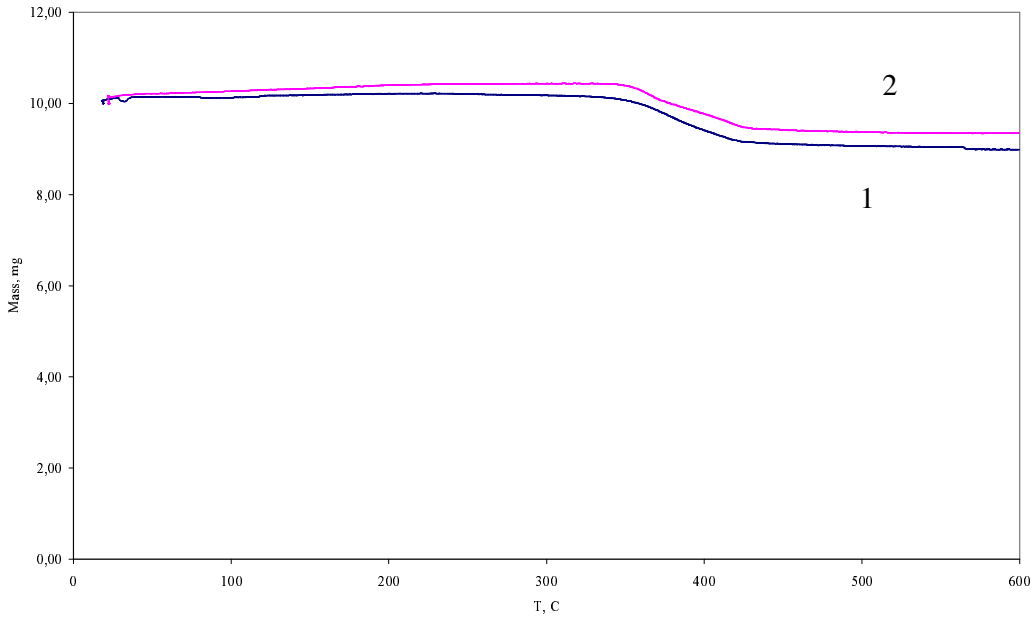

Fig.5.5 TGA curve of commercial ZB. (1:ZB-2335, 2:Chinese ZB).

TGA curves of both ZB samples indicated they were thermally stable up to 350ºC. ZB 2335 and Chinese ZB showed a mass loss of 6 and 8%, respectively starting from 350ºC and ending at 430ºC.

The SEM microphotographs of the commercial ZB and raw materials are also given in figures between Fig.5.6 (a), (b), (c) and (d).

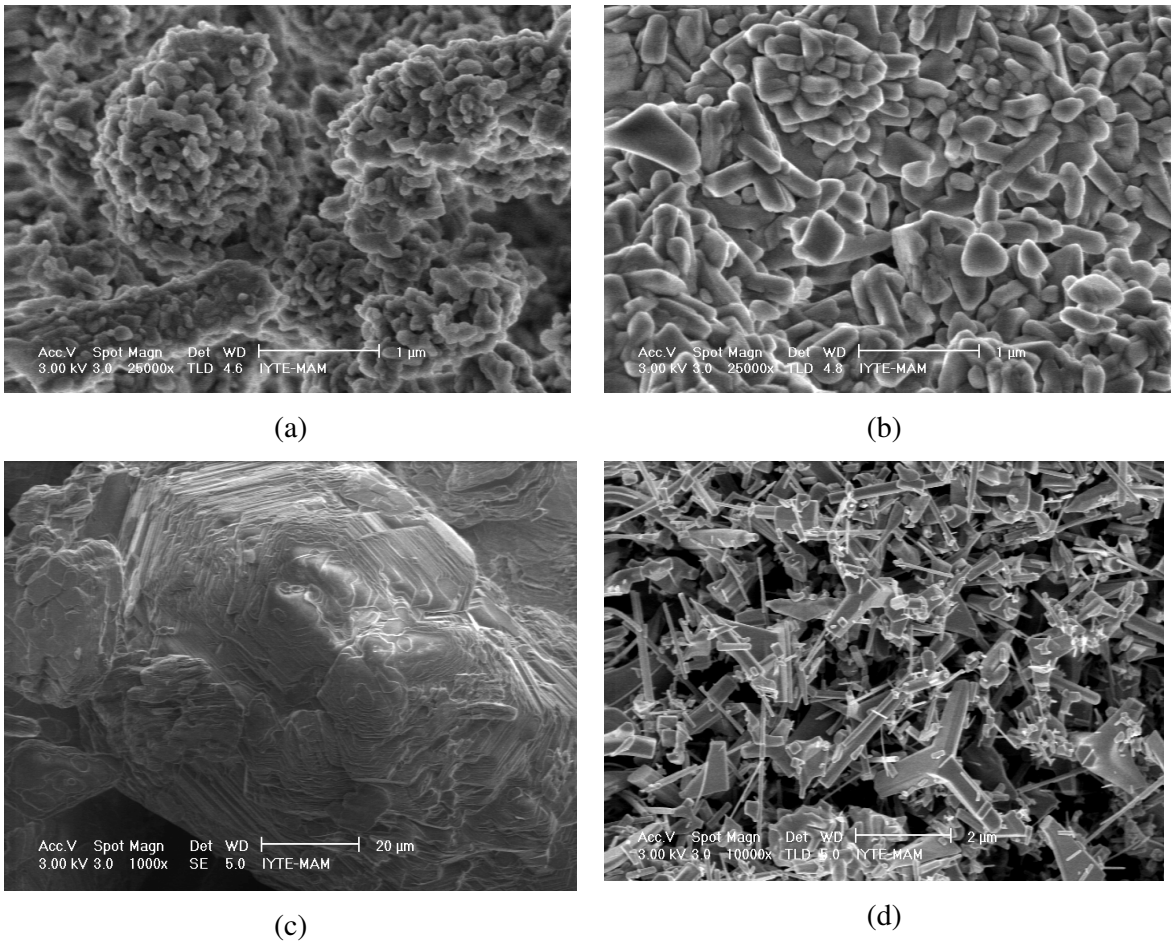

Fig.5.6 SEM microphotographs of commercial ZB and raw materials

(a) ZB-2335 (25000x), (b) Chinese ZB (25000x),

(c) Boric acid (1000x), (d) Zinc oxide (25000x).

Fig.5.6 (a) used as reference to check the success of the experiments in which the production was aimed. It is seen that the average particle size of the product is around 1 – 2 microns. The size of primary particles that are in the form as agglomerates is around 0.1 – 0.2 microns. Depending on how well the pigment is processed, the agglomerates will be dispersed and the pigment's effect will be proportionally increased with this dispersion management. Apart from a successful reaction this fine particle size could only be achieved by an advanced grinding operation. It is clearly seen that this pigment has been very successfully ground. If this pigment can be well dispersed in other words dispersed down to primary particle, outstanding results will be achieved during application in terms of fire retardancy and anticorrosion.

Fig.5.6 (b) shows that the average particle size of the product is around 0.2 – 0.6 micron and the particles are round shaped.

Table 5.2 Composition by EDX and Dehydration Temperature.

	B_2O_3/ZnO	**Dehydration Temperature, ºC**	**Dehydration % at 600ºC**	**Zn, %**	**B, %**	**O, %**
ZB 2335	1.21	350	8.0	33.3		41.5
Chinese ZB	2.48	350	6.0	30.4		37.9
ZnO	0.0	-	0.0	80.4	-	19.6

ZnO had 80.4% Zn close to its theoretical value of 80.5 ZnO as seen in Table 5.2.

Commercial ZB samples had B_2O_3/ZnO ratio different from theoretical value of 1.5. ZB product prosess which was reaction of boric acid and zinc oxide is a heterogeneous reaction which is first order with respect to boric acid concentration as shown by Shete et.al.[2003]. Rate of stirring, impeller type, particle size of zinc oxide are other variables that affect the rate of the process. The strong dependence of rate on temperature should it be controlled by chemical reaction step by Shete et.al.[2003].

On the other hand Igarashi et.al.[2001] prepared $2ZnO{\cdot}3B_2O_3{\cdot}3.5H_2O$ from boric acid and zinc oxide in two steps. The first step at 60ºC for 90 minutes zinc borate crystals form and in the second step 90ºC for 4 hours the crystal growth occurs. Schubert et.al.[2002] indicated formation of $2ZnO{\cdot}3B_2O_3{\cdot}7H_2O$ formed initially from ZnO and boric acid it is transformed to $2ZnO{\cdot}3B_2O_3{\cdot}3H_2O$ by slow polymerization of borate ion in solid state.

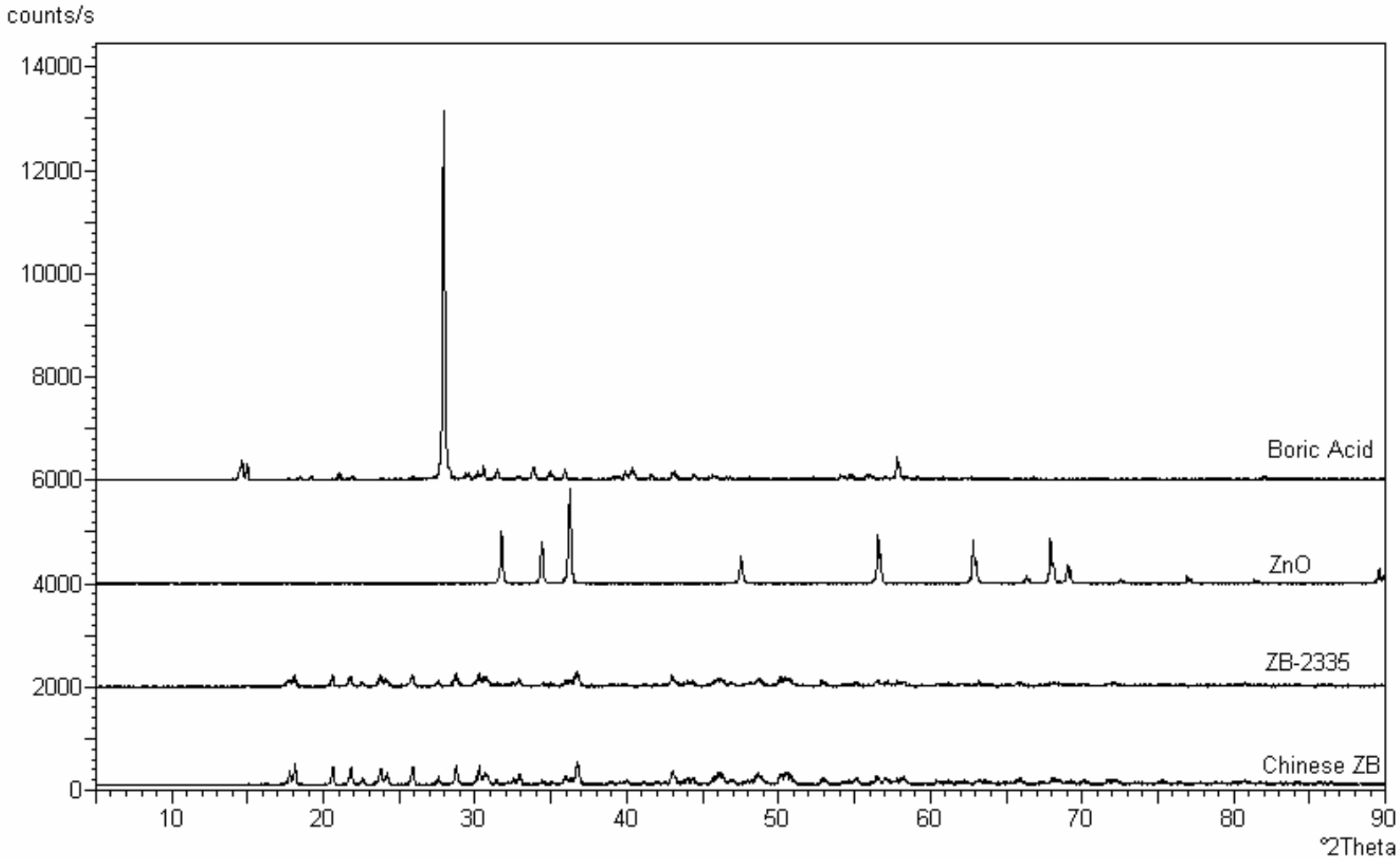

Fig.5.7 The X-ray diagram of the raw materials and reference materials (ZB 223 and ZB stands for another commercial ZB).

In Fig.5.7, X-ray diffraction diagram of boric acid, ZnO and three commercial ZB samples are seen. The X-ray diagram of boric acid and ZnO confirmed they were pure boric acid and ZnO.

5.1.1 The Viscosity and pH Change During ZB Production

The specific gravity of ZnO and $2ZnO\cdot 3B_2O_3\cdot 3H_2O$ are 5.3 and 2.77 g/cm^3 respectively. In patent by Igarashi et.al.[2001] one liter water contained 240 gr.boric acid and 96 gr.ZnO while boric acid present in dissolved form ZnO is a solid. The B_2O_3/ZnO ratio was 2.0 but in the product B_2O_3/ZnO was 1.5.

The mass of the solid fraction increases from 96 gr.to 313.5g.causing the viscosity of the mixture to increase. In the present study in applying Igarashi et.al.'s patent had difficulties of mixing the product and water loss by evaporation at long heating periods. The viscosity of suspension,

$$\eta = \eta_s \left(1 + k_E \phi\right) \tag{5.1}$$

where η is viscosity of suspension, η_s is the viscosity of the solvent, k_E is 2.5 for spherical particles and ϕ volume fraction of dispersed solid phase.

$$\rho_{ZnO} = 5.56$$
$$\rho_{ZB} = 2.7$$
$$5.56 = \frac{96}{V_{ZnO}} \rightarrow V_{ZnO} = 17.3\,cm^3$$
$$\phi_{ZnO} = \frac{17.3}{1000} = 0.017$$
$$2.7 = \frac{314}{V_{ZnO}} \rightarrow V_{ZnO} = 116\,cm^3$$
$$\phi_{ZnO} = \frac{117}{1000} = 0.116$$
$$\left(\frac{\eta}{\eta_s}\right)_{ZnO} = 1 + 2.5x0.017 = 1.04$$
$$\left(\frac{\eta}{\eta_s}\right)_{ZB} = 1 + 2.5x0.116 = 1.29$$
$$\frac{1.29}{1.04} = 1.24$$

The relative viscosity will increase to at least 1.24 times thus a mechanical mixer which will stir the mixture even when the viscosity is high should be used.

An additional experiment was performed (as experiment 6) to follow the pH change during reaction at 60°C. The pH of boric acid solution in the beginning is 4.3. The pH of

boric acid solution and pH of the mixture after ZnO was added was measured at different time periods by using Methrom pH-meter with a glass electrode. The results are tabulated in Table 5.3.

Table 5.3 pH change of experiment 6 at 60ºC.

Time, s	0	10	30	60	120	180	240	360	420
pH	4.30	5.33	5.63	5.68	5.70	5.72	5.72	5.72	5.72

Since an excess of boric acid was used in the patent of Igarashi, the solution pH is expected to be acidic. In the experimental run to follow pH change during reaction it was found that pH of boric acid solution was 4.3 and there was a step change to 5.33 in 10 sec., after ZnO was added as seen in Table 5.3. pH was stabilized at 5.72 after 180 s. Thus, during preparation of ZB, pH was lower than pH of 7 and reaction medium was acidic as expected.

This experiment shows that the formation of ZB occurs instantly after the addition of ZnO to boric acid as there was a step change to pH 5.33 in 10 sec. However the formed product is not the desired crystal modification of ZB. It is probably a form which contains 10 hydrate water. By looking at figures of FTIR, X-ray, TGA and SEM it is obvious that the desired form of ZB is not formed at 60ºC for 90 min. The further mixing of ZnO and boric acid at 90ºC for 4 hours under reflux, results in a ZB formation which has the desired chemical formula thus the desired dehydration temperature.

5.2 Characterization of Synthesized Zinc Borate

5.2.1 Thermogravimetric Analyses

To have an idea about the thermal behaviour of the ZB samples, TGA instrument used to carry out the investigations which is a good way in studying dehydration of water in the zinc borate.

TGA curves of Experiments 1, 2 and 3 are given in Figure 5.8. In Experiment No.1 ZB starts to lose its crystal water at 109°C and then at 145°C and finally at 225°C with a total mass loss of 20.63% and in Experiment No.2, ZB starts to lose its crystal water beginning from 133°C and 186°C with a total mass loss of 6.51% and in Experiment No.3 ZB starts to give its hydration water first at 355°C and then it goes on until at 445°C with a total mass loss of 9.65% which is a desired result for a ZB which can be used commercially as a flame retardant pigment.

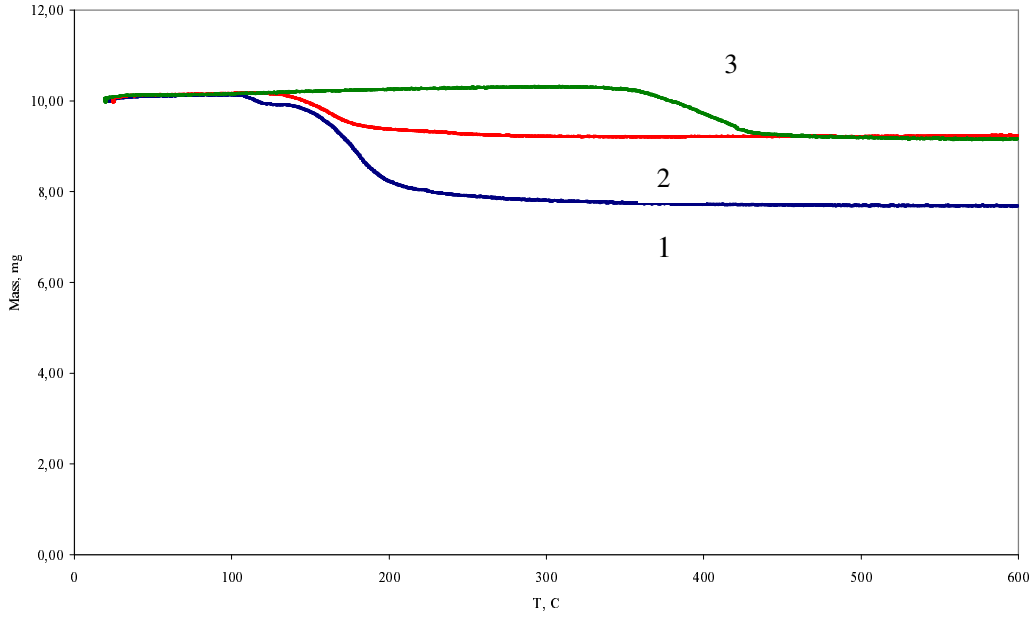

Fig.5.8 TGA curve of Experiment No.1, No.2 and No.3

TGA curves of Experiment Nos.4 and 5 at 60°C and 1.5h are given in Figure 5.9. In Experiment No.4 at 60°C, 1.5h ZB starts to lose its hydration water at 130°C until 403°C with a mass loss of 19.05% and in Experiment No.5 at 60°C, 1.5h ZB starts at 131°C until 403°C with a mass loss of 25%.When these two samples are compared it is observed that the one with seed crystals have a less mass loss which shows less degradation of the compound which can be said to be a better flame retardant.

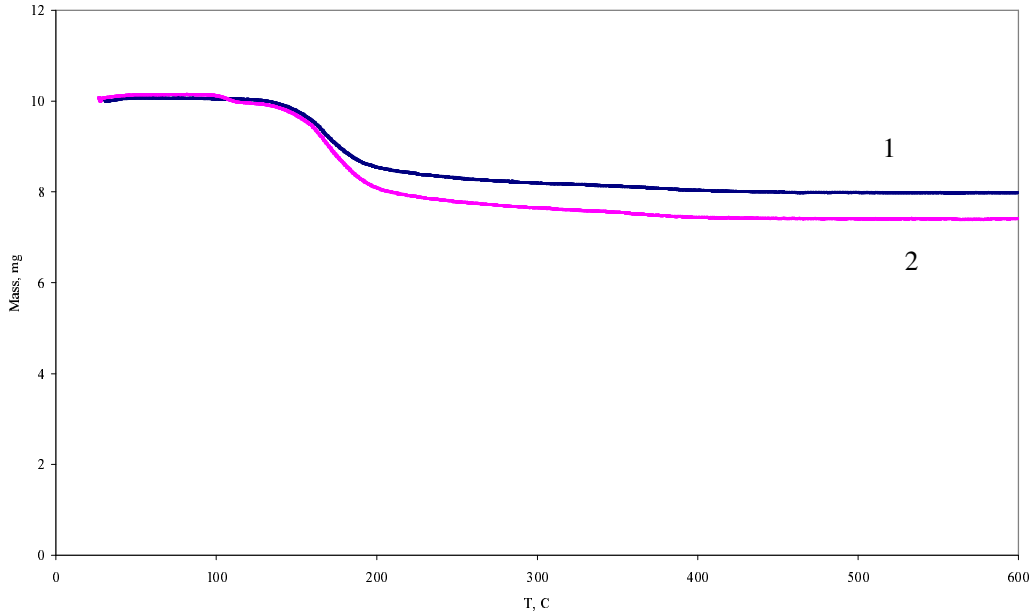

Fig.5.9 TGA curves 1:Experiment No.4 at 60ºC, 1.5h, 2:Experiment No.5 at 60ºC, 1.5h.

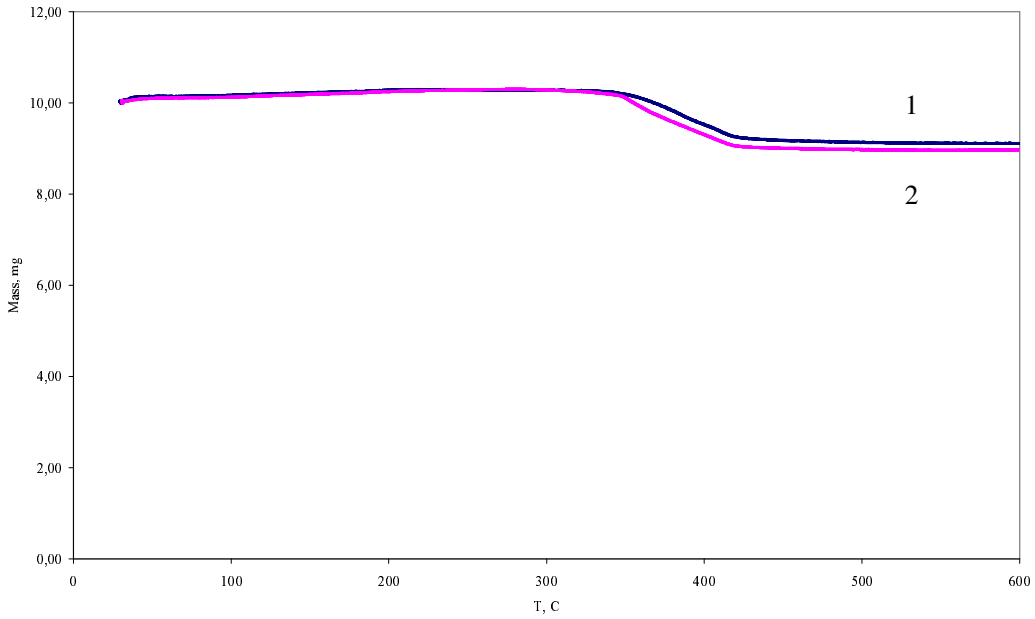

Fig.5.10 The effect of seed crystal on product formed at 90ºC, 4h. 1:Experiment No.4 (with seed crystal), 2:Experiment No.5 without seed crystal (without seed crystal. They were heated at 60º C for 90 minutes initially).

In Figure 5.10, the TGA curves of the Experiment Nos.4 and 5 at 90º C, 4h. are shown. In Experiments 4 and 5, ZB starts to lose its crystal water at 340º C at both

experiments until 439°C and 426°C with total mass losses of 9.72% and 11.38%, respectively. Again Experiment No.4 gave a less mass loss which is an advantage.

Dehydration results and molar results according to the experiments carried out were tabulated in Table 5.4.

Table 5.4 Dehydration results of the experiments

	H_2O loss at 600 °C %	**Dehydration Temperature, °C**	**B_2O_3/ZnO (Molar ratio)**
Experiment No.1	24	110 and 130	1.74
Experiment No.2	8.1	130	0.085
Experiment No.3	10	350	1.27
Experiment No.4-a	21	140	1.49
Experiment No.4-b	10	350	1.40
Experiment No.5-a	27.25	100 and 140	1.78
Experiment No.5-b	12	340	1.68

If $2ZnO \cdot 3B_2O_3 \cdot 3.5H_2O$ were obtained, mass loss should be 14.9%. Experiment No.5 which has a closer mass loss (12%) contained a product closer to $2ZnO \cdot 3B_2O_3 \cdot 3.5H_2O$ than experiment No.4b.

5.2.2 Scanning Electron Microphotographs

Experiment No.1. When compared with the SEM photographs of commercial ZB and raw materials it is seen that the product formed has not completed the formation of ZB. The shapes of the particles are not rounded like the commercial products that are taken as reference. The angular shape and needle like shape of the particles prove that the product obtained is not ZB but a composition that is richer in ZnO and boric acid. The TGA, EDX and FTIR analyses also support this idea. The average particle size is around 5 -7 micron like ZnO's. SEM microphotograph of this experiment is shown in Figure 5.11.

Experiment No.2. Again comparing the photo of this experiment with commercial ZB and raw materials it is seen that the desired reaction between ZnO and H_3BO_3 could not be achieved. ZnO and H_3BO_3 particles are clearly seen as unreacted. Thus according to the EDX result the B_2O_3/ZnO ratio is found as 0.085 as seen in Table 5.5 which shows that the product obtained is rich in ZnO. The average particle size of

this product is like that of ZnO's which is around 5 – 7 microns. SEM microphotograph of this experiment is shown in Figure 5.12.

Experiment No.3. The obtained product has an average particle size around 0.2 – 1 micron as seen in Figure 5.13 which is approximately the same as two commercial products studied as a reference. The round shapes of the particles prove that the experiment has been successful and ZB is obtained.

Here the agglomerated particles are to be dispersed when the pigment is being processed in the equipment chosen according to the application.

The shape of the particles looks neither like ZnO nor like H_3BO_3. It is clearly seen that the reaction between ZnO and H_3BO_3 has taken place and desired product was successfully obtained.

Experiment Nos.4 and 5. When SEM microphotographs of these two experiments are compared it was clearly seen that the similar morphology was obtained and this morphology is similar to those which are used as reference products. An additional note about experiment 4 which contains ZB-2335 as seed crystal is that morphologywise it is more like the reference product ZB-2335. Finer particles and agglomerates as bigger groups while experiment 5 has also fine particles but agglomerated in smaller groups. They are figure in Fig.5.14.

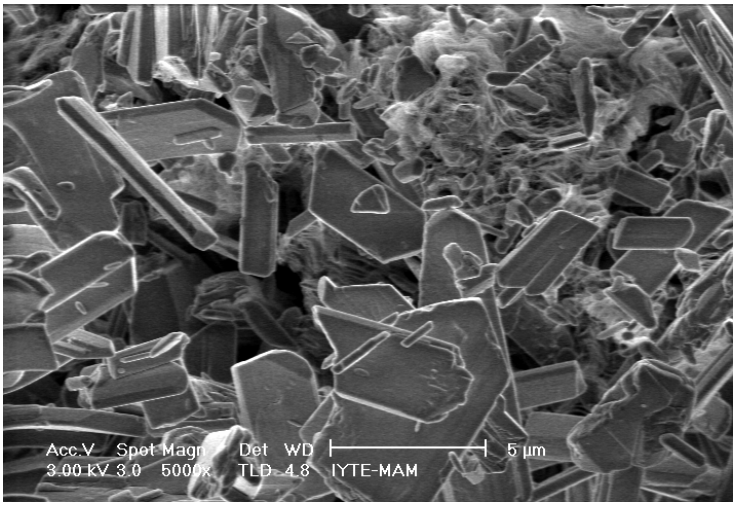

Fig.5.11 SEM microphotographs of Experiment No.1 (5000x).

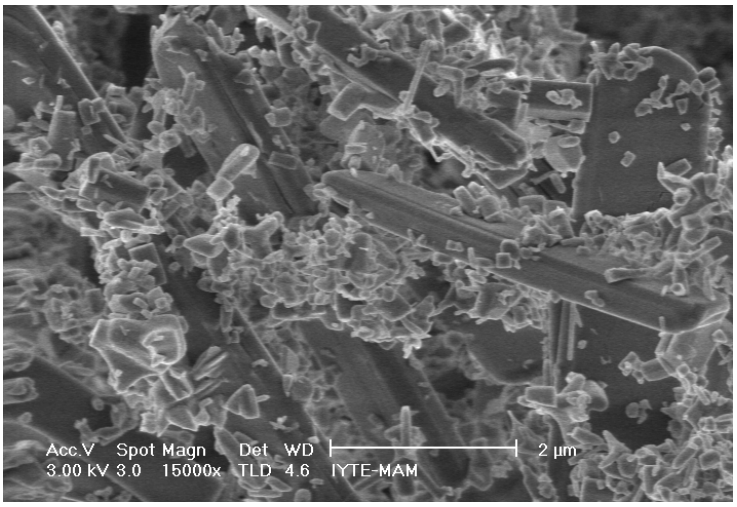

Fig.5.12 SEM microphotographs of Experiment No.2 (15000x).

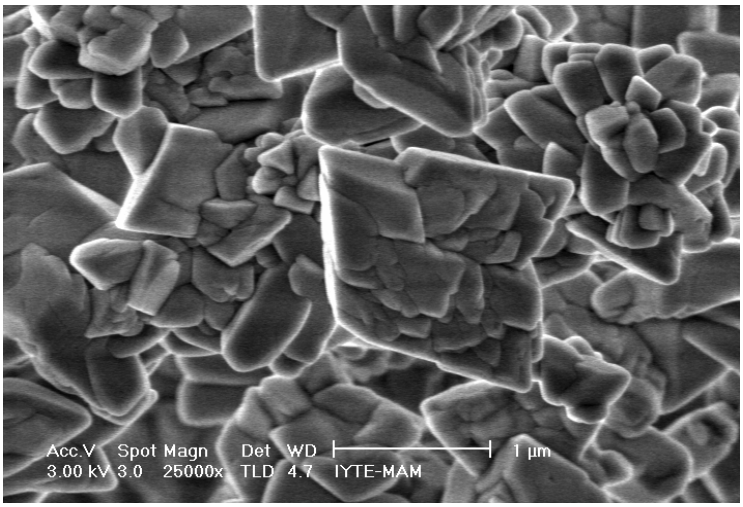

Fig.5.13 SEM microphotographs of Experiment No.3 (25000x).

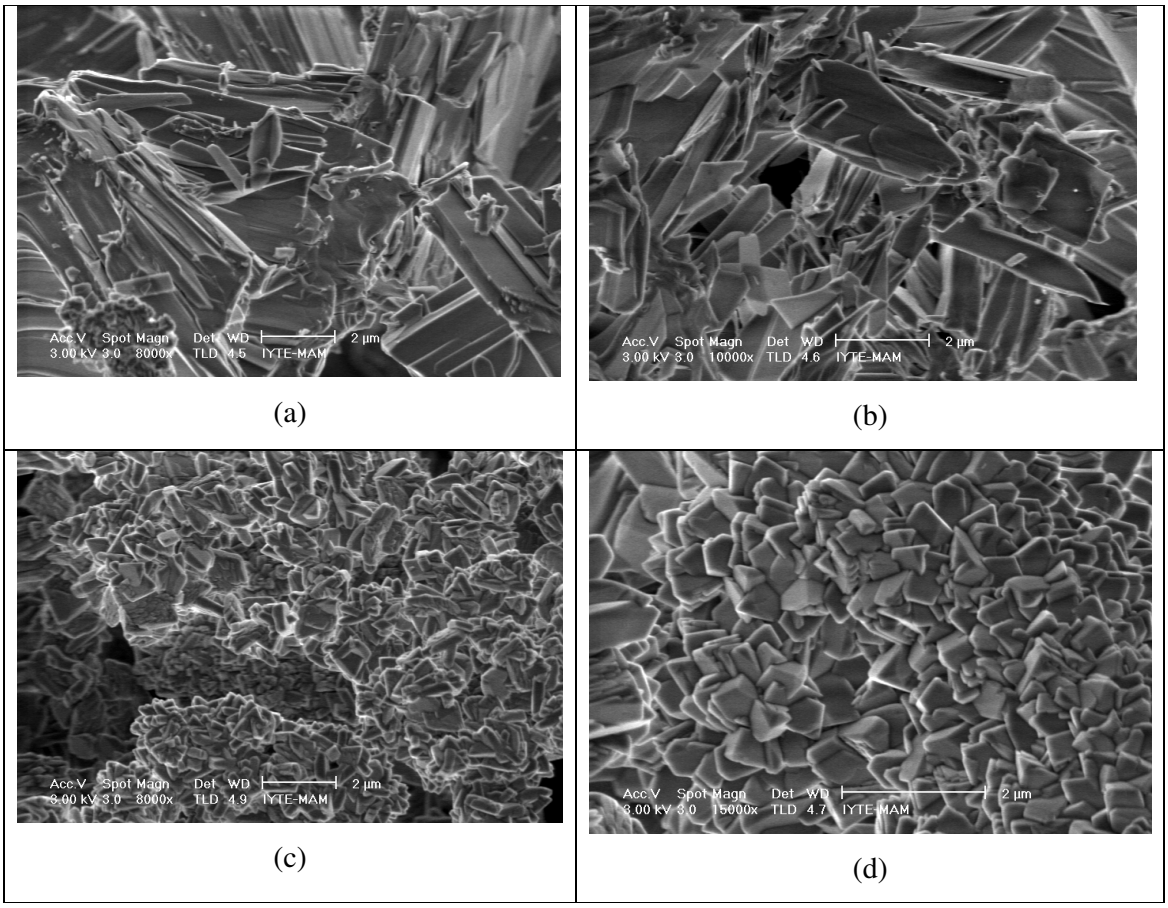

Fig.5.14 (a) SEM microphotographs of Experiment No.4 at 60C, 90min. (8000x) (b) SEM microphotographs of Experiment No.5 at 60C,90 min.(10000x), (c) SEM microphotographs of Experiment No.4 at 90C, 1.5h (8000x), (d) SEM microphotographs of Experiment No.5 at 90C, 1.5h (15000x).

5.2.3 FTIR Spectra

The observed peaks of FTIR spectra of the experiments are tabulated in Table 5.5. The main peak of $ZnO \cdot B_2O_3$ at around 3227 cm^{-1} is clearly seen in Fig.5.17, Fig.5.20 and Fig.5.21. The peaks between 900 and 1300 are all visible in these figures which were reported to be other characteristic peaks of zinc borate and they are also observed in reference ZB's FTIR spectra (Xie et.al., 2001). When these values are compared with the values in Table 3.11 of $MgB_6O_{10} \cdot 7H_2O$ by a study of Yongzhong et.al.[1999], it is clear that the same peaks at 1423, 1351 (belonging to $B_{(3)}$-O) are observed around 1360 cm^{-1}; the peaks at 1098, 1026 (belonging to $B_{(4)}$-O) are observed around 1067 cm^{-1}; the peaks at 957, 898 (belonging to $B_{(3)}$-O) are observed at around 992 and 898 cm^{-1}; 863, 812 (belonging to $B_{(4)}$-O) are observed are around 838 cm^{-1}.

The characteristic peaks of tetrahedral (BO_4) and trihedral (BO_3) borate groups are clearly seen between 1100 and 800 cm^{-1} and between 1450 and 1200 cm^{-1}, respectively between Figures 5.17, 5.20 and 5.21 just like reference's FTIR spectra. The characteristic peak of trihedral borate groups are also obvious at peaks below 800 cm^{-1} in these figures as well. These peaks are much clearer in the experiments where reflux is used and the material is heated for 4h under 90°C.

In Fig.5.15, 5.16, 5.18 and 5.19 the characteristic peak of $ZnO \cdot B_2O_3$ at 3227 cm^{-1} is not observed but the peak of isolated OH between 3350 cm^{-1} and 3500 cm^{-1} is observed. This peak is also observed in FTIR spectra of reference commercial products. This means that the formation of ZB has not fully been achieved in these experiments.

The formation of ZB crystals requires heating under reflux at 90ºC for 4h.

For experiments 1 and 2, the formation of ZB crystals could not be achieved due to the lack of reflux which is seen in Fig.5.15 and 5.16. The experiments 4 and 5 were carried out in two steps with proper mixing. The FTIR spectra of first stages showed that mixing the material at 60°C for 90 minutes does not lead to production of desired zinc borate crystals. Thus, comparison of the FTIR spectra of these experiments (Fig.5.18 and 5.19) with the reference ZBs are proof of this statement.

The peak seen in Fig.5.15, 5.16, 5.18 and 5.19 at 1600 cm^{-1} which is the characteristic peak of water, is not observed in the other figures which belong to the experiments where ZB formation completely achieved. This peak is also not observed in FTIR spectra of commercial ZBs used as reference.

The peak at 2500 cm^{-1} is significant in Fig.5.17, 5.20 and 5.21, and the reference ZBs.

Table 5.5 The observed peaks of FTIR spectra of the experiments.

Exp.3		**Exp.4a**		**Exp.5a**		**Exp.4b**		**Exp.5b**	
Wave number	Abs.	Wave number	Abs.	Wave number	Abs.	Wave number	Abs.	Wave number	Abs.
3355	1.75	3360	0.75	3355	0.82	3465	0.98	3462	0.53
2664	0.70	2662.5	0.41	1365	0.9	3217	1.11	3220	0.58
1360	2.1	1363	0.93	1225	0.76	1420	1.47	2510	0.3
1222	1.60	1222.5	0.745	1125	0.775	1297.5	1.56	1420	0.66
1125	1.55	1122.5	0.79	1057.5	0.81	1255	1.08	1295	0.68
1067	1.8	1065	0.87	1000	0.875	1195	1.04	1256	0.56
927.5	1.485	992.5	0.95	890	0.76	1118	1.4	1194	0.55
887	1.56	887.5	0.78	838	0.705	1068	1.36	1115	0.65
763	1.2	760	0.63	760	0.675	955	1.695	925	0.75
643	1.25	644	0.63	716	0.645	860	1.22	750	0.64
525	0.94	525	0.51	642.5	0.652	752	1.24	657	0.52
						570	0.65	615	0.44
						548	0.7	548	0.42
						520	0.8	520	0.48

Exp.4a: 60ºC, 90 minutes.

Exp.4b: 90ºC, 4 hours.

Exp.5a: 60ºC, 90 minutes.

Exp.5b: 90ºC, 4 hours.

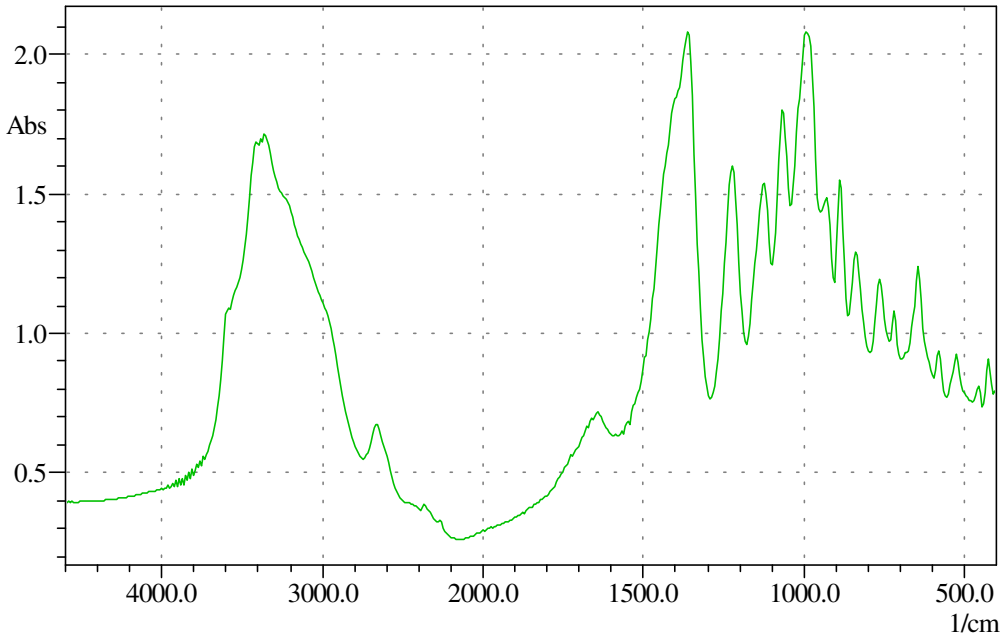

Fig.5.15 FTIR spectrum of Experiment no.1

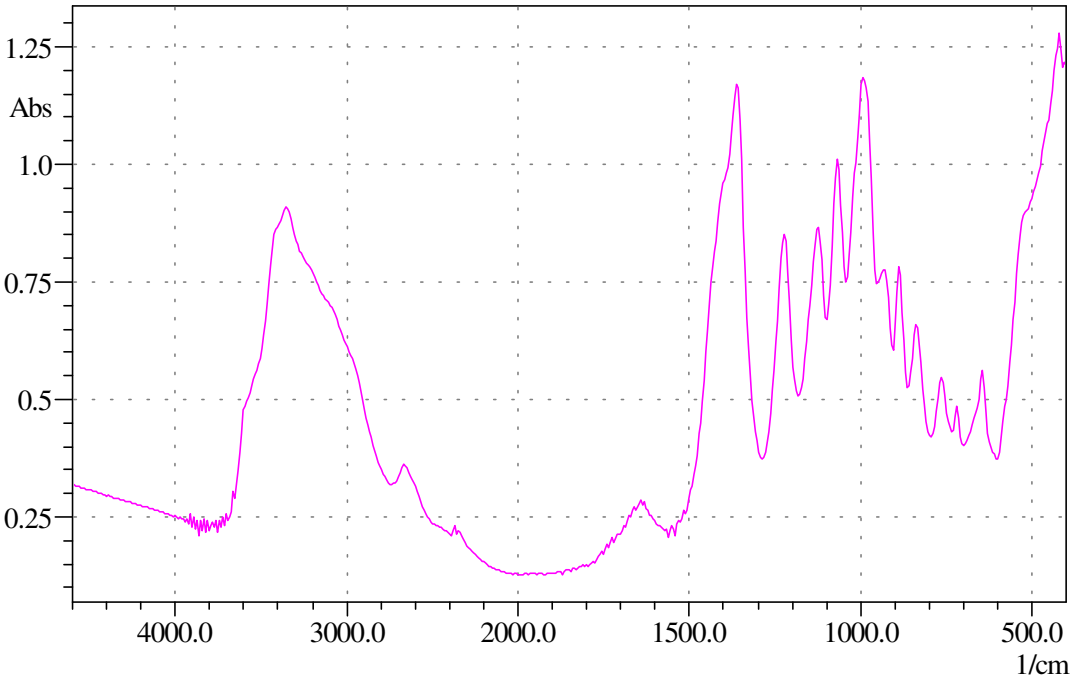

Fig.5.16 FTIR spectrum of the Experiment No.2.

In Fig.5.15, unreacted ZnO was present as understood from the IR peak at 400 cm^{-1} characteristic of ZnO spectrum in Fig.5.3.

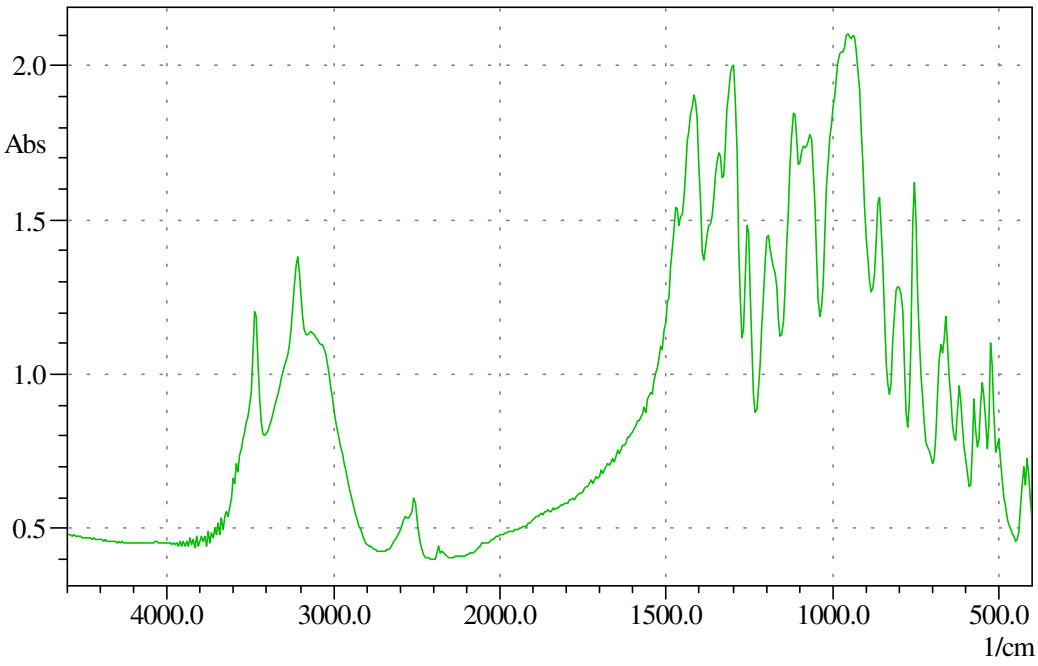

Fig.5.17 FTIR spectrum of the Experiment No.3

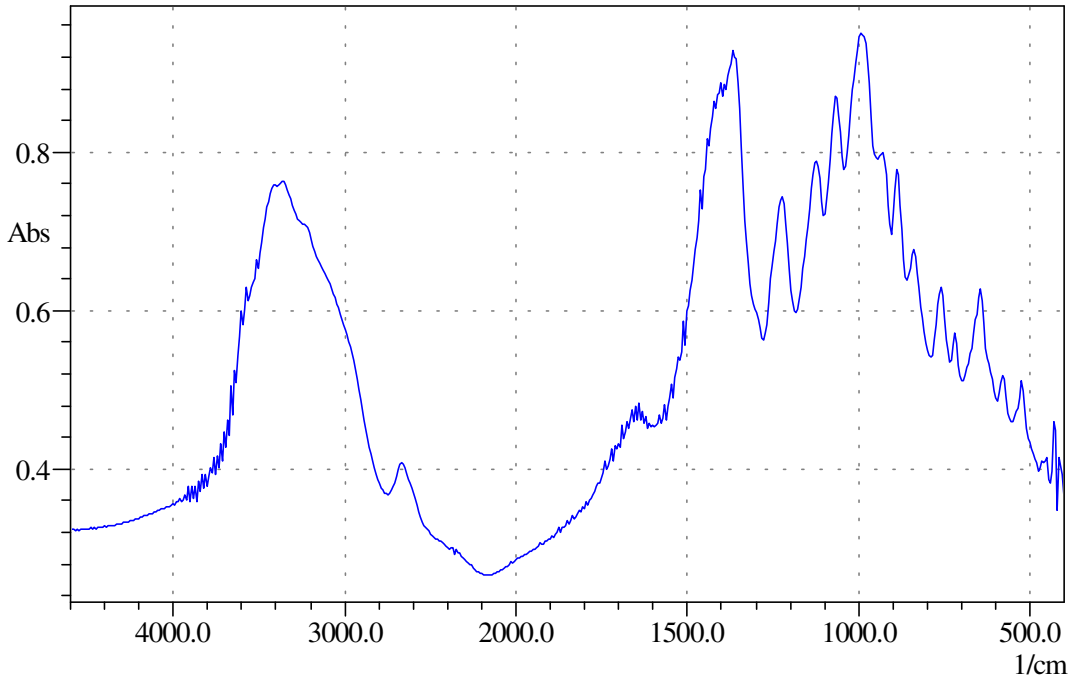

Fig.5.18 FTIR spectrum of the Experiment No.4 at 60ºC, 90min.

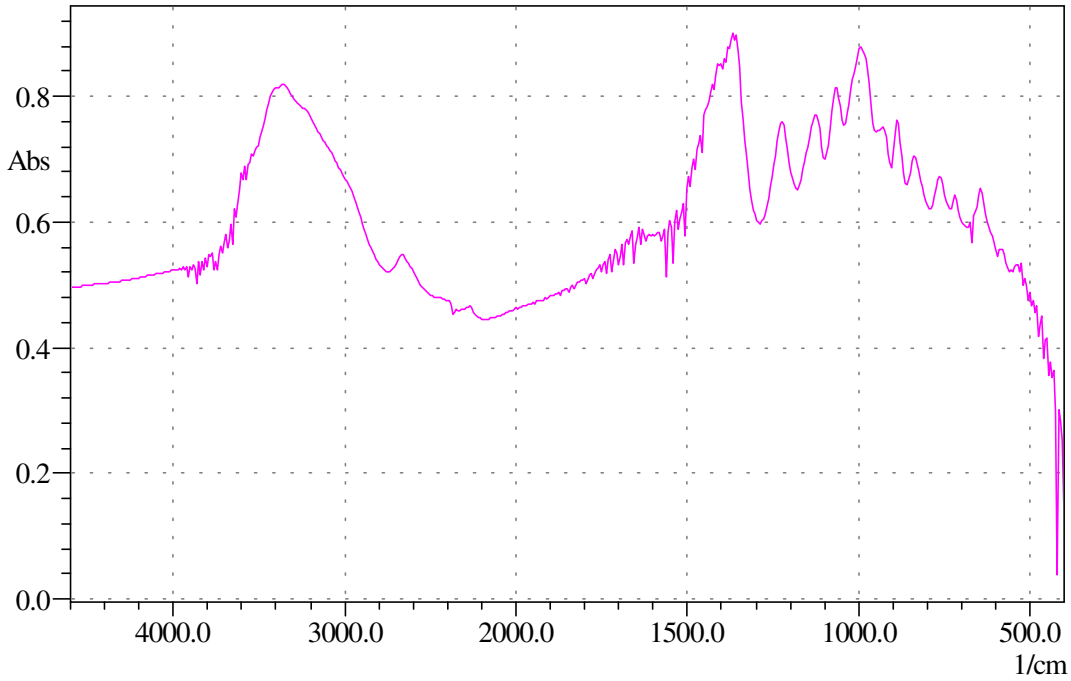

Fig.5.19 FTIR spectrum of the Experiment No.5 at 60ºC, 90min.

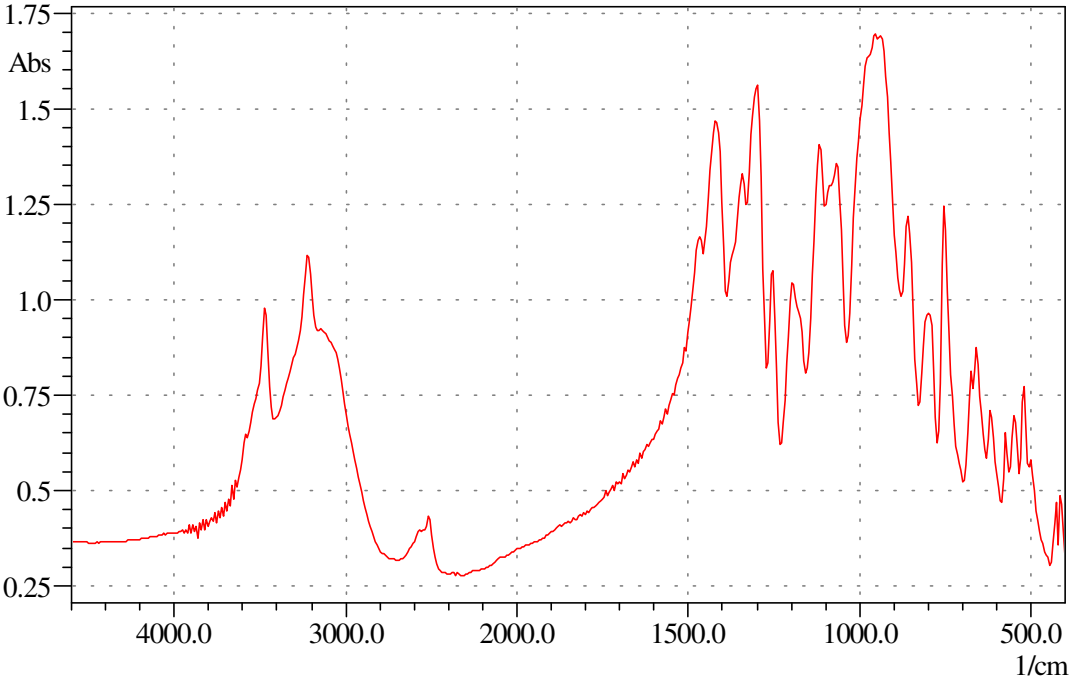

Fig.5.20 FTIR spectrum of the Experiment No.4 at 90ºC, 4h.

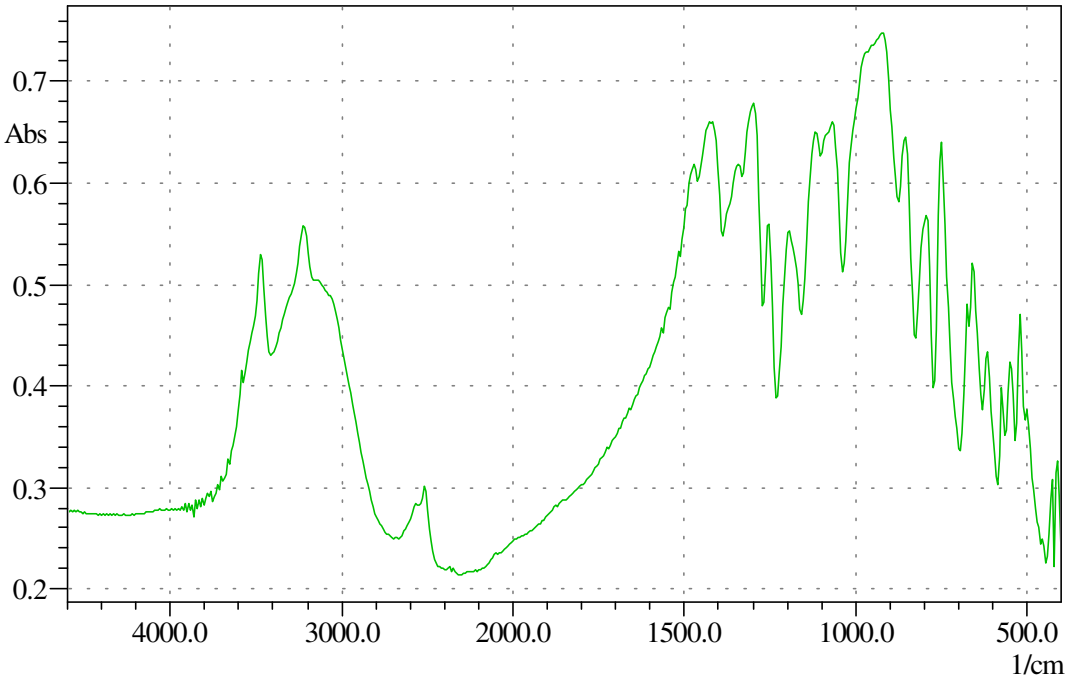

Fig.5.21 FTIR spectrum of the Experiment No.5 at 90ºC, 4h.

5.2.4 X-Ray Diffraction Analysis

X-ray diffraction diagram of the products of this project were compared with X-ray diffraction diagram of $2ZnO \cdot 3B_2O_3 \cdot 3.5H_2O$ reported by Igarashi et.al.[2001] as seen in Figures 5.22 – 5.26. In none of ZB products of Igarashi et.al.had any diffraction peak at 2θ values lower than 17°. On the other hand for experiments 1, 2, 4a and 5a there are strong diffraction peaks at 2θ value of 8°.

From Bragg equation,

$$n\lambda = 2d\mathrm{Sin}\theta$$

where n is order of diffraction, λ is wavelength of incident X-rays. 1.546A° for CuKα radiation used in the experiments, θ is diffraction angle and d is the interplanar distance.

$$1x1.546 = 2xdxSin(8/2)$$
$$d = 11.08A^o$$

this corresponds to a d value of 11.08 A° for experiments 4b and 5b which were carried in two steps at 60°C for 90 minutes and at 90°C for 4 hours, this peak at 2θ value of 8 is not present. The X-ray diffraction diagram of these two products was the same with those of Igarashi et.al.and ZB 2335 and Chinese ZB. X-ray intensities of samples with ZB seed crystals were higher than the unseeded ones indicating higher crystallinity while intensity at 2θ of 28.4 was 27 for unseeded sample, it was 44 for seeded sample.

The primary particle size, B of the crystals was found from Scherer equation.

$$B = \frac{0.9\lambda}{LCos\theta}$$

where L is the breadth of the peak at θ value at half height.

$$B = \frac{0.9x1.546}{{}^{1}\!/\!_{180}\,x3.14xCos\left(\frac{17}{2}\right)} = 81.2\,A^o$$

From the breadth of the peaks of 2θ 18.0 for [020] plane of experiment 5b. The X-ray diffraction values are given in Table 5.6.

Table 5.6 X-ray diffraction values of Experiments

Exp.1		**Exp.2**		**Exp.3**		**Exp.4a**		**Exp.5a**		**Exp.4b**		**Exp.5b**	
2θ	Int.	2θ	Int	2θ	Int	2θ	Int	2θ	Int	2θ	Int	2θ	Int
17.5	27	17.6	24	17.8	25	17.5	11	17.6	19	17.7	31	17.9	53
20.6	11	19.7	6	20.2	9	20.8	6	20.4	5	20.3	44	20.3	53
21.6	4	21.3	5	22.3	6	23.0	4	22.8	5	21.4	27	21.6	48
22.7	4	23.2	10	23.4	9	23.5	4	23.3	11	23.4	26	23.5	49
23.8	8	23.9	5	24.0	7	27.4	9	24.0	7	25.5	37	25.5	48
24.7	5	27.2	12	27.2	13	28.7	9	27.0	21	27.2	11	27.2	19
27.4	16	28.8	10	28.1	45			28.1	23	28.4	27	28.5	44
28.8	9												

Exp.4a: 60ºC, 90 minutes.

Exp.5a: 60ºC, 90 minutes.

Exp.4b: 90ºC, 4 hours.

Exp.5b: 90ºC, 4 hours.

The X-ray diagrams of the ZB sample from the experiments

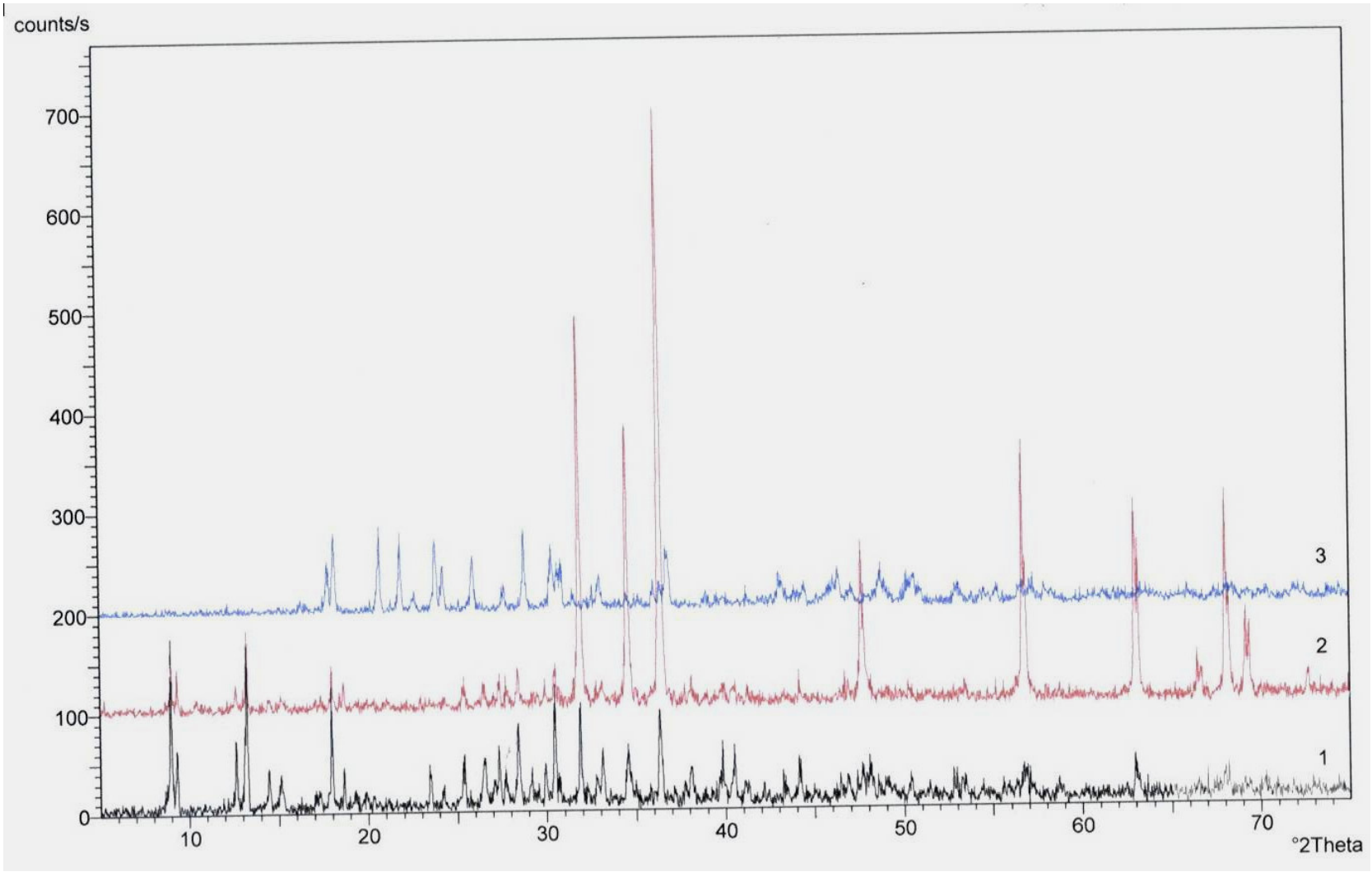

Fig.5.22 X-ray diffraction image of Experiment No.1, No.2 and No.3.

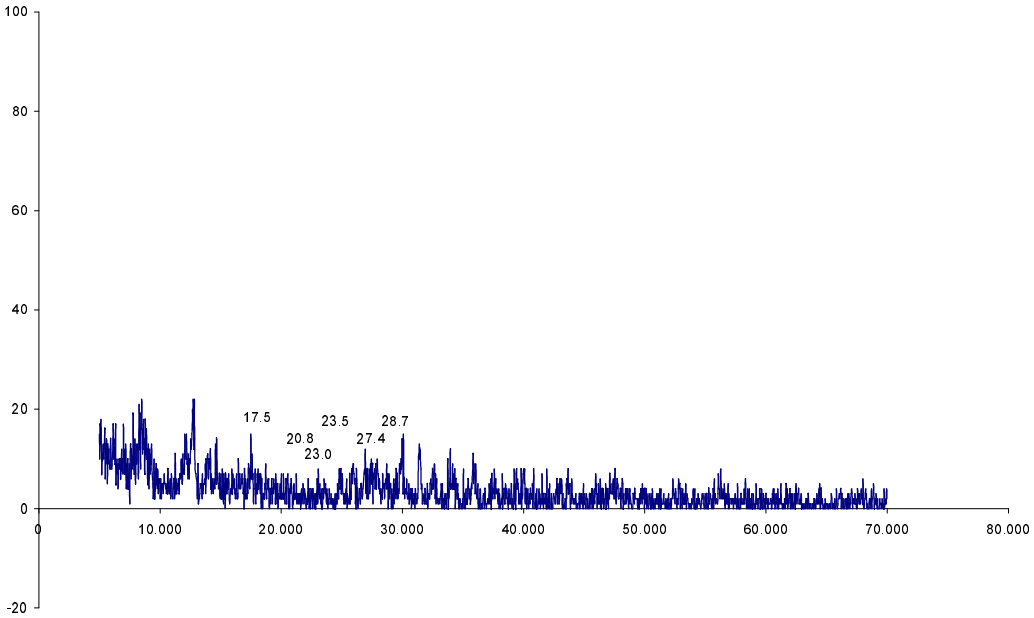

Fig.5.23 X-ray diffraction image of Experiment No.4 at 60ºC, 90 min.

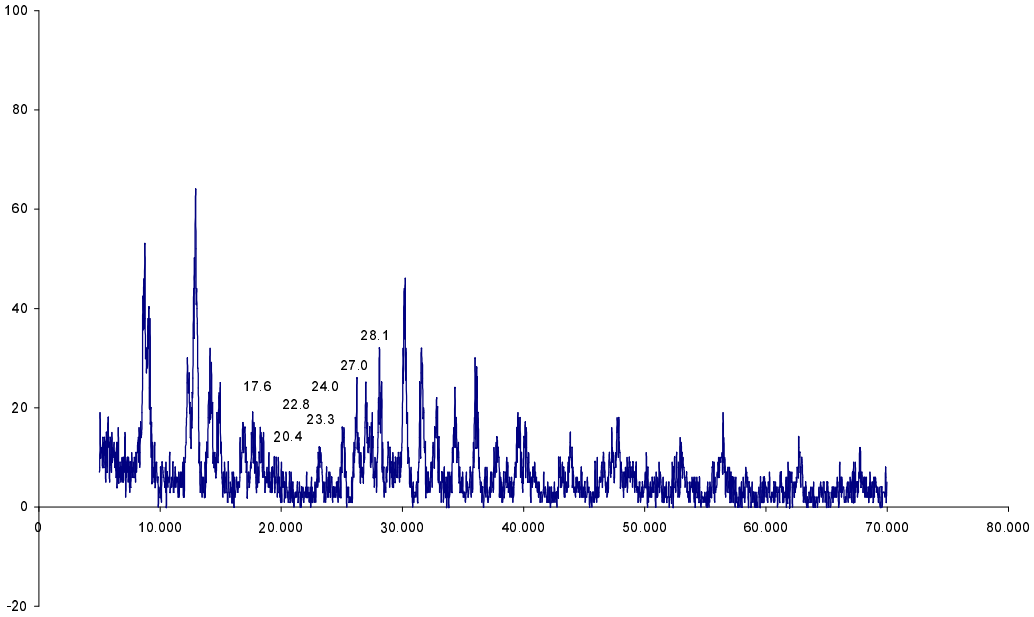

Fig.5.24 X-ray diffraction image of Experiment No.5 at 60ºC, 90 min.

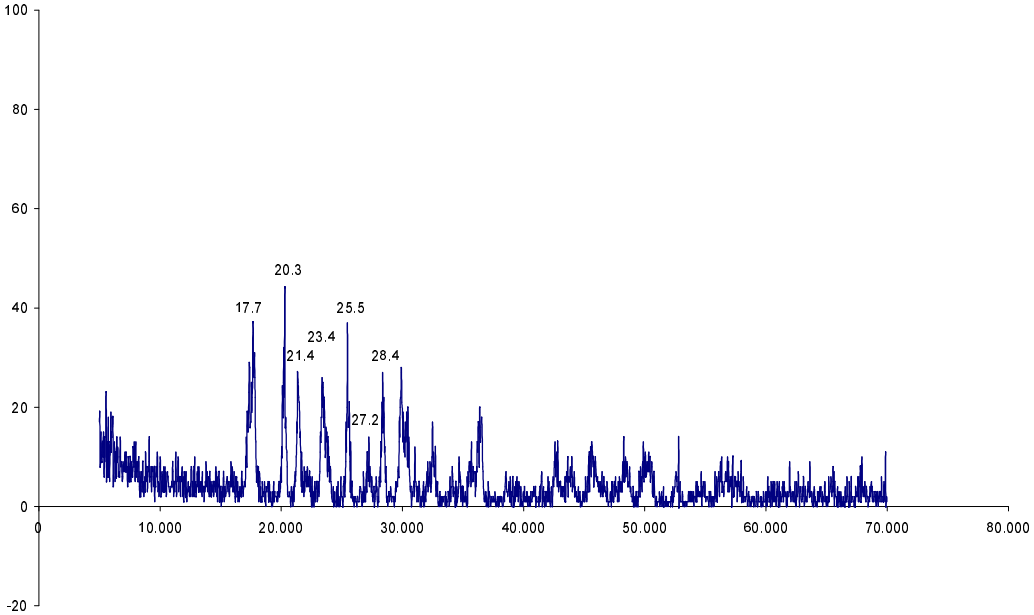

Fig.5.25 X-ray diffraction image of Experiment No.4 at 90ºC, 4h.

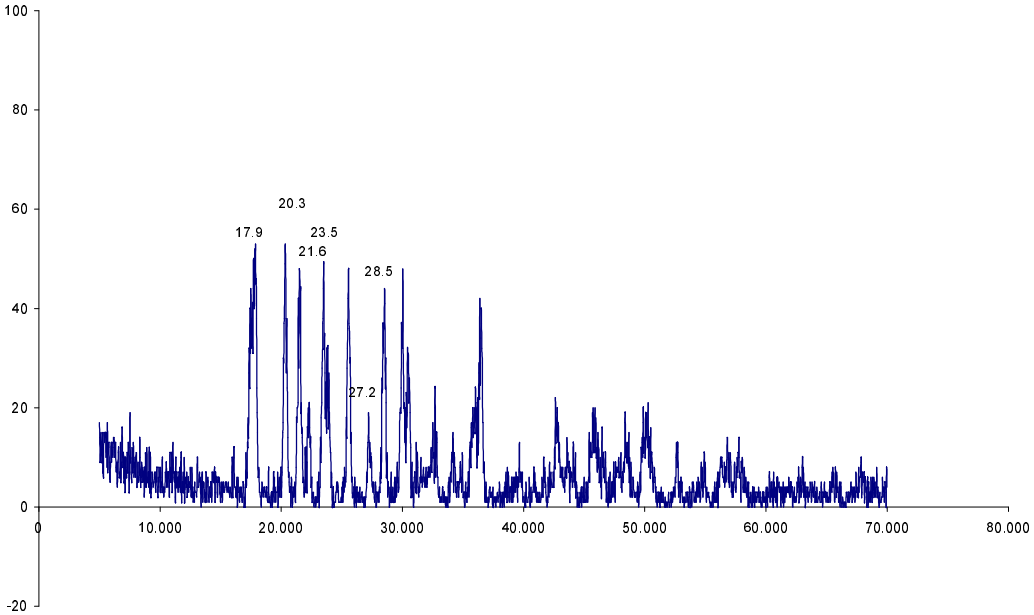

Fig.5.26. X-ray diffraction image of Experiment No.5 at 90ºC, 4h.

5.3 Discussion

In this study, the development of zinc borate production process was investigated. The produced zinc borates were then characterized by SEM, TGA, X-ray diffraction, FTIR and the results were discussed in the previous chapters.

First of all, thermogravimetric (TGA) analyses were done to investigate the thermal behaviour of the samples of zinc borate in view of the crystal water and mass losses. The mass loss of the experiment no.1, 2, 3, 4 and 5 at 60°C for 1.5h and 4 and 5 at 90°C for 4h. were 20.63%, 6.51%, 9.65%, 19.1%, 25%, 9.72 and 11.4%, respectively. It is appearent that the one with seed crystal had got a less mass loss than its counterpart.

The morphology of all of the samples of zinc borate was investigated by a scanning electron microscope (SEM) by taking the microphotographs. This instrument gives information regarding the structures of the films in micron scales. When the first two experiments are compared with the SEM photographs of commercial ZB and raw materials, it is seen that the product formed has not completed the formation of ZB. The shapes of the particles are not rounded like the commercial products that are taken as reference. The angular shape and needle like shape of the particles prove that the product obtained is not ZB but a composition that is richer in ZnO and boric acid. The obtained product in experiment No.3 has an average particle size around 0.2 – 1 micron which is approximately the same as two commercial products studied as a reference. The round shapes of the particles prove that the experiment has been successful and ZB is obtained. When SEM microphotographs of the latest two experiments are compared, it is clearly seen that the similar morphology was obtained and this morphology is similar to those which are used as reference products. An additional note about experiment 4 which contains ZB-2335 as seed crystal is that morphologywise it is more like the reference product ZB-2335.

FTIR spectra of the zinc borate samples were analyzed to have an idea on the structures which are present in the samples. The main peak of $ZnO \cdot B_2O_3$ at around 3227 cm^{-1} is clearly seen. The characteristic peaks of tetrahedral (BO_4) and trihedral (BO_3) borate groups are clearly seen between 1100 and 800 cm^{-1} and between 1450 and 1200 cm^{-1}, respectively. The characteristic peak of trihedral borate groups are also obvious at peaks below 800 cm^{-1} in these figures as well. These peaks are much clearer in the experiments where reflux is used and the material is heated for 4h under 90°C.

In the experiments 1, 2, 4(at 60°C, 90min.) and 5(at 60°C, 90min.), the characteristic peak of $ZnO \cdot B_2O_3$ at 3227 cm^{-1} is not observed but the peak of isolated OH between 3350 cm^{-1} and 3500 cm^{-1} is observed. This peak is also observed in FTIR spectra of reference commercial products. This means that the formation of ZB has not fully been achieved in these experiments. The experiments 4 and 5 were carried out in two steps with proper mixing. The FTIR spectra of first stages showed that mixing the material at 60°C for 90 minutes does not lead to production of desired zinc borate crystals.

For a proper understanding of the crystal structure of the produced zinc borate samples, X-ray diffraction diagrams were used throughout the study. In none of ZB products reported in literature had any diffraction peak at 2θ values lower than 17°. On the other hand for experiments 1, 2, 3, 4a and 5a there are strong diffraction peaks at 2θ value of 8° which corresponds to a value of 11.08A°. X-ray intensities of the samples with ZB seed crystals were higher than the unseeded ones indicating higher crystallinity while intensity at 2θ of 28.4 was 27 for unseeded sample. It was 44 for seeded sample.

The primary particle size of the crystals was found from Scherer equation as 81.2A° from the breadth of the peak of 2θ 18.0 for [020] planes.

An investigation on the relative viscosity change was also carried out during the study which will help to understand the mixer type of the reactor. The relative viscosity will increase to at least 1.24 times thus a mechanical mixer which will stir the mixture even when the viscosity is high should be used.

Also, pH was measured to determine the condition during the experiments. Since an excess of boric acid was used, the solution pH is expected to be acidic in literature. In the two experimental runs to follow pH change during reaction, it was found that pH of boric acid solution was 4.2 and there was a step change to pH 6 as soon as ZnO was added. Thus the pH of reaction mixture was very close to neutral pH during preparation. The result of the experiments shows that the production of ZB should be done under reflux and addition of seed crystal. It is also vital to have reaction temperatures around 90°C and reaction times around 4 hours at this temperature to achieve the desired quality of ZB.

CHAPTER 6

CONCLUSION

For 29.6 g.boric acid and 9.6 g.ZnO per 100 g.water heating at 60ºC for 90 minutes and at 90ºC for 120 minutes, water reflux gave ZB crystals having the same IR spectrum and X-ray diffraction diagram of commercial ZB.

ZB which has 10 – 12 % crystalline water and which dehydrates above 290ºC was obtained from ZnO and boric acid by heating under reflux.

Because of the viscosity increase during reaction, using a powerful mixer and a good temperature control and keeping the volume constant by using reflux are important parameters in ZB production.

Further studies in pilot scale are recommended.

REFERENCES

- Bourbigot S., Bras M.L., Leeuwendal R., Shen K.K., Schubert D., "Recent Advances In the Use of Zinc Borates In Flame Retardancy of EVA", Polymer Degradation and Stability, 64, 419 – 425, 1999.
- Burns P.C., Hawthorne F.C., Can.Mineral. 31, 297 – 304, 1993.
- Christ C., Clark J.R., Physical Chemistry Minerology, 2, 59 – 87, 1977.
- Giudice C.A., Benitez J.C., "Zinc Borates As Flame-retardant Pigments In Chlorine-containing Coatings", Progress In Organic Coatings, 42, 82 – 88, 2001.
- http://minerals.usgs.gov, 2001.
- http://www.etiholding.gov.tr
- http://www.samuelbanner.co.uk/storey/home.htm
- Igarashi H., Tatebe A., Sakao K., Zinc Borate, and Production Method and Use Thereof", EP.Patent No.1 205 439 A1, 2001.
- Kirk-Othmer Encyclopedia of Chemical Technology, Vol.10 and Vol.4, 4th ed., John Wiley and Sons, 910 – 961 and 407 – 408,1994, N.Y.
- Kirk-Othmer Encyclopedia of Chemical Technology, Vol.22, 2nd ed., John Wiley and Sons, 606, 1970, N.Y.
- Schubert D.M., 'Zinc Borate", US.Patent No.5472644, 1995.
- Schubert D.M., Alam F., Mandana Z.V., Knobler C., 'Structural Characterization and Chemistry of The Industrially Important Zinc Borate, $Zn[B_3O_4(OH)_3]$", Americal Chemical Society, 15, 866 – 871, 2003.
- Shete A.V., Sawant S.B., Pangarkar V.G., 'Kinetics of Fluid-Solid Reaction With An Insoluble Product: Zinc Borate By The Reaction of Boric Acid and Zinc Oxide", Journal of Chemical Technology and Biotechnology, 79, 526 – 532, 2003.
- Tektaş E., Mergen A., "Çinko Borat", Etibank, 2003.

- Ullmann's Encyclopedia of Industrial Chemistry, Vol.A11, 5th ed., VCH Publication, 123 – 139,1988, Weinherm.
- Xie R., Qu B., Hu K., "Dynamic FTIR Studies of Thermo Oxidation of Expandable Graphite-based Halogen-free Flame Retardant LLDPE Blends", Polymer Degradation and Stability, 72, 313 – 321, 2001.
- Yongzhong J., Shiyang G., Shuping X., Jun L., Spectrochimica Acta Part A, 56, 1291 – 1297, Elsevier, 1999.